Západočeská univerzita v Plzni

Fakulta elektrotechnická

Katedra technologií a měření

DISERTAČNÍ PRÁCE

PLZEŇ, 2014

Ing. Petr Mráz

Fakulta elektrotechnická

DISERTAČNÍ PRÁCE

k získání akademického titulu doktor
v oboru

Elektrotechnika

Ing. Petr Mráz

Aspekty hodnocení výbojové činnosti

Školitel: prof. Ing. Václav Mentlík, CSc.

Konzultant specialista: prof. Ing. Rainer Haller, Dr.

Datum státní doktorské zkoušky: 11. 7. 2011

Datum odevzdání práce:

V Plzni, 2014

Faculty of Electrical Engineering

DISSERTATION THESIS

To obtain academic doctor's degree PhD in field

Electrical Engineering

Ing. Petr Mráz

Aspects of partial discharge activity evaluation

Supervisor: prof. Ing. Václav Mentlík, CSc.

Consultant specialist: prof. Ing. Rainer Haller, Dr.

Pilsen, 2014

Prohlášení o duševním vlastnictví

Tímto předkládám k posouzení a obhajobě disertační práci na téma „Aspekty hodnocení výbojové činnosti“ zpracovanou během doktorského studia na Fakultě elektrotechnické Západočeské univerzity v Plzni pod vedením prof. Ing. Václava Mentlíka, CSc. a konzultanta prof. Ing. Rainera Hallera, Dr.

Prohlašuji, že jsem tuto práci vypracoval samostatně s použitím literatury a zdrojů uvedených v seznamu na konci této práce.

V Plzni, ...

Petr Mráz

Mráz, P.

ASPEKTY HODNOCENÍ VÝBOJOVÉ ČINNOSTI

Disertační práce se zabývá měřením a vyhodnocováním výbojové činnosti v elektrických zařízeních, především metodikou měření částečných výbojů u strojů s vinutími.

Práce se zaměřuje na měřené a odvozené parametry částečných výbojů určené pro vyhodnocování dopadu výbojové činnosti na izolační systém. V práci jsou diskutována omezení nejrozšířenějšího hodnotícího parametru zdánlivého náboje Q_{iec} a následně je navržena vhodná metodika měření a vyhodnocování výbojové činnosti. Jsou rozebrány dílčí limity dané mezinárodní normou pro měření částečných výbojů IEC 60270, které je nutné uvažovat při měření i následném vyhodnocování naměřených dat. Je rozebrána problematika paralelních zdrojů výbojové činnosti a jejich možné rozlišení a identifikace v časovém a frekvenčním spektru. Je představena nová měřicí technika přenosové frekvenční charakteristiky u strojů s vinutími a z toho plynoucí odhad kapacity stroje v různých frekvenčních spektrech, na jehož základě lze určit vhodnou velikost vazební kapacity pro dosažení efektivní citlivosti měření.

Problematika práce byla podpořena výzkumným záměrem MŠMT České republiky MSM 4977751310 – „Diagnostika interaktivních dějů v elektrotechnice“ a grantem Studentské grantové soutěže ZČU SGS 2012-026 **„**Materiálové a technologické systémy v elektrotechnice**“**.

121 stran 105 obrázků 10 tabulek 2 přílohy

KET, FEL ZČU v Plzni 2014

Mráz, P.

ASPECTS OF PARTIAL DISCHARGE ACTIVITY EVALUATION

This doctoral thesis deals with measurement and evaluation of discharge mechanisms in electrical devices, especially by using a method of measuring partial discharges in devices with winding.

It focuses on both measured and derived parameters of partial discharges designated for evaluation of the impacts of discharge activity on insulation system. The scope also includes limitations of the apparent charge parameter of evaluation Q_{iec} which is the most widely used in practice. Their identification then led to a proposal of an appropriate methodology for measurement and evaluation of discharge activity. Particular limits established by the international standard for measurement of partial discharges IEC 60270 that need to be followed during measuring and subsequent data evaluation stages are also mentioned. The topic of parallel sources of discharge activity along with their potential differentiation and identification within the time- and frequency- domain is tackled as well. One of the next contributions of this thesis is the development and introduction of a new measuring technique of the transmission frequency characteristic for the devices with winding. The proposed methodology enables estimation of the device capacity in various frequency-domains which then provides a basis for an appropriate amount of binding capacity to be established in order to achieve an effective sensitivity of the measurement.

The aims addressed by this project have been supported by research objectives of MŠMT Czech Republic MSM 4977751310 – 'Diagnostics of Interactive Processes in Electrical Engineering" and Student Grant Agency of the WBU in Pilsen, grant No. SGS 2012 – 026 ‚Material and Technology Systems in Electrical Engineering'.

121 pages 105 pictures 10 tables 2 annexes

KET, FEL ZČU in Pilsen 2014

Mráz, P.

ASPEKTE DER BEWERTUNG DER ENTLADUNGSAKTIVITÄT

Die Dissertation befasst sich mit der Messung und Auswertung der Entladungsaktivität in elektrischen Geräten, vor allem mit der Methodik der Teilentladungsmessung an Maschinen mit Wicklungen.

Der Schwerpunkt der Arbeit liegt in den gemessenen und abgeleiteten Parametern der Teilentladungen, die zur Auswertung der Auswirkungen der Entladungsaktivität auf Isolationssystem dienen. In der Arbeit werden die Einschränkungen des am meistverbreiteten Auswertungsparameter der scheinbaren Ladung Q_{iec} diskutiert und anschließend ist die geeignete Methodik für die Messung und Bewertung der Entladungsaktivität entworfen. Es werden die Limits nach dem internationalen Standard für die Messung von Teilentladungen IEC 60270 erläutert, die bei der Messung und anschließender Auswertung der Messdaten berücksichtigt werden müssen. Analysiert wird die Problematik der Parallelquellen der Entladungsaktivität und ihre mögliche Unterscheidung und Identifikation im Zeit- und Frequenzbereich. Vorgestellt wird eine neue Messtechnik der Übertragungsfrequenzcharakteristik der Maschinen mit Wicklung und die resultierende Schätzung der Maschinenkapazität in unterschiedlichen Frequenzspektren, an deren Grundlage die passende Größe der Kopplungskapazität für die Erreichung der effektiven Messempfindlichkeit bestimmt werden kann.

Das Thema der Arbeit wurde von dem Forschungsvorhaben der MŠMT der Tschechischen Republik MSM 4977751310 – „Diagnostik der interaktiven Prozesse in der Elektrotechnik“ und der Förderung des Studentenwettbewerbs ZČU SGS 2012-026 „Materielle und technologische Systeme in der Elektrotechnik“ unterstützt.

121 Seiten 105 Bilder 10 Tabellen 2 Beilagen

KET, FEL ZČU in Pilsen 2014

Content

List of symbols and abbreviations

AC	Alternating current
BW	Bandwidth
CIGRE	International Council on Large Electric Systems
CT	Current Transformer
DC	Direct current
DGA	Dissolved Gas Analysis
DUT	Device Under Test
FFT	Fast Fourier Transform
FRA	Frequency Response Analysis
GIS	Gas Insulated Switchgear
HNQ	PD diagram, where y axis is a pulse rate and x axis is a apparent charge
HP	High Pass
IEC	International Electrotechnical Commission
IEEE	The Institute of Electrical and Electronics Engineers
ISD	Intensive Slot Discharges
LP	Low Pass
MIDAS	Mobile Insulation Diagnosis & Analyzing System
N(t)	PD diagram, where y axis is the pulse repetition rate and x axis is a measuring time
PD	Partial Discharge
PD-AC	Partial Discharge measurement under the AC stress
PD-DC	Partial Discharge measurement under the DC stress
PDEV	Partial Discharge Extinction Voltage
PDIV	Partial Discharge Inception Voltage
PET	Poly Ethylene Terephthlate
PRPD	Phase Resolved Partial Discharge diagram or fingerprint
Q(t)	PD Diagram, where y axis is the apparent charge and x axis is the measuring time
Q(t)U(t)	PD diagram, where y_1 axis is the apparent chare, y_2 axis is a test voltage and x axis is the measuring time
Q(U)	PD diagram, where y axis is the apparent charge and x axis is the test voltage
SNR	Signal to Noise Ratio
UHF	Ultra High Frequency
VPI	Vacuum Pressure Impregnation
VT	Voltage Transformer
ϕ-q	PD Pulse Diagram
ϕ-q-n	Phase Resolved Partial Discharge diagram or fingerprint
C	Capacitance
C_k	Coupling capacitor
C_t	Test object
f_1	Low cut-off frequency
f_2	High cut-off frequency
f_c	Cut-off frequency
HV	High Voltage
I	Discharge Current
i(t)	Compensating current
L	Inductance

LV	Low Voltage
M	Measuring device
MV	Medium Voltage
N	Pulse repetition frequency
n	Pulse repetition rate
O_3	Ozone
P	Discharge power
Q	Apparent Charge
q	Instantaneous value of the apparent charge
q_i	Instantaneous value of the apparent charge
Q_{iec}	Apparent Charge measured according to IEC 60270
Q_m	Measured charge
R	Resistance
R_M	Measuring resistor
R_{max}	Maximum reading of PD measuring instrument
R_{min}	Minimum reading of PD measuring instrument
T	Time interval
t_d	Dead time
t_f	Fall time
t_{on}	Pulse peak time, see Fig. 35
t_r	Rise time
T_{ref}	Reference time interval
t_t	Total pulse duration
U	High voltage power supply
U_1	Test voltage, specific definition can be found the thesis and IEC 60076
U_2	Test voltage, specific definition can be found the thesis and IEC 60076
U_e	Extinction voltage
$U_{e/avg}$	Average value of extinction voltage
U_i	Inception voltage
u_i	Instantaneous value of the test voltage
$U_{i/avg}$	Average value of inception voltage
U_m	Maximum voltage
U_n	Nominal Voltage
U_{test}	Test voltage
Z	Impedance
Z_0	Characteristic/surge impedance
Z_m	Measuring impendence
Δf	Bandwidth
ΔU_t,	Voltage drop
ΔU_t	Residual voltage drop

1 Introduction and motivation

Nowadays, the consumption of electrical energy increases all around the world. Because of that it is very important to focus on devices that produce and provide this kind of energy. Electrical rotating machines, transformers, reactors, switchgears, cables, all of these are the key elements in chain of electrical energy production and distribution. There are a lot of parameters that should be studied and improved e.g. efficiency and reliability. Diagnostic of electrical devices is well-known and frequently used tool for determining state. It is necessary to aim the research effort at reliability of these devices the lack of which can cause enormous financial losses and big problems in the function of state infrastructure or even the functionality of the whole society if they stopped operating.

One of the very important diagnostic parameters is partial discharge (PD) activity detection in insulating system of electrical devices. The well-known rule stating that the system is reliable only as much as its weakest part, is naturally also applicable in the field of electrotechnics. It was found that in case of electrical rotating machines, the weakest segment (from the reliability point of view) is the insulating system of a motor. The question is why we should even deal with partial discharge activity. History of PD investigation goes back to the 1920s, when the partial discharge phenomenon was first detected, but no significant attention was paid to this topic. [35, 36] An important turn arose in the 1960s, when the fundamental transformation came in the insulating system of rotating machines – the change from so called "soft" to "hard" insulation system. "Soft" insulation system consisted from paper and foliated mica, where shellac was used as a binder, (resin type) [34] and tar. [65, 68] When temperature of a generator reached the operating temperature (around 60 °C – 70 °C) the bitumen perfectly filled all spaces between the stator winding bar and the slot. So the system became perfectly compact and homogenous. However, this system had certain disadvantages as well. Hence the so called "hard" insulation system came. Glass fibre or PET (Poly Ethylene Terephthalate) foil together with reconstructed mica (Bardet or Heyman process [34]) and epoxy-resin are used instead. Three-component composite has better electrical and thermal properties, but despite modern technological processes it is almost impossible to produce it without any air voids or non-uniformities in the outer structure of the winding. These cavities are the source of partial discharges, which has negative impact on the lifetime of insulating materials. The main problem is caused by slot discharges, up until then an unknown problem. Slot discharges were defined and discussed at global scale from the early 1950s

[67] up to the present day literature [29, 68]. In our country several studies dealt with slot discharges in the 1980s and used to call them the Intensive Slot Discharges (ISD) to distinguish them from the rest of partial discharges because of their large energy content and significant erosion effect [65, 66]. Another problem was surface discharges at the end-winding part of the stator with rated value more than 3 kV. No semi-conductive paints or tapes were used and hence the machine room used to be full of O_3 produced by PD. Nevertheless the end-winding part is the source of PD activity even nowadays since the semi-conductive paints or tapes can only reduce the PD activity.

Detection and evaluation of PD activity helps during the design of new segments of electrical machines and devices (primarily insulating systems), but it is also a suitable diagnostic tool helping to determine current state of the device. Thanks to PD detection it is possible to prevent destructive changes in the device and plan lay-offs as well as regular maintenance of machines and devices. Nowadays, the PD detection as a non-destructive diagnostic tool is used in a wide range of applications, e.g. in case of generators, transformers, cables, switchgears and many others.

Partial discharge measuring has recently become quite a popular and discussed diagnosis method. The main reasons for that have been outlined in the introduction. The following chapter tries to find out and describe why it so, on particular examples and discuss whether the measuring of partial discharges makes sense and is worth it if the amount of resources invested is considered.

Rotating machines, switchgears and transformers are the key elements of electro energy grid. These elements should fulfil strict requirements and should be under continuous monitoring or at least an increased attention should be paid to these particular components. Several surveys of these devices have been already done to find out the weakest points to enable satisfactory focus on excluding possible failures. Critical parts and causes of main failures are mentioned in the following paragraphs.

1.1 Rotating machines

Several statistical analyses regarding power generators have been conducted, but they have been mostly done with small amount of samples or only specify the part of machines where the failure occurred, but no deeper examination of the cause of a failure has been carried out. [12] An interesting and useful statistic was done by CIGRE, working group A1.10 and described in brochure number 392. [1] The brochure deals with hydro generators, but in general a very similar behaviour can be observed in case of all rotating machines since the design is very much alike. The survey was done at 16 utilities and one machine manufacture. Total number of observed generators was 1199 pieces. 69 incidents was recorded and analysed.

Fig. 1 shows that most failures occurred in the stator part. Opposite to that, rotor part has almost four times lower amount of failures. End windings flashovers are quite a rare issue, same as slip ring flashovers. It means that the focus of designers and test engineers should be concentrated at the stator of power generators.

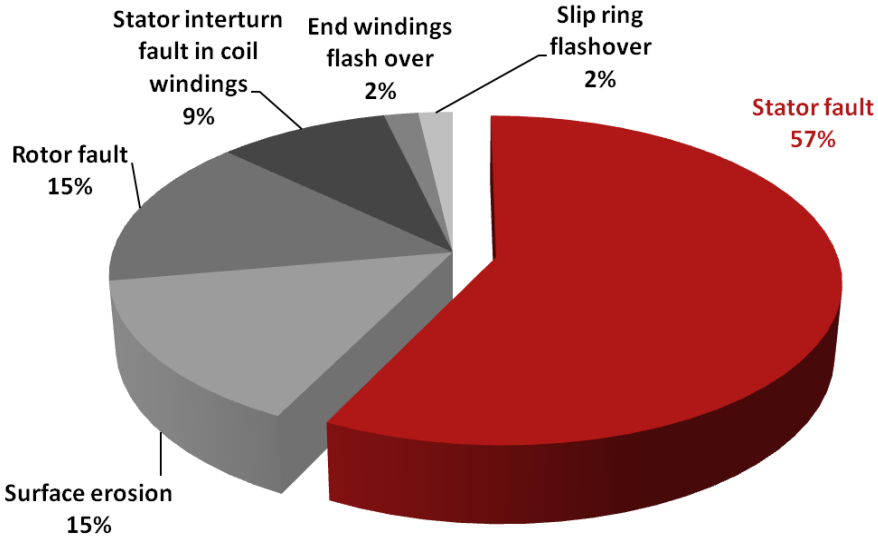

Fig. 1 Localisation of faults during the construction of machines [1]

What type of damage causes the failure can be concluded from Fig. 2 where it is clearly stated that more than 50 percent of failures are again caused by insulation damage. Mechanical and thermal damages have half the probability to make the machine fail.

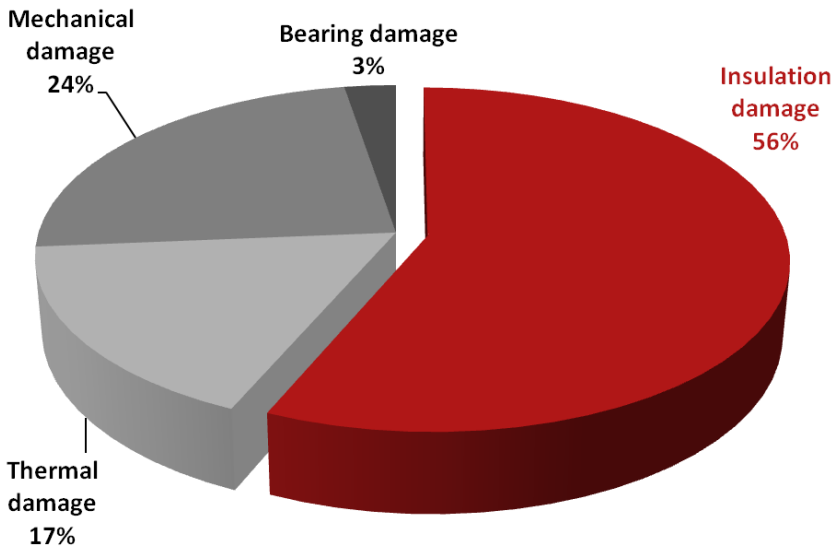

Fig. 2 Localisation of faults regarding the type of damage [1]

Finally Fig. 3 shows the root causes of machines fault. Internal partial discharges (IPD) cause almost one quarter of defects. IPD might be caused by improper technological process, but in general it is impossible to make an absolutely homogenous insulation, especially nowadays when three-component composite materials are used to produce insulation of rotating machines. The carrying element is in this case glass fabric or a PET foil, whereas mica is mostly used as a filler and resin like a binder to interconnect all parts together. The structure of this insulation material might cause the IPD, because the combination of glass fabric where the joints of single fibres are and resin might cause formation of small cavities and bubbles mostly filled with air or other gases. There are two technological processes how to produce this kind of insulation - resin-rich and VPI (Vacuum Pressure Impregnation). [32] Both of the technological processes try to minimise the possible creation of cavities, but despite the pressure and vacuum which is used in case of the technological VPI process, small air cavities usually occur in the insulation material. Nevertheless the VPI process is more immune to creating the cavities. This imperfection should be suppressed as much as possible and controlled at the output inspection of the final product.

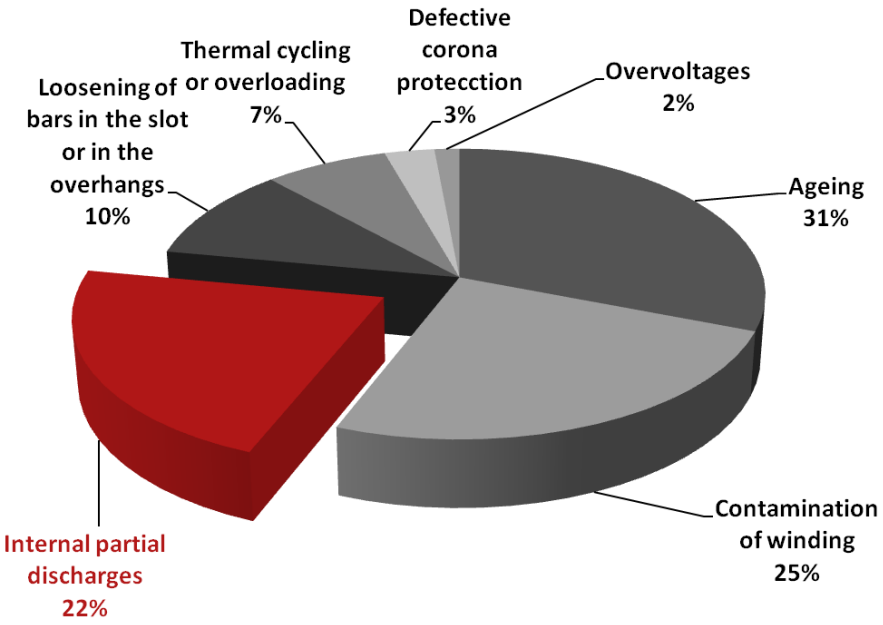

Fig. 3 Particular causes of failures [1]

The second most common problem in rotating machines is winding contamination. This issue causes partial discharges which has negative and erosive impacts on the winding and finally causes a failure. 31 percent of accidents are caused by ageing. Ageing can be induced by many parameters, but apart from the other ones, also by partial discharges with negative electrical, chemical, erosive and mechanical impacts. [33]

On-line partial discharge monitoring was found to be a reliable predictive system for rotating machines. [8] On-line PD monitoring together with regular off-line tests can prolong the lifetime of a machine up to 20 years. During this period a relatively low amount of money has to be invested into regular maintenance and accidental repairs, which are returned in short period of time. On-line PD monitoring can save a lot of funds and make the system more reliable, which is an important benefit. [22-31]

1.2 Switchgears and GIS (Gas Insulated Switchgears)

In case of GIS (Gas Insulated Switchgears, mostly insulated by insulation gas SF_6) an interesting study was made by CIGRE joint working group 33/23.12, and summarized in Electra article number ELT_176_4. [2] The survey was done together with companies EDF, Enel, Eskom, Tepco, Ontario, Hydro, Wienstrom and five German utilities. It means quite a

wide range of institutes worldwide. Study was conducted on GIS installed between 1967 and 1992.

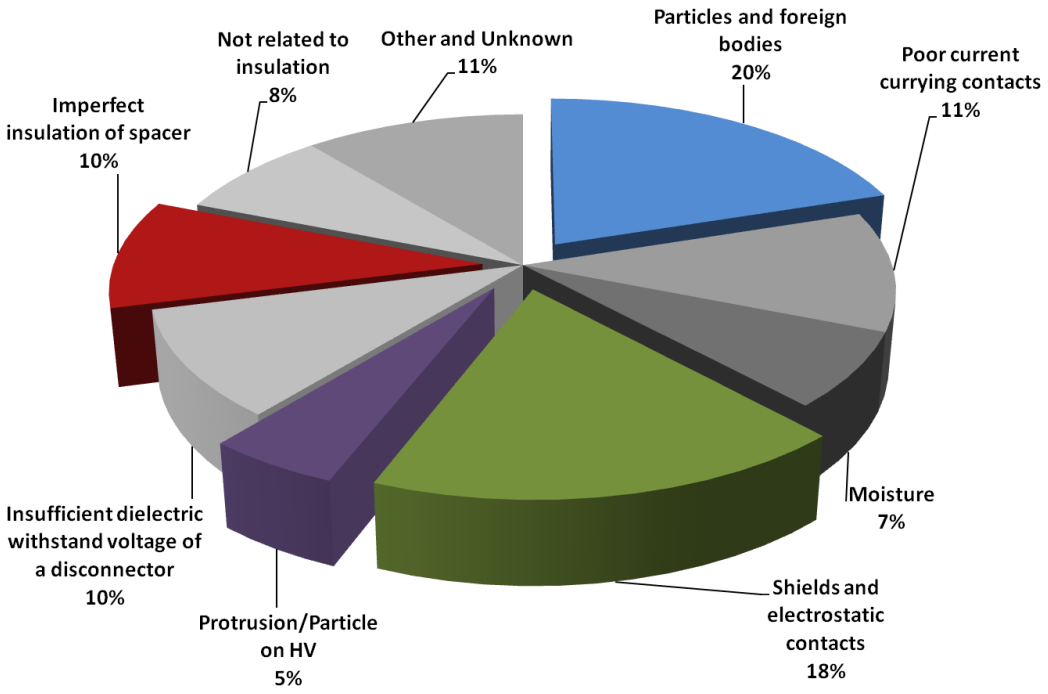

Fig. 4 Failures at GIS sorted by type [2]

The main failures are caused because of particles or foreign bodies which left close or on spacer surface, by sharp protrusions or particles occurring on high voltage conductor, by poor electrostatic contacts and shield and by imperfect insulation of the spacer. Most of all above mentioned failures produce partial discharges, which consequently has a negative impact on the system and causes the failures. These failures can be mostly recognized by partial discharge measurement. [2]

For GIS there are two main groups of failure causes. Fast Front Overvoltages and Very Fast Front Overvoltages belong into the first group. This is caused by a lightning, which hits over-headlines, dis-connectors or circuit breakers. Second group of failure causes are internal faults such as protrusions, particles, loose shields etc. To distinguish the internal faults, it is recommended to use partial discharge detection diagnosis method [3, 4] since this is in fact more or less the only method which enables to detect these kind of failures relatively easily and effectively. It was found and generally agreed upon that for PD detection method all of the available techniques are useful and can help to recognise the defect. But there is currently no relation between all of these methods regarding the

measured parameters. Because of that a CIGRE Joint Task Force 15/33.03.05 was established to standardise the UHF (Ultra High Frequency), acoustic and conventional PD measurements. The main task is to gain experience and try to find correlation between these methods. [2]

1.3 Transformers

Regarding the overview of transformer failures a survey has been done by CIGRE group SC D1. Data has been collected from 48 utilities and 16 countries. Total amount of recorded failures has been 685 from the time period between 1996 and 2010. Transformers which have been included in the survey were manufactured from the 1950's up to 2009. This project is still in progress. [5]

Localisation of faults was done on Substation Transformers with operation voltage level above 100 kV, number of recorded faults was 364. Next type of observed power transformers was Generator Step-up Transformer, again above 100 kV operation voltage. Number of recorded faults in this case was 82 failures. The rest of faults belong to transformers with lower operation voltages. [5]

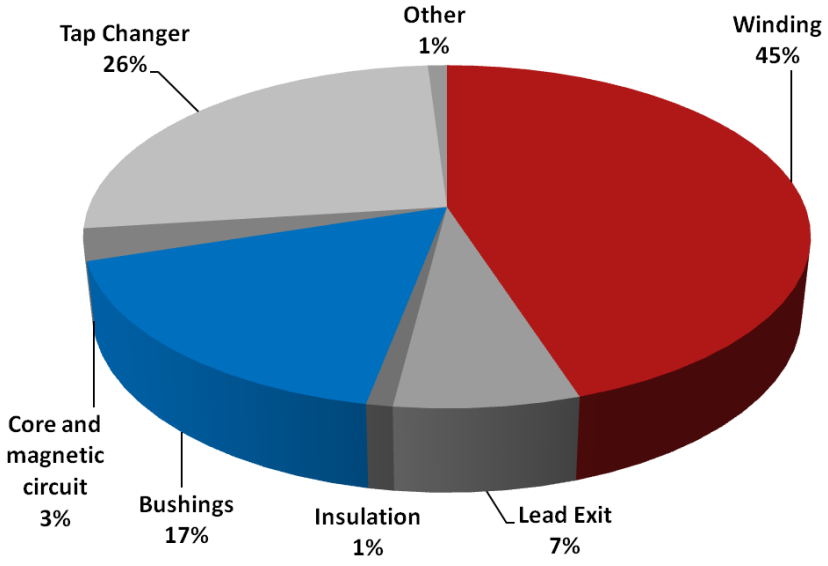

Fig. 5 Faults of Substation Transformers [5]

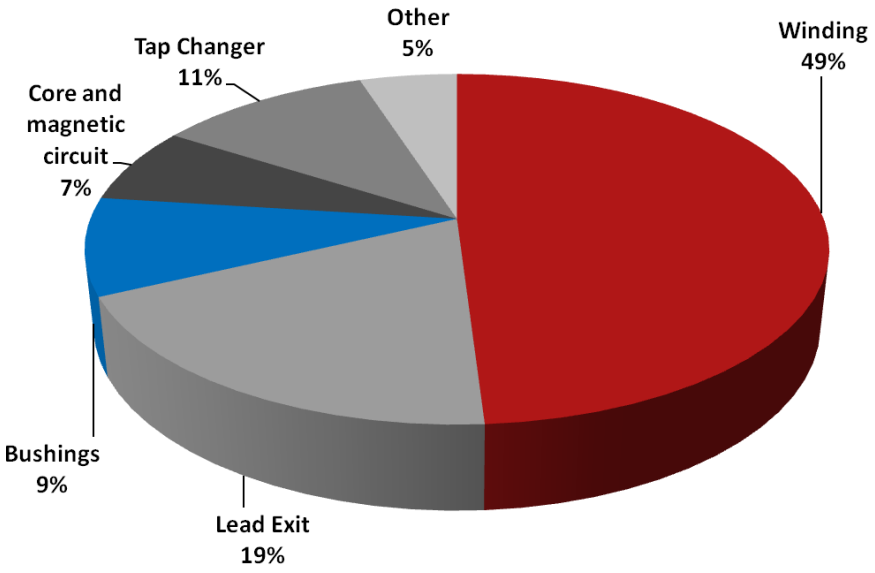

Fig. 6 Faults of Generator Step-up Transformers [5]

From the Fig. 5 and Fig. 6, it is clear that the weakest point in case of power transformer is winding. Increased attention should be also paid to the bushings. Although, tap changers produce relatively high amount of faults as well. Unfortunately, this work does not yet offer more detailed description of failures. Hopefully, this can be expected in upcoming final report which should be carried out by this working group. The core causes of failures can be therefore only estimated at this time. Locations are stated, but the core causes should be specified. Nevertheless, based on experience from generators and GIS, it can be expected that the faults in winding might be caused by partial discharge activity, of course besides other factors like over-heating, mechanical dislocation etc. But it can be certainly assumed that the PD activity is the origin or at least the consequence of major faults in case of winding or bushings. The final step is the breakdown, but before that partial discharges can be observed for sure. It means that PD measurement can bring valuable information about the transformer's condition [6] and can be much more effective and plausible in comparison with other diagnostic techniques which in some cases can be insufficient.

Suitable example of possible misinterpretation of the insulation condition is mentioned in an experiment described in the reviewed literature [7]. Experiment dealt with partial discharge measurement and dissolved gas analysis (DGA) regarding the biodegradable oils and standard mineral oils. Result achieved in this research shows that DGA outcomes are not the same for mineral and biodegradable oils. Specification done for mineral oils cannot

be used for biodegradable oils. It was found that biodegradable oils produce only a limited amount of gases during the PD faults. So in case of biodegradable oils being used in transformers, DGA method might have problems to recognise possible failures. Opposite to that, partial discharge measurement was able to recognise PD faults in both mineral and biodegradable oils.

It seems to be that PD measurement in the case of power transformers is currently a little bit neglected, but this will hopefully change soon. As it has been already shown in case of rotating machines [8] PD measurement can be very useful diagnostic technique and can help to save a lot of funds and prolong the operating lifetime of the device.

2 Basic PD measurement requirements

This chapter shows and describes basics about PD measurement, and in particular the relation to discussed topics. Closer description of PD basics can be found in following literature [33, 35-39, 42]. This work describes the basic measuring circuit and explains and discusses its behaviour. It points out the limits of current PD galvanic measurement technique, where coupling capacitor C_k together with measuring impedance Z are used. And finally it describes the calculation technique of apparent charge Q_{iec} according to IEC 60270.

The aim of this work is not to discuss the fundaments of apparent charge or to discuss equivalent circuit of the PD defect. The up to date discussions related to this topic are opened and outlined in papers from Lemke [40, 41]. In fact the problem where the PD defect cannot be represented by capacitance as was previously presented by Gemant and Philippoff is described, but it should be defined as dipole model as Pederson and his co-workers proposed in past. Prof. Lemke continues in this idea and offers new and relevant demonstrations to proof this theory. This work takes the whole test object into consideration like a unit.

2.1 Measuring circuit according to IEC 60270

The PD high frequency current pulses should be de-coupled in suitable way from the measuring test circuit. There can be many variations of a PD test circuit. This chapter deals only with the global galvanic PD measurement method according to IEC 60270. Three basic measurement test circuits can be found in the literature [9 and 35-39].

- Measuring impedance Z_m is in series with coupling capacitor C_k
- Measuring impedance Z_m is in series with specimen C_t
- Measuring test set-up with balanced (bridge) circuit

There are more possible variants which can be derived from those three basic test set-ups.

Only the basic and the most widespread PD measuring test circuits, where the measuring impedance Z_m is in series with coupling capacitor C_k (see Fig. 7) will be described for the purposes of this work.

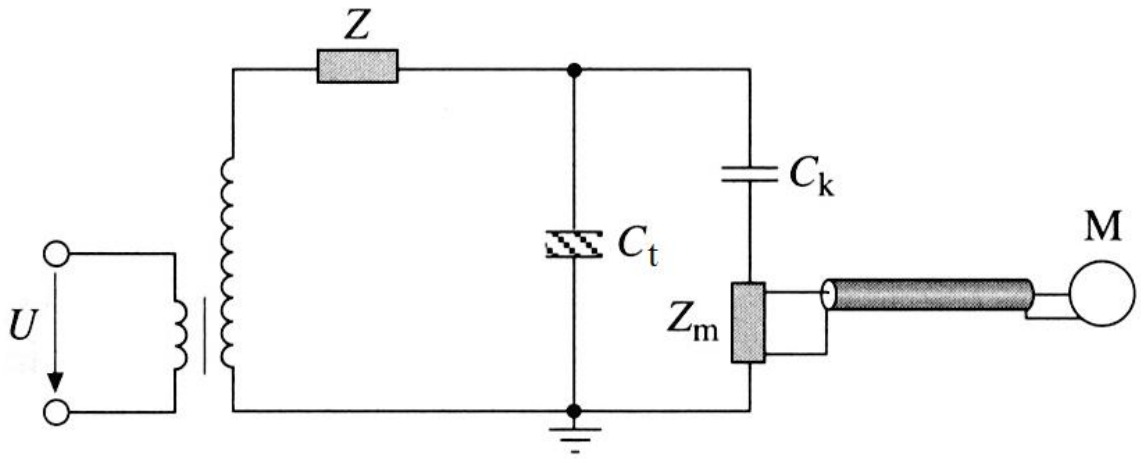

U - High voltage power supply
Z - Filter
C_t - Test object
C_k - Coupling capacitor
Z_m - Measuring impedance
M - Measuring device

Fig. 7 Basic PD measurement test circuit [35]

The measuring circuit contains a high voltage power supply which should be PD free and with a sufficiently low level of internal noise. Filter Z is usually connected on the output of power supply to block possible disturbances from the power source and also to prevent leakage of PD current pulses through the power source. The filter has usually inductive character and its values are in range of mH. Test object C_t should be grounded in this test arrangement. Since the PD measurement is usually focused on insulation of the tested device, character of the load is mainly capacitive and hence the DUT (Device Under the Test) can be characterised as the capacitor for easier understanding. The coupling capacitor

fulfils the function of a de-coupling unit. It should cover the voltage drop caused by the PD event. This voltage drop is read by the measuring impedance and transferred to the current impulse, or in other words the charge which is induced by the original PD event.

According to the standard IEC 60270 PD measurement should be done in flat area of the frequency response curve. A signal drop should not be more then - 3 dB (- 6 dB respectively), see Fig. 8 . Frequency f_1 is given by High Pass (HP) filter and frequency f_2 is given by Low Pass (LP). The above mentioned international standard states that PD measurement should be done in frequency range 30 kHz < f_1 < 100 kHz,f_2 < 500 kHz, 100 kHz < Δf < 400 kHz. In general the frequency range 100 kHz - 500 kHz is used. This frequency range has been most probably chosen based on empirical experience since most of the PD pulses have more or less flat frequency behaviour in this range. The frequency range and maximum defined bandwidth have significant impact on the pulse shape and in general on the PD measurement and recognition. Those impacts should be defined and taken into account.

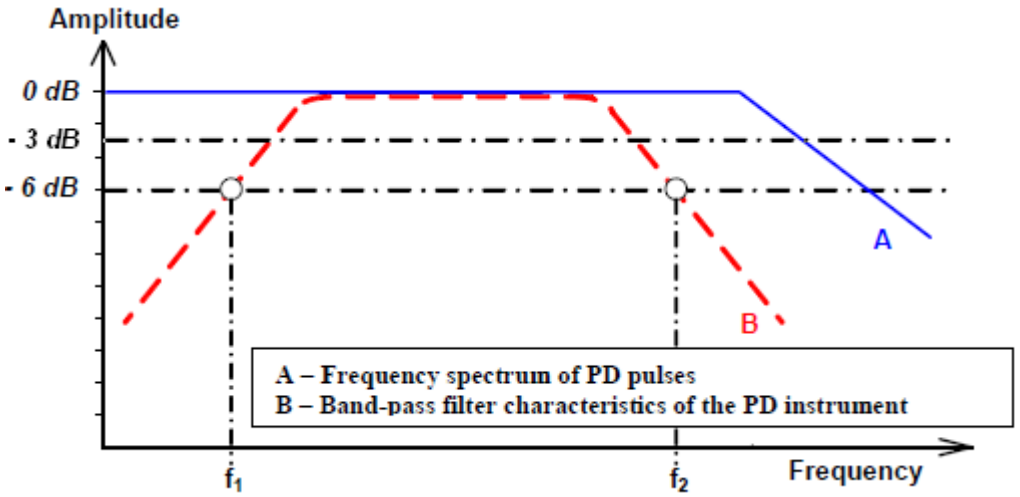

Fig. 8 Frequency characteristics of PD pulse and measuring circuit (schematically)

Pulse behaviour (such as e.g. shape and polarity) is given by many aspects. Dominant aspects are mentioned below.

a) Applied voltage polarity (AC)
b) Transfer function between the point of PD origin and point of PD reading
c) Measuring impedance Z and coupling capacitor C_k makes HP filter (but only 1st order and hence the attenuation is not so dramatic), but at the same time RC of measuring impedance and coupling capacitor constant influence on the duration of a

PD pulse. Higher C_k means longer duration of PD pulse and hence lower cut-off frequency in frequency- domain

d) Detector filter settings (even within IEC range the pulse shape and polarity might be influenced)
e) Location of measuring impendence (in series with test object or in series with C_k)
f) Type of PD source

2.2 Definition of apparent and measurable charge

This chapter is based on literature [37, 38]. In general it can be stated that coupling capacitor C_k should be much higher than capacitance of test object C_t since the charge delivered from coupling capacitor C_k is the highest and hence measurable charge is equal to charge caused by the PD event. This charge compensates the voltage drop caused by local breakdown at the test object side.

The theoretical assumption that $C_k >> C_t$ can be hardly fulfilled in practise since the large C_k would be too big of a load for the power source, and from the economical point of view this would be rather ineffective and expensive solution. It means that if the coupling capacitor is only slightly higher than the capacitance of the test object, the ratio between measurable charge and charge caused by the PD fault is reduced because the compensating current *i(t)* is lower. It should be mentioned that the correctness of measured charge is not influenced by this effect thanks to the calibration process, see e.g. chapter 8 in literature [37]. The Signal to Noise Ratio on the other hand is influenced and therefore even the measuring sensitivity and possibility to detect lower values of partial discharge activity. When the charge transfer between C_t and C_k is taken into consideration the following formula can be written

$$Q = C_t \times \Delta U_t = (C_t + C_k) \times \Delta U_t' \quad (1)$$

$\Delta U_t'$ is the residual voltage drop after the charge transfer. The measured charge Q_m can be obtained at the coupling capacitor C_k side and it is defined as

$$Q_m = C_k \times \Delta U_t' \quad (2)$$

The ratio of measured to apparent or real charge can be then defined as

$$\frac{Q_m}{Q} = \frac{C_k}{C_t + C_t} \tag{3}$$

Dependence on measured and real (respectively apparent) charge ratio versus C_t and C_k ratio is demonstrated in the Fig. 9. It can be seen that if the coupling capacitor C_k is 10 times higher than capacity of the test object, the Q_m/Q ratio is 90 percent. When C_k is equal to C_t, the Q_m/Q ratio is only 50 percent. To reach 100 percent reading of the charge caused by PD fault it is necessary to have a ratio of 100:1 (C_k/C_t).

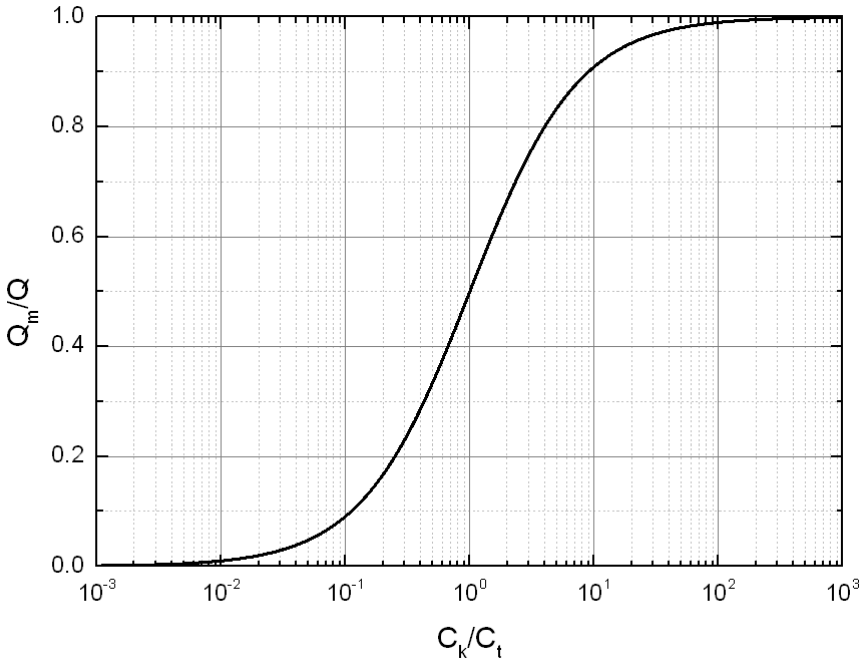

Fig. 9 Q_m/Q dependence on C_k to C_t ratio [37]

Fig. 10 shows a relation between the most typical values of coupling capacitors C_k versus capacities of test objects C_t. It can be concluded that sufficiently big coupling capacitor should be used for sensitive measurement of partial discharges.

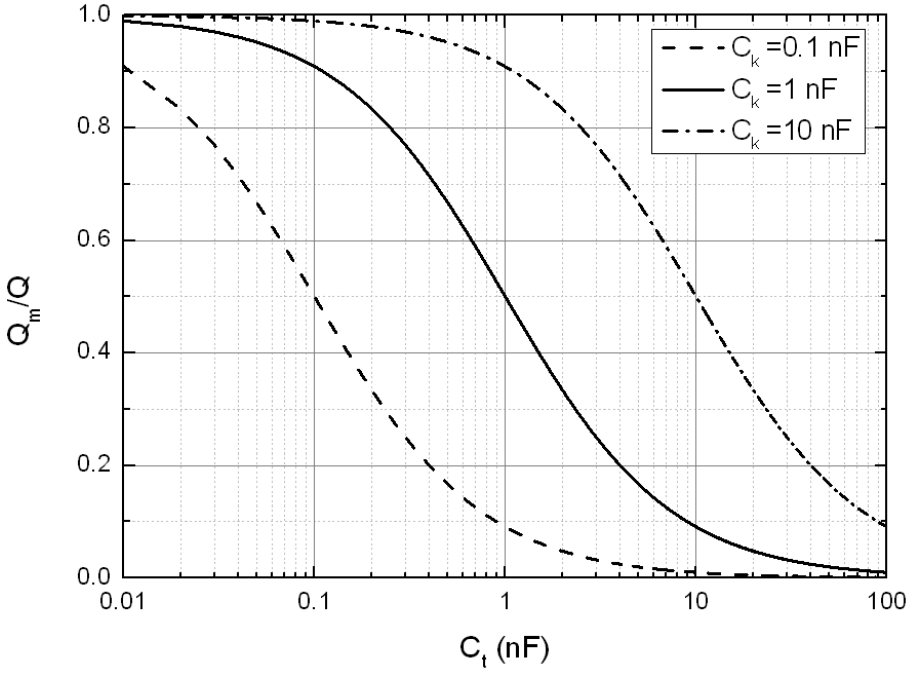

Fig. 10 Q_m/Q dependence on C_t versus various C_k values [37]

2.3 Evaluation of PD activity

There are several evaluation methods for PD measurement. In general the main evaluation PD parameter is apparent charge Q measured according to the IEC 60270 [9]. One of the key evaluation diagrams which helps to distinguish between various PD sources is PRPD diagram/pattern. This chapter describes the main two evaluation tools and adds several additional PD parameters' description.

2.3.1 Apparent charge and another PD quantities definition according to IEC 60270

Concerning conventions and standards (international and in-house) apparent charge Q should be measured. This value is then defined in IEC 60270 [9] as follows.

Chapter 4.3.3 states that it is recommended to record *largest repeatedly occurring PD magnitude, which should be based on digital peak detection by software with very short electrical charging and discharging time constant shorter than 0,44 s*.

It is also required that *the response of the system to a pulse train consisting of equally large equidistant pulses with a known pulse repetition frequency N, shall be such that the reading*

R of the instrument indicates magnitudes as given in Table 1. *The range and gain of the instrument is assumed to be adjusted to read full scale or 100 % for N = 100.*

Table 1: Pulse train response of PD instruments [9]

N (1/s)	1	2	5	10	50	≥ 100
R_{min} (%)	35	55	76	85	94	95
R_{max} (%)	45	65	86	95	104	105

Concerning first recommendation or better to say requirement it can be understood that value of apparent charge Q_{iec} corresponds to the charge peak value of a cluster with the highest number of pulses. Moreover in case that frequency of pulses N is not ≥ 100, value of Q_{iec} is reduced in accordance to Table 1. Regarding information mentioned above, it is clear that gaining of apparent charge Q_{iec} is relatively complicated and its plausibility is rather debatable to say the least. In practise the Q_{iec} value is the peak value of the measured data if the pulse repetition rate is over 100 pulses per second. If not, the apparent charge Q_{iec} value is reduced by a corresponding figure in the given table.

For purposes of this work following two additional PD parameters are mentioned. One of the plausible PD parameters seems to be average discharge current I, which is the integral magnitude calculated as a sum of apparent charge during defined time interval T. [9, 33, 42]

$$I = \frac{1}{T_{ref}}\left[|q_1| + |q_2| + ... + |q_i| + ... + |q_m|\right] \quad \text{(A; s, C)} \tag{4}$$

Provided that all PD current pulses have the same amplitude of apparent charge Q, the equation 4 can be simplified subsequently.

$$I = nq \quad \text{(A; s}^{-1}\text{, C)} \tag{5}$$

Next complementary PD magnitude is discharge power (integral magnitude as well). It is the instantaneous energy of single PD pulses during defined time interval T. [5, 6] In the international standard IEC 60270 [9] determines additional PD parameters.

$$P = \frac{1}{T_{ref}}\sum_{i=1}^{m} q_i u_i \quad \text{(W; s, C, V)} \tag{6}$$

Pulse Repetition Rate N (1/s)

Ratio between the total number of PD pulses in selected time interval and the duration of this certain time interval.

2.3.2 PRPD pattern

One of the most important parameters for PD measurement under the AC stress is so called PRPD (Phase Resolved Partial Discharge) pattern/diagram, sometimes also called fingerprint or ϕ-q-n diagram. In general ϕ-q-n diagram is extended ϕ-q diagram - sometimes called Pulse diagram or Scope diagram, which is a basic evaluation PD diagram, in fact it is an oscilloscopic view, where y axis is the charge and the phase of test voltage is plotted on x axis. PRPD diagram has an apparent charge on its y axis, the phase of the test voltage is displayed on x axis, but there is an added third parameter - repetition rate. The repetition rate is represented by colour points in the diagram, which expresses intensity of partial discharge activity in given position. It depends on the set pallet, but it is customary that red colour represents the highest PD occurrence and black colour to lowest.

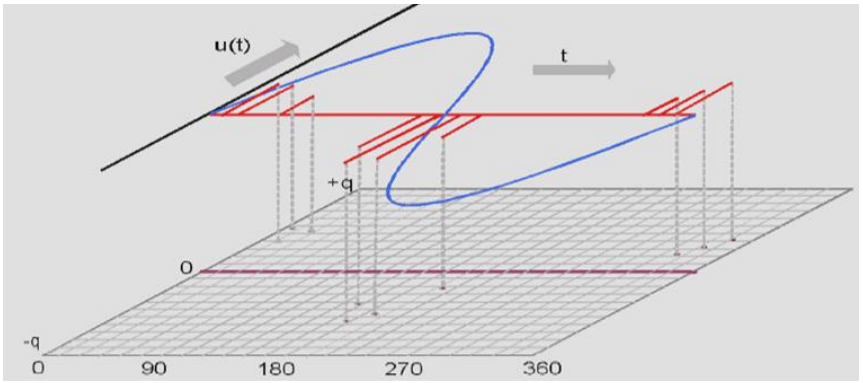

Fig. 11 PRPD pattern construction principle [93]

This diagram offers the new and modern view on PD evaluation. Typical fingerprints or patterns are the output of this diagram. Thanks to these specific patterns it is possible to distinguish between various kinds of PD activity, such as internal PD activity, corona discharges or surface (gliding/creeping) discharges etc. Pattern recognition mostly depends on experience of the operating engineer. No official PD patterns database currently exists and each company which deals with PD has its own database which it mostly protects and does not share completely. Many PRPD patterns can be also found in technical papers and documents. Based on personal experience and technical papers or literature reviewed, each PD expert builds their own PD database. But in general there are some very basic fingerprints which can be recognised easily. For specific examples, see Annex 1.

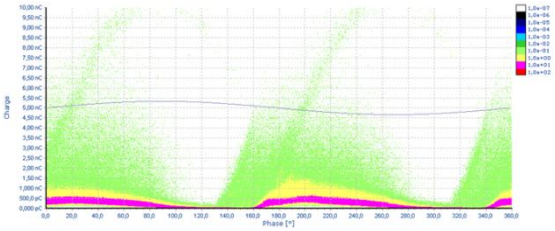

Doble Lemke GmbH - PD Smart

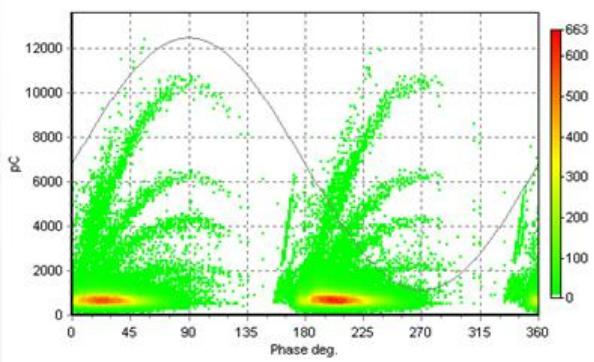

Haefely Hipotronics – Tettex - DDX 9121b

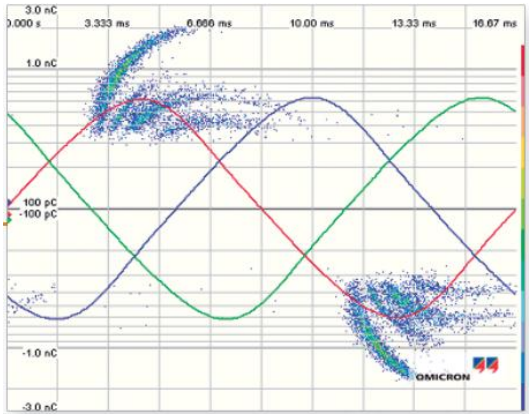

Omicron GmbH – MPD 600 [94]

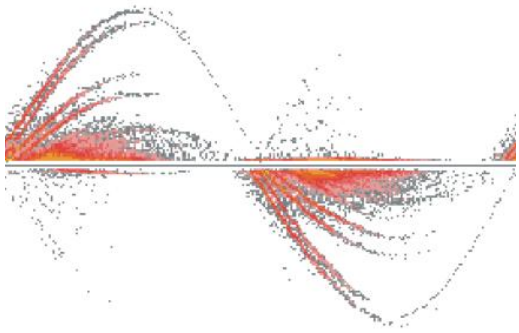

Power Diagnostix – ICM System [95]

Fig. 12 Illustrative examples of PRPD diagram

Limitation of PRPD pattern arises in case of multiple PD sources. In that case single defects can be overlapped and it can be difficult or even impossible to discriminate all single PD faults. For example surface discharges typically have high amplitudes and are defined by symmetrical triangular cluster in both half sinus waves of test voltage. A pattern of corona discharges with generally much lower amplitude can be hidden in the cluster as well as another pattern of for example internal PD or floating potential patterns with various amplitudes, which can also hide or overlap.

For further PD evaluation diagrams, such as Q(t)U(t), Q(U) diagrams and others, see author's publication [49].

2.4 Pulse recognition technique

Pulse recognition technique is the key element and know-how of every partial discharge detector, which is in fact basically a peak detector. Peak detection technique varies for

every single PD detector. What is a common feature for all detectors is the parameter called dead time. This parameter is very important for single PD event recognition and hence for the correct determination of repetition rate. Principle is graphically shown in Fig. 13 – dead time t_d is marked as a yellow coloured area. Peak detection can be done as a trigger to a rising edge, a peak etc.

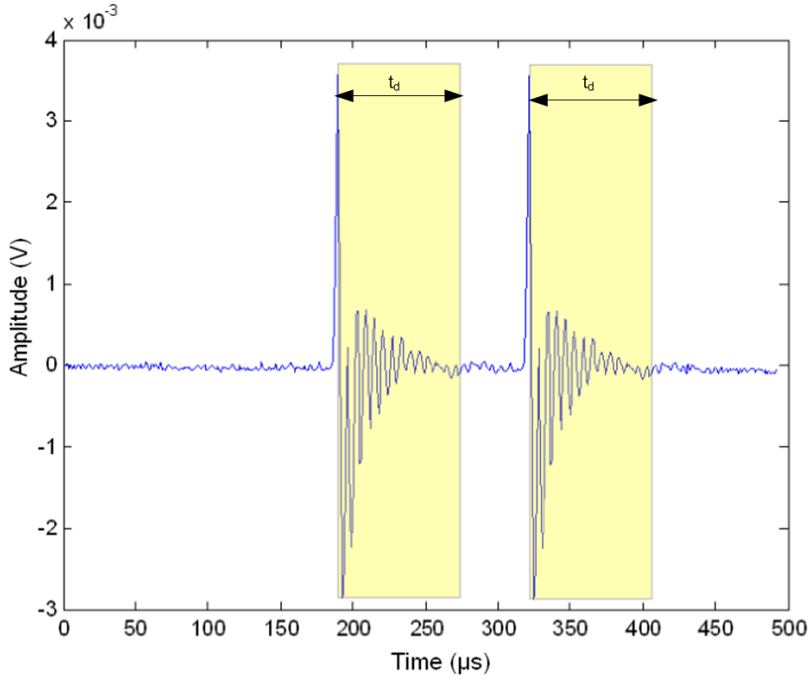

Fig. 13 Principle of dead time t_d function

When peak detection is done, it is necessary to interrupt peak detection for given time – the dead time. This is caused by the oscillation of detected PD pulses. Oscillations are caused by several causes, e.g. travelling path, measuring impedance, frequency bandwidth and range etc. dead time function therefore ensures that one pulse with oscillations will not be detected as several pulses, but as a single pulse. In other words, dead time is the time when no pulses are detected.

It is essential to mentioned that each PD detector has different settings for dead time. Some detectors have floating dead time based on frequency settings of detector, other detectors have a set fixed dead time, and yet another group of detectors enables to set dead time by the users themselves etc. This effect causes various PD repetition rate numbers. For PD measurement under the AC voltage this does not have to be a crucial problem. PD-AC measurement is mainly based on amplitude-phase PD recognition and evaluation – PRPD (Phase Resolved Partial Discharge) diagram or Φ-q-n diagram. But in case of PD measurement under the DC measurement repetition rate plays in many cases an important

role. In literature [69-74] the authors use dependence of repetition rate on time N(t) as an evaluation parameter. In general, the PD-DC measurement currently uses apparent charge on time dependence Q(t). But as additional evaluation parameter some groups suggest to use N(t) dependence instead.
Q(t) dependence can be compared between various PD detectors, since apparent charge is calibrated for capacitive test objects [9, 29], but in case of repetition rate it is not possible to compare values between the various PD detectors as mentioned above.

3 Selected PD measurement requirements for specific electrical devices

From the previous chapter it can be concluded that partial discharges can be substantial source of device's faults and failures. At the same time, PD measurement can help to reveal other sources of potential fails as well, because partial discharges can be also sub-sequences of different failure types and sources (as aging, over-heating, mechanical disproportion and defects etc.).

PD measurement has recently become an accepted diagnostic method in many fields of electrical engineering. The goal of this chapter is to show how the international standards deal with this subject. And after that, to discuss if the definitions or limits defined in standards are suitable, plausible and appropriate.

The following chapter discusses PD measurement conditions and limits for transformers, switchgears/GIS, rotating machines and cables. All of the particular standards are based on the basic international standard IEC 60270:2000, High-voltage test techniques - Partial discharge measurements [9], where the fundamentals and test technique of PD measurement are described and defined.

3.1 Transformers

Transformers can be divided into three main categories – power transformers, distribution transformers and instrument transformers. Power transformers are then divided to substation transformers, which transform high voltage to lower voltage levels, which can still be considered as high voltage levels. Step up transformers are usually located at power plants and convert the voltage from generators to high voltage for transmission lines.

3.1.1 Power transformers

For transformers test there is a standard IEC 60076-3:2000 [10]. Partial discharge measurements should be performed for transformers with U_m above 72.5 kV to prove that the machine operates within defined partial discharge limits. For transformers which have the highest voltage for equipment under the 72.5 kV the PD test is optional and depends on agreement between the manufacturer and the customer.

PD test is done together with short-duration induced AC withstand tests. The test procedure is clearly defined in the standard. The PD test itself is defined in Fig. 14.

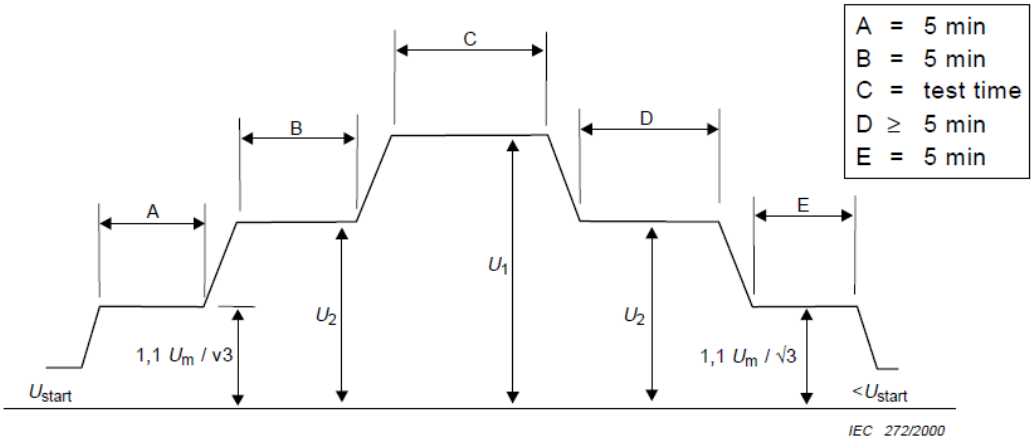

Fig. 14 Test procedure for partial discharge measurement for transformers [10]

Test procedure is following:

- Stage A: increase the test voltage to 1.1 $U_m/\sqrt{3}$ and wait at this level for 5 minutes. The starting test voltage should not be higher than $U_2/3$
- Stage B: Increase the test voltage to U_2 and wait at this voltage level 5 minutes
- Stage C: Increase the test voltage to U_1 and wait for defined time period, which is specified in standard and depends on test and rated frequency.
- Stage D: Afterwards decrease the test voltage to U2 again and wait 5 minutes
- Stage E: Decrease the test voltage 1.1 $U_m/\sqrt{3}$ and wait 5 minutes. Finally reduce the applied test voltage below $U_2/3$ and switch test voltage off-

Voltage level U_2 is defined as 1.3 $U_m/\sqrt{3}$ for three phase-to-earth and 1.3 Um for phase-to-phase measurement.

Voltage level U_1 is defined in EIC 60076-:2000, Annex D. It depends on the rated maximum voltage of transformers.

Acceptance test limits from PD point of view are following:

- At stage B and D the apparent charge cannot exceed the limit 300 pC
- At stage A and E the apparent charge cannot exceed the limit 100 pC
- Partial discharge activity cannot have increasing time trend in any of the stages

3.1.2 Instrument transformers

Partial discharge measurement on instrument transformers is defined in IEC 60044, which is divided into 8 parts. Each part deals with different type of instrument transformers. Nevertheless the recommendation for PD measurement and limits are mostly the same, in general there are differences in test voltage levels. Following information is for Current transformers [11]. Currently the family of IEC 60044 is replaced by IEC 61869:2007, General Requirements for Instrument Transformers.
PD measurement is required for current transformers which operate above 7.2 kV. The limits differ for different earthing of the system. The second parameter is the type of insulation - immersed in liquid or solid insulation.

For earthed neutral system there are two voltage test levels with two PD levels. PD limit is defined by concrete value of apparent charge here.

Insulation - immersed in liquid	Solid insulation
$U_{test} = U_m$, $Q_{iec} = 10$ pC	$U_{test} = U_m$, $Q_{iec} = 50$ pC
$U_{test} = 1.2\ U_m/\sqrt{3}$, $Q_{iec} = 5$ pC	$U_{test} = 1.2\ U_m/\sqrt{3}$, $Q_{iec} = 20$ pC

Background noise level should be below 5 pC.

Standard allows changing the frequency range against the IEC 60270. Low Pass can be set up to 1.2 MHz for wide-band measuring devices (nowadays major technique). The bandwidth should be at least 100 kHz. The maximum value is not stated so it can be only assumed that it should be set according the IEC 60270.

3.2 Switchgears and GIS

In case of middle-voltage switchgears there is no international standard that would define partial discharge measurement. However PD measurements are performed. Mostly according to limits which are done by factory tests defined by utilities, customers etc. Test procedures are mostly based on voltage progress and apparent charge limits at given voltage levels. In the case of MV switchgears limits are mostly from 20 pC to 50 pC on given voltage levels. [14]

For HV switchgears which are mostly constructed as Gas-Insulated Switchgears (GIS), an international standard IEC 62271-203:2011 is available [13]. Partial discharge measurement should be performed after pre-stress voltage is applied for 1 minute. The level is given by the standard and differs according to the operating voltage of the device. The voltage is then decreased to the PD test voltage. This level is different for system with solidly earthed neutral ($U_{test} = 1.2\ U_n/\sqrt{3}$) and without solidly earthed neutral ($U_{test} = 1.2\ U_n$). The maximum acceptance of a PD level is defined by the value of apparent charge and it is 5 pC. This limit is for a complete system, including all sub-assemblies which are installed in the system. However some exceptions can be quoted. The exception is for sub-assemblies containing other components which have a different defined acceptance level for PD. In this case the acceptance level for the whole system is 10 pC. If the components are rated for higher PD activity they should be tested separately.

3.3 Rotating machines

The main two documents for partial discharge measurements on rotating machines are IEEE Trial-Use Guide to the Measurement of Partial Discharges in Rotating Machinery [15] and IEC 60034-27:2006 [16].

The PD measurement on rotating machines is well and thoroughly specified in the international standard IEC 60034-27:2006. Performance check is intrinsically important, and it should include the test of a background noise level, which should not exceed 100 pC. This test should be done on the entire measurement circuit. The test object should be replaced by relevant PD free capacitor; if the capacitor is not available the test can be performed with no load as well. Test should follow the complete voltage range as the real

test is then performed. Typical test procedure can be seen in Fig. 15. It is the so-called gradual stepped power-up test.

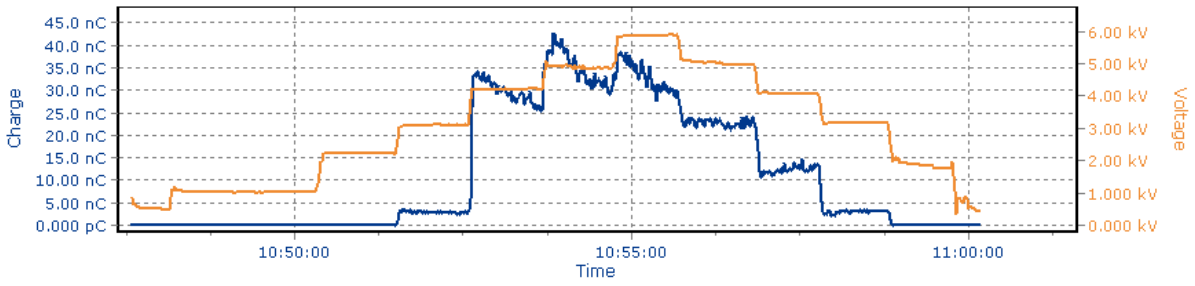

Fig. 15 Test procedure for partial discharge measurement on rotating machines

The partial voltage steps are rated as 20 percent of maximum test voltage steps. Maximum test voltage can be chosen from 3 variants [16]:

$U_1 = U_n/\sqrt{3}$, or operating (line-to-ground) voltage of the insulation system

$U_2 = 1.2\ U_n/\sqrt{3}$, or 120 % of operating (line-to-ground) voltage of the insulation system

$U_3 = U_n$, or rated line to line voltage of the insulation system

PD parameters (such as apparent charge, pulse repetition rate, etc.) should be recorded at each voltage step as defined in the standard and the Phase Resolved Partial Discharge (PRPD) diagram, so called fingerprints ought to be recorded as well.

Limits in the meaning of apparent charge levels are also not defined in any standard. Evaluation in case of rotating machines is a more complex procedure based on several aspects, such as the number of measured PD magnitudes, PRPD pattern etc. Condition of the background environment is important for the evaluation.

The apparent charge limits with a rather informative character also exist and help the evaluation [14]. Based on this evaluation DUT can be divided into three groups

- Class A - up to 5000 pC – normal behaviour but pattern needs to be considered
- Class B - from 5000 - 15 nC – still acceptable, trending and pattern analysis
- Class C - starting from 15 nC – trending and monitoring intervals needs to be set or increased

Note: Class A, B, C –the pattern needs to be always analysed and the insulation design to be considered. Machine comparison is always recommended. Offline and online tests cannot be compared.

3.4 Cables

Partial discharge tests on cables are defined by following two basic standards:

- IEC 60885-2:1987, Electrical test methods for electric cables – Part 2: Partial discharge tests [17].
- IEC 60885-3:1988, Electrical test methods for electric cables – Part 3: Test methods for partial discharge measurements on lengths of extruded power cables. [18]

Based on these two standards, many others standards are derived, upon which the tests for particular voltage ranges for cables are defined. For example:

- IEC 60502-2:1998, Power cables with extruded insulation and their accessories for rated voltages from 1 kV (U_m = 1,2 kV) up to 30 kV (U_m = 36 kV) – Part 2: Cables for rated voltages from 6 kV (U_m = 7,2 kV) up to 30 kV (U_m = 36 kV) [19]
- IEC 60840:1999, Power cables with extruded insulation and their accessories for rated voltages above 30 kV (U_m = 36 kV) up to 150 kV (U_m = 170 kV) – Test methods and requirements [20]
- IEC 62067:2001, Power cables with extruded insulation and their accessories for rated voltages above 150 kV (U_m = 170 kV) up to 500 kV (U_m = 550 kV) – Test methods and requirements [21]

Partial discharge measurements defined in these standards do not differ too much. The main and practically the only evaluated parameter is apparent charge, measured according to IEC 60270, with the only thing which slightly differs being the voltage test level. For example the extract from PD test performance definition in IEC 62067:2001 says following:

Chapter 9: Routine tests on cables and cable accessories - cables and the main insulation of prefabricated cable accessories.

Partial discharge test should be performed according to IEC 60885-3, but the background noise level should be 5 pC or lower. Test voltage should be increased gradually. A 10 second ramp should be present at the voltage level 1.75 U_0 (U_0 is nominal voltage) after which the voltage should be decreased down to 1.5 U_o. The apparent charge of partial discharges should not exceed 10 pC at test voltage level 1.5 U_0.

Chapter 11: Type tests on cable systems, cable and accessories

Test procedure is the same as in previous case, but the limits are stricter. Background noise level should not exceed 2 pC and the maximum accepted level of apparent charge at 1.5 U_0 is 5 pC.
Limits are common for all kinds of cables, such as PE, HDPE, EPR or XLPE cables as can be seen in chapter 13.2, Table 2.

3.5 Conclusion

Chapter 2 gave a basic and brief overview about the state of the art of partial discharge measurement. The main goal of that chapter was to find out how the PD activity is evaluated and which parameters and procedures are used and standardised. It can be concluded that in the majority of cases there is only one evaluation parameter – apparent charge, measured according to international standard IEC 60270, so called Q_{iec} value. The only exception is the PD measurement on rotating machines, where the PD evaluation is a more complex method and there are no fixed apparent charge limits in the standards.

4 Goals

1. New methodology of partial discharge recording and analysis

According to current trends and international standards the apparent charge Q measured in compliance with the IEC 60270 becomes the only evaluated parameter in case of electrical devices, such as transformers, gas insulated switchgears or cables. In case of rotating machines this parameter is a major one, but there is a recommendation to do further PD observations. Practical experience shows that this attitude is rather insufficient. It is therefore desirable to review the plausibility of Q_{iec} parameter in certain cases. The goal is to design plausible, easy to perform and robust methodology for PD measurement.

2. Analysis of time- and frequency- domain of partial discharge activity

Phase Resolved Partial Discharge diagram (so called PRPD pattern/diagram or fingerprint) is a key evaluation diagram for PD source recognition. Nevertheless the PRPD pattern

provides significant limits in case of multiple PD sources, where single PD sources can be overlapped or hidden by each other. The goal is to provide possible solutions for multiple PD sources recognition in time- and frequency- domain. The issue of time- and frequency domain is closely connected to IEC 60270 frequency range and bandwidth limitations in the meaning of influences to the PD recognition technique.

3. Evaluation of measurement issues of test objects with winding

There is a direct relation between capacity of a test object C_t and capacity of coupling capacitor C_k. Ratio 1:1 seems to be a minimum criterion to reach reasonable and sufficient measuring sensitivity for charge measurement. It is therefore necessary to inquire the issue of PD measurement on machines with winding, such as transformers or rotating machines. It is well know that the capacity of rotating machines is in range of 100 nF (medium size machines) up to 1 μF (large hydro generators) and higher. Transporting such a large coupling capacitor on-site as well as feeding the measuring circuit would be rather complicated and expensive. The maximum limit of used coupling capacitors is generally in range 10 to 40 nF. This implies, that due to the very bad C_k:C_t ratio the measuring sensitivity would be so low, that measurement could not be even performed. Last but not least, the goal is to answer and show the possibilities of measuring objects with large capacitances without losing measuring sensitivity.

5 New methodology of partial discharge recording and analysis

This chapter discusses parameter Q_{iec} as the only measured parameter and show its advantages, potential disadvantages and limitations and if possible offer the solutions and hints to make comprehensive partial discharge measurement and consequently evaluation.

In case of apparent charge level Q (pC) measurement, several important parameters are neglected, for example the repetition rate N (1/s), phase position of discharge current pulses etc. Partial discharge measurement is very sensitive and demanding in signal to noise ratio. When only apparent charge visual display unit is used, the information about the PD type is lost. Also distinction between the real PD impulses and noise is not possible.

The noise can have various forms. The most common is the flat character, it means the noise pulses are distributed over the whole sinus period (in case of AC testing) and the

pulses have similar amplitude. But the noise can also have the character of a single pulse or a group of pulses caused by for example switching elements, which are included in the test circuit. When the amplitude of noise pulses is higher than amplitude of the real PD pulses coming from the test object, incorrect reading of the PD activity can be obtained.

If the repetition rate of PD activity is not recorded, the information about the complex energy impact of PD activity is not provided. Hence the incorrect overview and statements about the test object condition can be done.

There is a significant difference of PD activity impact if one pulse with amplitude 3000 pC (it corresponds to the discharge current I = 0.003 μA) or impact of six thousand pulses per second with the apparent charge level 2900 pC (it corresponds to the discharge current I = 17.4 μA) occurs. Well in the IEC 60270 apparent charge Q_{iec} take into consideration the repetition rate as was shown in chapter *3.3 Apparent charge definition according to IEC 60270*. So in the case of one pulse per second and an amplitude 3000 pC, the Q_{iec} value would be reduced to the 40 percent, it means to 1200 pC. But since the repetition rate would be more than 50 per second, the apparent charge level Q_{iec} would be de facto the maximum level of given pulses, which means 3000 pC and the 0.15 μA. Let us have a look at Table 2, where the overview of the information mentioned above is presented.

Table 2: Comparison table of various PD magnitudes

	Case A	Case B	Case C
Q (pC)	3000	2900	3000
N (1/s)	1	6000	50
Q_{iec} (pC)	1200	2900	3000
I (μA)	0.003	17.4	0.15

Table 2 shows how the sole comparison of the apparent charge Q_{iec} can lead to severe misinterpretation of the global PD activity. If the case A and the case B are compared, the apparent charge Q is lower in case B, but at the same time the discharge current is significantly higher and hence the total impact of PD activity to the insulation system of test object is higher as well. More pulses affect higher level of degradation processes. Whether it is the electrical impact (caused by the pulses themselves) or thermal process

(caused by the higher current flow), erosion, or chemical processes. In case C which represents apparent charge according to IEC 60270 Q_{iec}, given manner of repetition rate influence is taken into the account. But all in all it can be concluded that in case B the Q_{iec} value is lower than in case C, but the total impact of PD activity is more than 100 times higher. It means that only the apparent charge Q_{iec} evaluation can lead to incorrect conclusions. This theoretical assumption will be demonstrated on several practical case studies in the following chapters.

5.1 Case study - corona discharges arrangement

Simulation of typical corona discharges was chosen for the basic test measurement arrangement (Fig. 16). Brass needle tip shape was 24 μm before the test voltage was applied (electrical stress) and lower brass circular electrode had a diameter 75 mm, gap distance was 10 mm.

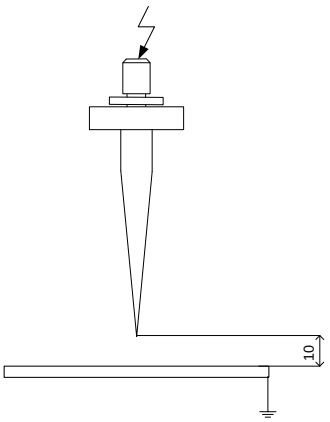

Fig. 16 Corona arrangement – needle – plate

Measurement was performed using a test circuit according to IEC 60270 [9] (Fig. 17). It consists of a 50 Hz- power transformer (0-50 kV), coupling capacitor (C=1000pF), measuring impedance (Z=50Ω) and partial discharge analyser PD SMART (LDIC PD fully digital measuring system (Doble Lemke)). The whole test circuit was located in a shielded test room, where a PD sensitivity of less than 1 pC was reached at a test voltage value up to 30 kV.

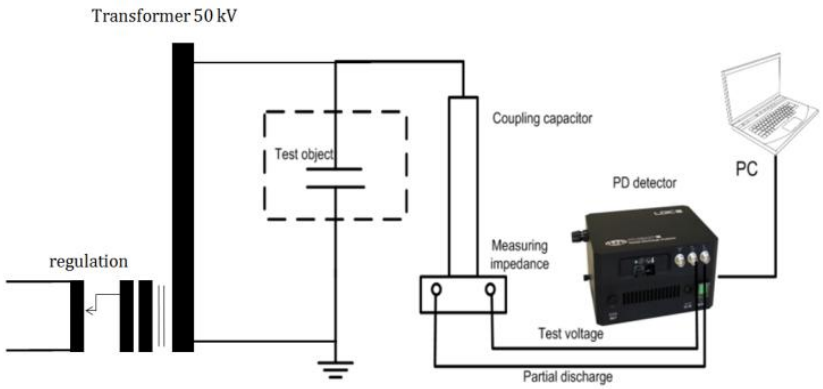

Fig. 17 Test circuit

Measurement results are summarized in Table 3. Values are related to the inception voltage U_i of this test arrangement. Apparent charge Q_{iec} remains more or less the same in both cases. So in case of a charge visual display unit, no significant difference would be registered. Nevertheless if the Φ-q diagram (Fig. 18) is taken into consideration, it can be noticed that there is a difference between the two cases. From Φ-q diagram clearly demonstrates that repetition rate increased noticeably.

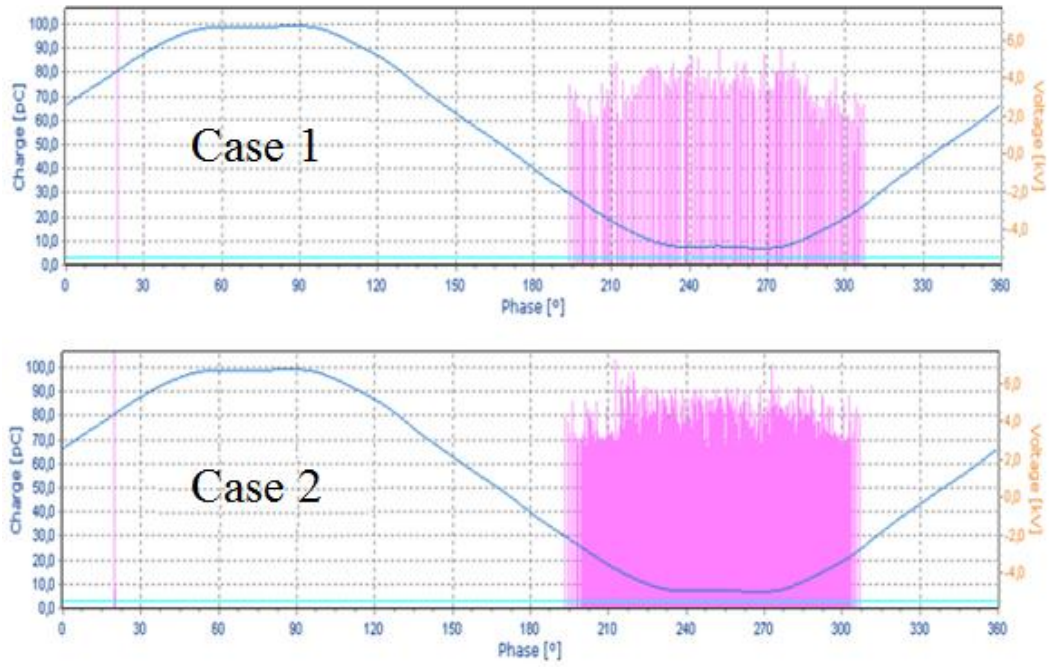

Fig. 18 Φ-q diagram for corona arrangement – two different cases

It is obvious from Table 3 that repetition rate N is more than three times higher in case 2. Discharge current relevantly reacted to this change when the value increased from 600 nA to 2100 nA. This corresponds to more than 3 times higher increment. This is caused by the

self-definition of an apparent charge Q_{iec}, which is in simplified way the maximum value of a measured apparent charge. On the contrary, discharge current takes into account every single PD event and hence calculates with the repetition rate.

Table 3: Comparison table of various PD magnitudes

	Apparent Charge Q_{iec} (pC)	*Repetition Rate N (1/s)*	*Discharge Current I (nA)*
Case 1	103	7000	600
Case 2	107	27000	2100

Further investigation of various corona arrangements (needle-plate, needle-insulated plane and needle-sphere) and limitations of apparent charge Q_{iec} can be found in author's paper [43]. Beside other issues, the paper deals with pulses occurrence during the pre-breakdown stage of corona and apparent charge Q_{iec} as well as a discharge current *I* response. It can be concluded that Q_{iec} values can cause misinterpretation of global PD activity.

5.2 Case study - PD activity in stator winding of rotating machines

Chapter 5.1 presented an experiment comparing corona measurement on basic test arrangement needle-plane. This chapter continues in previous work, but goes further. Results obtained from model experimental measurements can be one thing but different behaviour can also be observed in real electrical devices. Because of that, a following experiment was done on real sample of large rotating machines stator winding.

5.2.1 Test procedure

Measuring circuit was set according to IEC 60270. More details, including circuit diagram can be seen in previous chapter 5.1. Range of input filters was set to HP (High Pass) 100 kHz and LP (Low Pass) 500 kHz according to the standard. Before each measurement calibration was done at 1000 pC.

Measurement was done on real sample of large rotating machines stator winding (see Fig. 19). This model was made by resin-rich technology. Each bar was wedged in winding slot by radial wedges and side wedges. Bars had so called anti-corona protection in form of tapes in slot and end-winding parts. Measurement was done on two identical bars, where very similar results were obtained.

Fig. 19 Tested model of rotating machines stator winding

Concerning conventions and standards (international and in-house) apparent charge Q_{iec} was measured according to IEC 60270. Measuring test procedure was following. First, the inception and extinction voltage was measured ($U_{i/avg}$ = 4.1 kV, $U_{e/avg}$ = 3.7 kV). After that test voltage level was set to nominal voltage of test object ($U_n = 15.75/\sqrt{3} \approx 9\ kV$), where 15 minutes wait time was applied and so called self-extinguished phenomenon was observed. After stabilization of PD activity test voltage was decreased by 1 kV steps up to extinction voltage.

5.2.2 Test results

Experiment results are concluded in Table 4. If apparent charge Q_{iec} is observed it can be assumed that at higher voltage levels partial discharge activity is lower than in case of lower test voltage level. This fact by itself is misleading and confusing. Let us accept hypothetical situation that rotating machine which is measured has nominal voltage 9 kV. Acceptance standard states that new build rotating machine cannot exceed PD activity level of 3.5 nC at nominal voltage. It would mean that machine would be accepted, even though at 4 kV is PD level at 4.35 nC and machine should be therefore at least checked or even rejected.

Table 4: Comparison table of various PD magnitudes

U_{test} [kV]	Q_{iec} [nC]	I [μA]	P [μW]
9	3,17	7,49	3,47
8	3,14	6,07	2,97
7	3,23	4,86	2,40
6	3,66	2,83	2,16
5	4,30	1,07	1,87
4	4,35	0,23	0,82

Fig. 20 shows that average discharge current I (μA) and discharge power P (μW) increased together with test voltage. This also corresponds with PRPD (Phase Resolved Partial Discharge / dependency of apparent charge on phase angle of test voltage with repetition rate parameter) patterns displayed in Fig. 21 - Fig. 24, where it is clear that PD activity increases with applied voltage. Gliding and slot discharges can be observed in the case of two symmetrical triangle-shaped clusters in both test voltage half sinus waves with phase angle from 160° to 300°[58-60], which result in a decline of its activity with decreasing test voltage. Slot discharges are one of the most common degradation effects. An internal PD activity [44-47] represented by so called "rabbit ears" can be recognised from the diagrams.

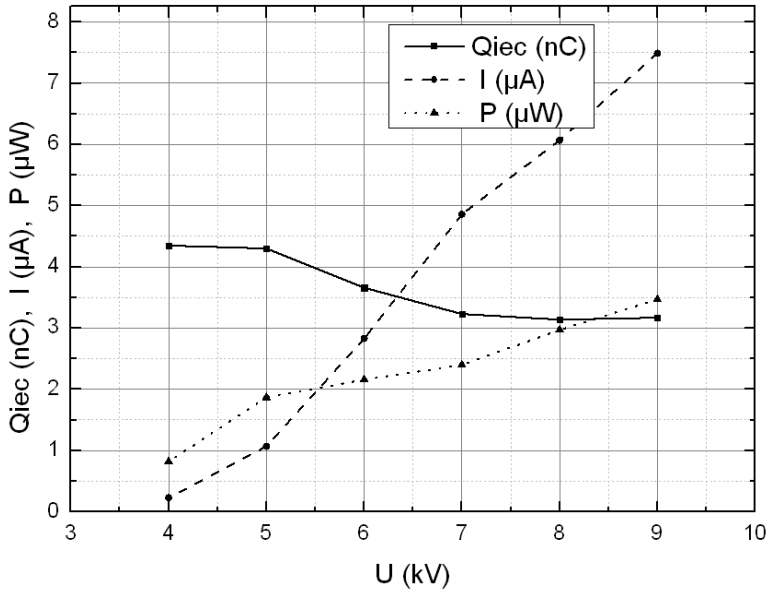

Fig. 20 Graphical comparison of measured PD magnitudes

It is important to notice that Q_{iec} value takes into account internal PD activity in lower test voltage levels, but in voltage level beginning at between 5 and 6 kV repetition level of gliding and slot discharge clusters prevails and Q_{iec} value changes its reading by 1000 pC. It means that at this particular voltage level, gliding and slot discharges are detected only

because of its high repetition rate, and internal discharges are suppressed, because of its lower repetition rate of PD current pulses. But as can be seen in PRPD patterns, the internal PD activity is presented at higher voltage levels as well. This fact cannot be recognised by Q_{iec}. As a result of the magnitude observation, it can be incorrectly concluded that PD activity generally increases with decreasing test voltage. Correct conclusion can be gained by an average discharge current and discharge power evaluation. These two magnitudes calculate with real frequency occurrence of PD pulses in comparison with apparent charge Q_{iec}.

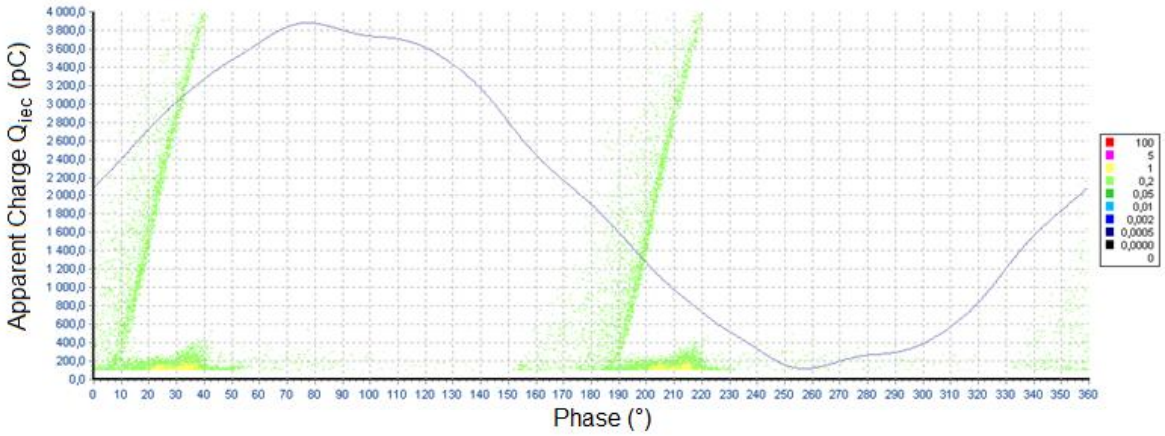

Fig. 21 PRPD pattern, 100-500 kHz (IEC), U_{test} = 4 kV

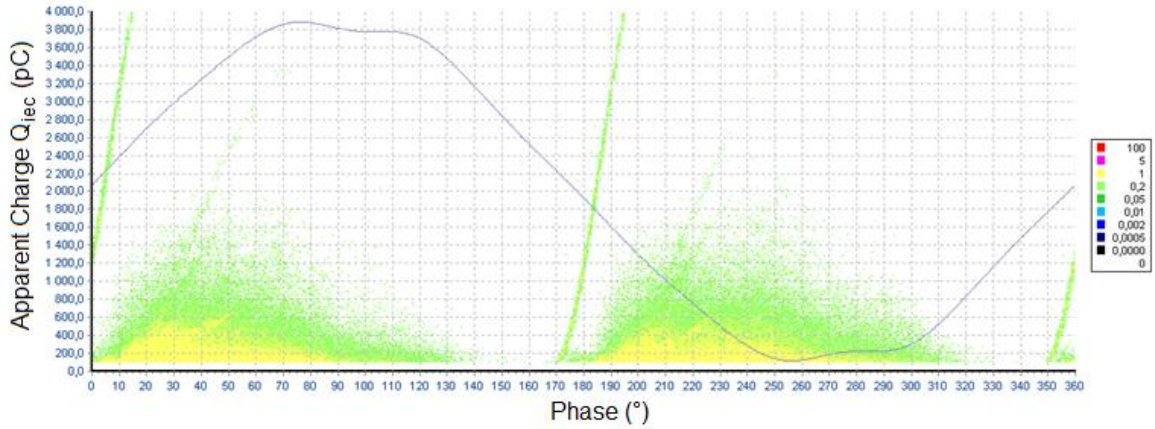

Fig. 22 PRPD pattern, 100-500 kHz (IEC), U_{test} = 5 kV

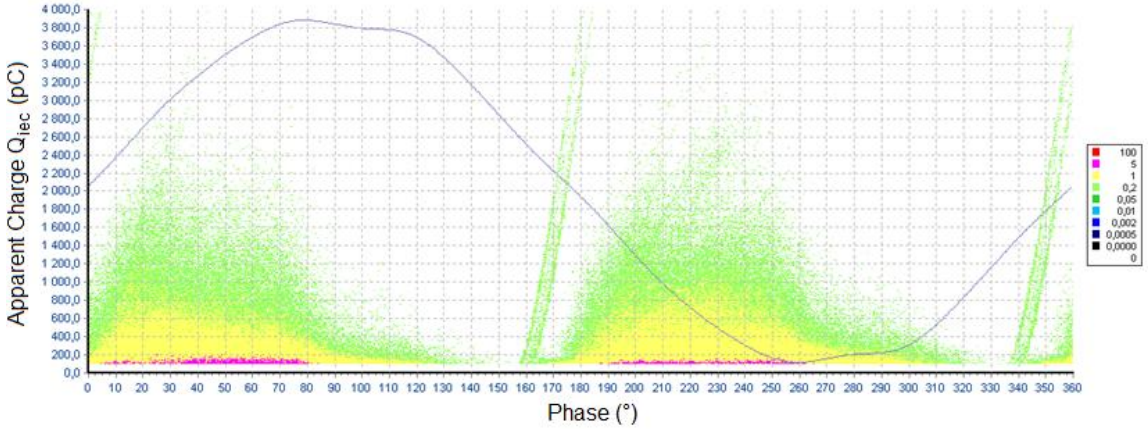

Fig. 23 PRPD pattern, 100-500 kHz (IEC), U_{test} = 6 kV

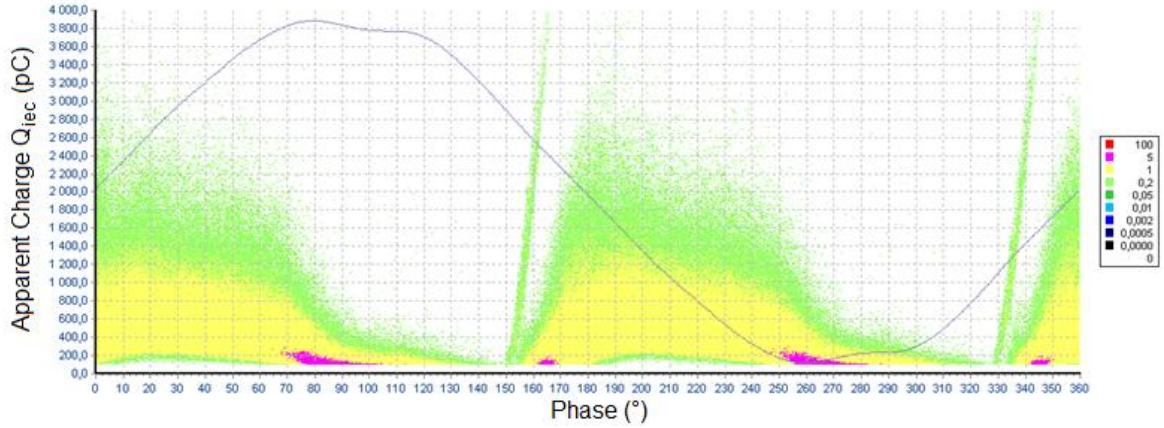

Fig. 24 PRPD pattern, 100-500 kHz (IEC), U_{test} = 9 kV

Similar results were obtained by measurement of a sister bar in the stator winding model. Time dependence of apparent charge Q_{iec} at two voltage levels (4 kV and 8 kV) is shown in Fig. 25. In case of 4 kV voltage the level average Q_{iec} was 4.70 nC. In case of 8 kV it was 4.36 nC. It can be therefore concludes that PD activity is very similar or even identical. But if PRPD patterns in Fig. 26 and Fig. 27 are checked, it is clear that PD activity is definitely not the same and not even similar.

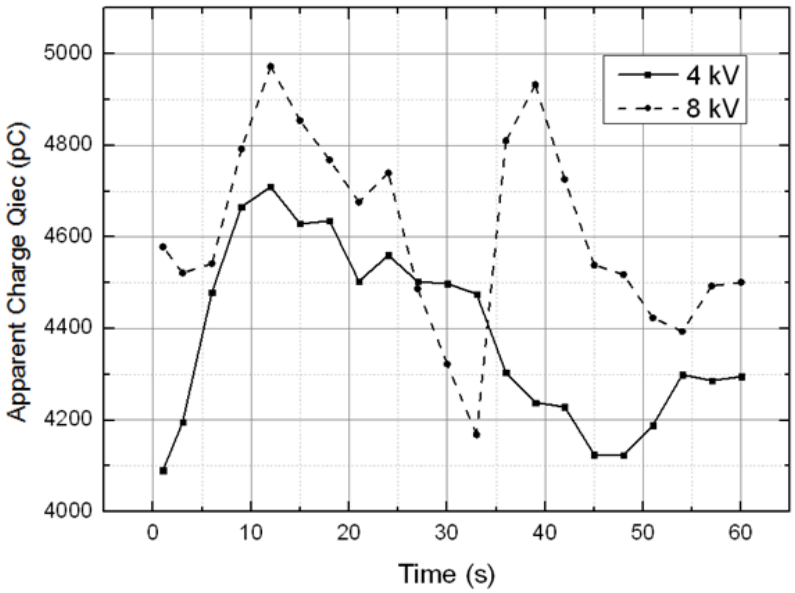

Fig. 25 Q(t)U(t) diagram U_{test} = 4 kV vs. 8 kV

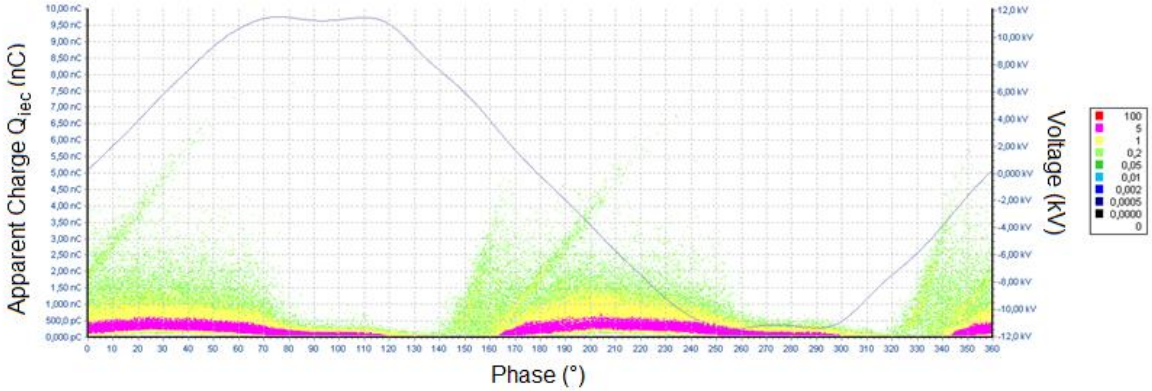

Fig. 26 PRPD pattern, second identical bar, U_{test} = 8 kV

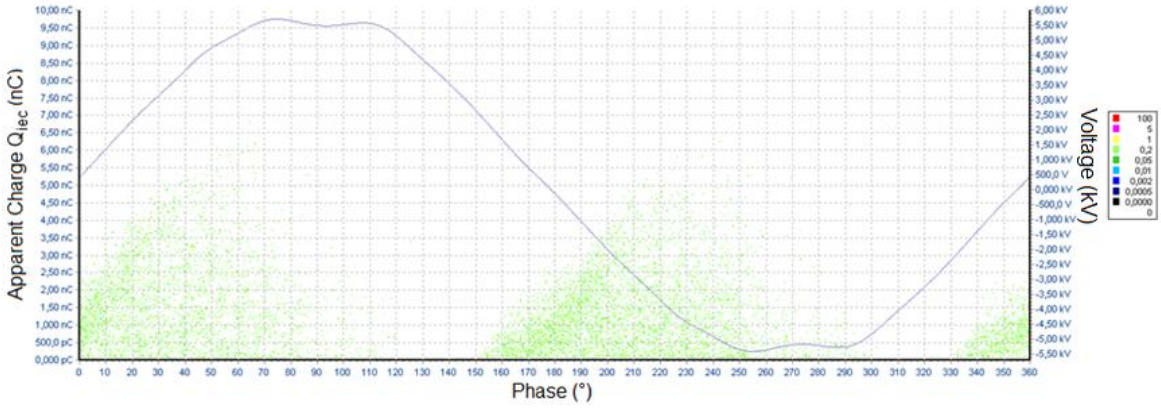

Fig. 27 PRPD pattern, second identical bar, U_{test} = 4 kV

Same assumption can be made by checking the HNQ line diagrams in Fig. 28 and Fig. 29. HNQ line diagram displays the rate (1/s) of each partial discharge pulse in dependency on its actual apparent charge level. Scaling of the x axis is the same in both cases, but difference is in the y axis, where there is a significant difference in the event rate. In case of 8kV there is a 100 times higher rate of partial discharge activity along the whole apparent charge range.

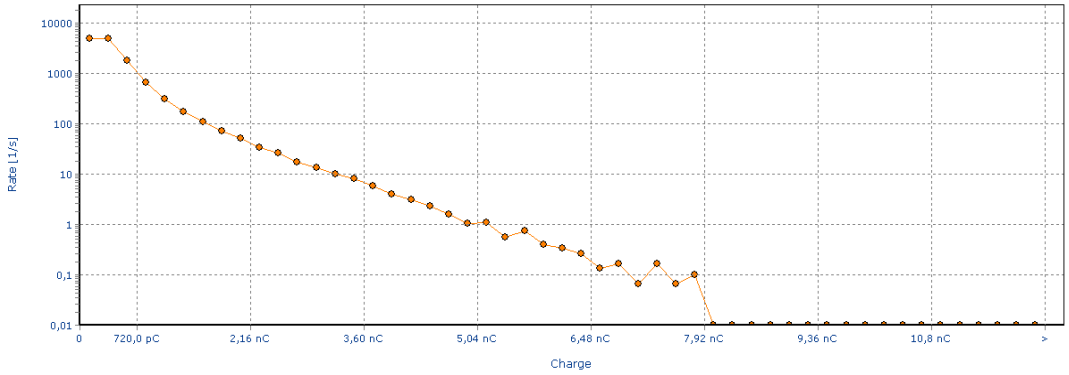

Fig. 28 HNQ line diagram, U_{test} = 8 kV

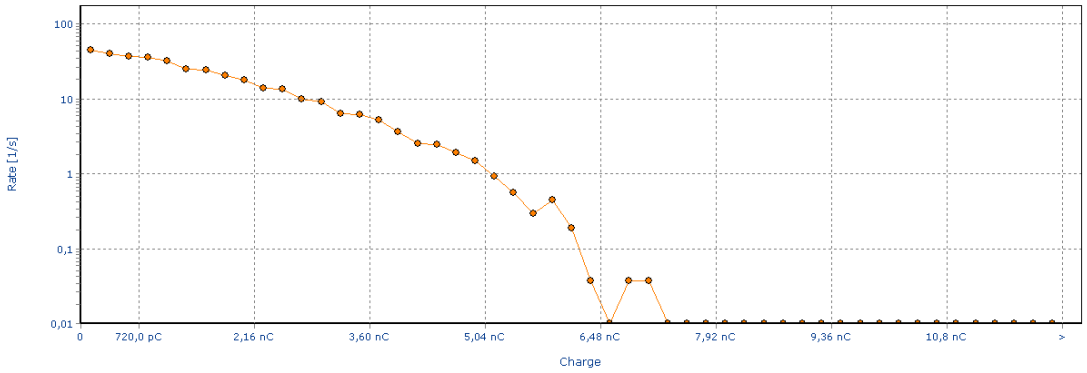

Fig. 29 HNQ line diagram, U_{test} = 4 kV

If average discharge current is taken into account it can be seen that PD activity is assessed correctly. See Fig. 30, where 60s time dependence of discharge current is displayed. Average value is I = 0.49 µA for voltage 4 kV. For 8 kV discharge current increased to I = 5.4 µA (Fig. 31). It means more than 10 times difference in PD activity. In case of evaluation of apparent charge Q_{iec}, PD activity looks more or less the same.

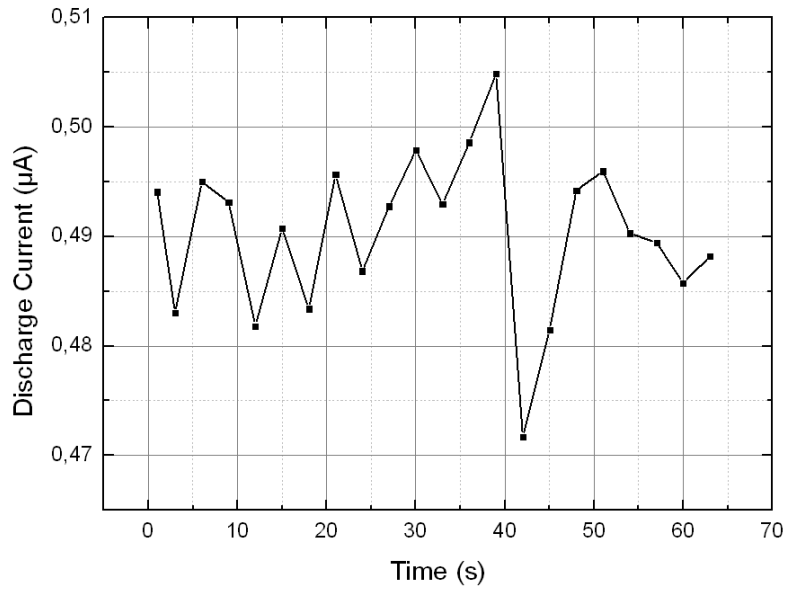

Fig. 30 Discharge current time dependence diagram U_{test} = 4 kV

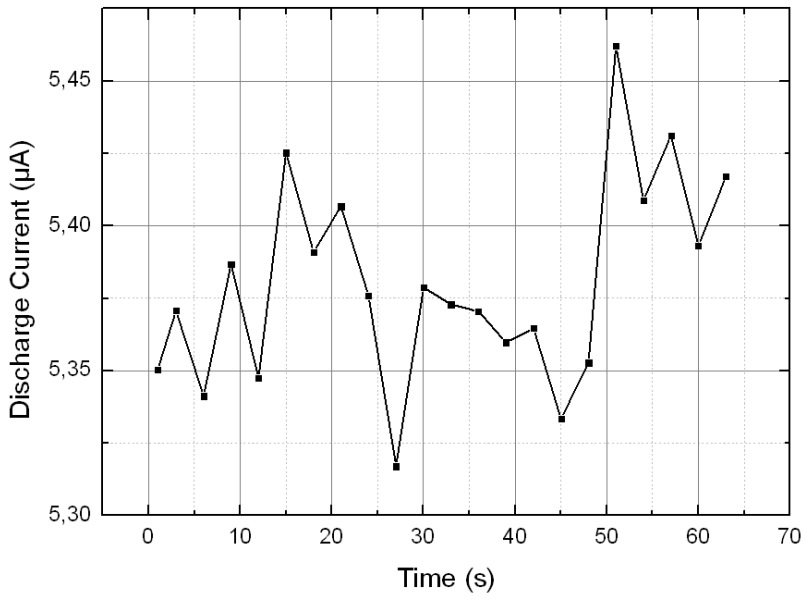

Fig. 31 Discharge current time dependence diagram U_{test} = 8 kV

Regarding results mentioned in this chapter and in continuity to previous experiments, it can be concluded that measurement and evaluation of apparent charge Q_{iec} might be strongly misleading and confusing, and incorrect interpretation of PD measurement can be done. Because of that, it is important to focus on other parameters such as average discharge current *I* or discharge power P, which calculate with repetition rate of single PD events as well. It does not mean that measurement of apparent charge Q should be ignored. The question is the post-processing of this value. Peak values of apparent charge Q might have substantial degradation effect on the dielectric materials, as can be observed in case of

electrical treeing in organic materials, where one short (or small amount) strong energetic current pulse occurs during a long time period. Step by step, this pulse forms a conducting track through the insulating material up to the electrical breakdown and leads to machine failure. Results and assumptions mentioned above were presented at 7th International Scientific Symposium on Electrical Power Engineering, 2013 [64].

5.3 Case study - VT/CT routine test

This describes made-up case of PD measurement event based on experience. Let's assume that there is manufacture of Voltage and Current Transformers (VT and CT). Manufacture makes output routine test to ensure it provides a good quality product, which is also required by costumers, since CTs and VTs play an important role in their systems. In this case, based on experience and international standards, an apparent charge Q_{iec} limit was set at **300 pC** as the operating voltage level. Company used basic PD detector which provides only Q_{iec} value and no another evaluation parameters. For manufactures and even for customers this seems to be sufficient, since in international standard for transformers only provide the apparent charge limits.

Fig. 32 shows a case number 1 – PD activity measurement from January 2013 – Routine test – Device VT_00111. PD detector showed value Q_{iec} = **200 pC**. This fulfilled requirements, which enabled the manufacture to produce the devices without any restraints.

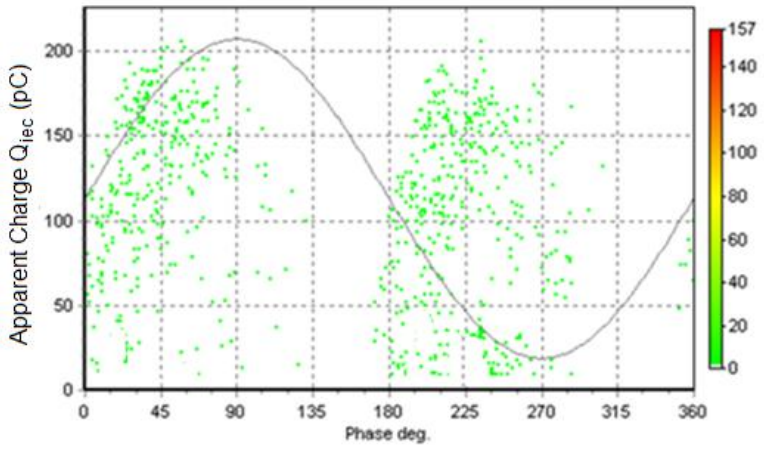

Fig. 32 **Case 1:** Measurement from January 2013 – Routine test – Device VT_00111

In May 2014, several operators changed and a number of new personnel were hired, since production expanded. The sub-supplier of resin was also changed, as a result of better pricing. Routine test which was done in June 2013 did not show any changes. Apparent

charge was still 200 pC – acceptable. Fig. 33 presents a detailed PRPD diagram of this routine, done on a device number 1500. It can be seen, that below the level 200 pC an internal PD activity can be recognised [51-57] – which could be caused by new resin making bubbles during application to the insulation system. Another negative effect could be caused by new operators who did not know or simply did not follow the procedure (timing, precision etc.) correctly. The internal PD activity occurred below the acceptance level, so it seems to be not important.

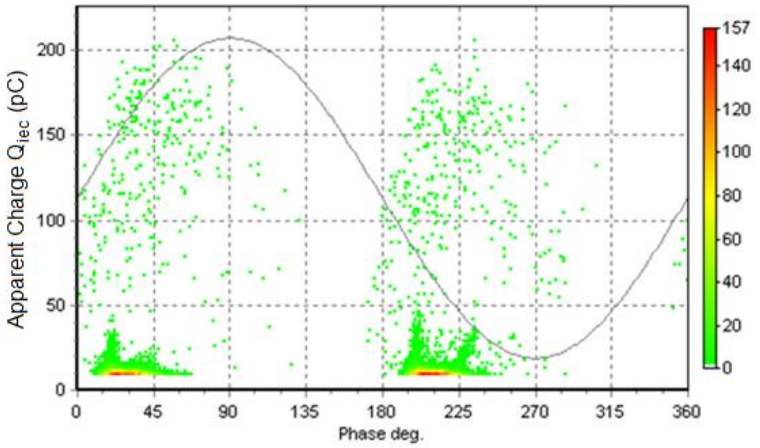

Fig. 33 **Case 2:** Measurement from June 2013 - Routine test – **Device VT_01500**

Fig. 34 shows PD activity of the same device number 1500 as in Fig. 33, but 2 months later. Since resin is an organic material, which is very sensitive to PD activity, air cavities increased their size and also PD activity of internal PD increased, but it is still under the acceptance level 300 pC. Manufacture didn't recognise any problem and produced hundreds and hundreds of new devices.

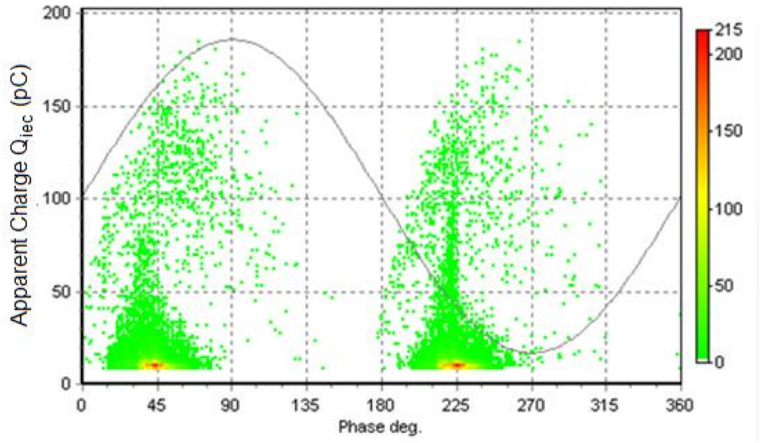

Fig. 34 **Case 3:** Measurement August 2013 - **Device VT_01500**

In November 2013, the internal PD reached a level of 1000 pC, where internal cavities turn into cracks, electrical treeing occurs and single air cavities start to connect together. But manufacture did only the routine test, no monitoring on-site and during routine test nothing was recognised. Year 2013 was concluded as a very good year. Manufacture received many new orders for the next one and sold over 2000 VT and CT units. Unfortunately, in January 2014, electrical treeing and cracks in insulation system reached its limits and breakdown of the first unit occurred. Next units followed on a weekly basis.

Conclusion is that additional parameters such as discharge current (which would increase its value since it calculates with the repetition rate, which obviously increased) or PRPD patterns should be measured and evaluated. The problem could have been recognised in time and company would have saved a lot of money, credibility and its reputation! If possible, online PD monitoring can be also recommended.

5.4 Conclusion and recommendations

This chapter discussed the apparent charge Q_{iec} as the only evaluation parameter. Some practical examples of apparent charge measurement were given, followed by evaluation and discussion of acquired information and given conclusions. The goal of this chapter was not to say whether Q_{iec} parameter is good, bad or even inappropriate, the goal of this chapter was to show possible limitations and offer alternatives and possibilities to perhaps a more complex, but still agreeable, evaluation of PD activity. It can be recommended to record additional parameters, such as discharge current *I*. It is clear and obvious that producers of various electrical devices do not have enough time to do complex, lengthy and hence expensive tests. Based on previous research and evaluation, following test procedure is proposed.

Optimal PD test procedure

1. First voltage test levels and time procedure should be defined – this can be defined by international or internal company standard
2. Then measure PDIV (U_i) and PDEV (U_e) [1], record Q_{iec} and I values for given voltage levels
3. Next step is to measure apparent charge Q_{iec} at given voltage test levels
4. Discharge current I should be recorded for given test voltage levels [2]
5. Also PRPD pattern should be recorded for given test voltage levels [3]

[1] PDIV means Partial Discharge Inception Voltage. PDIV (or U_i (kV)) can be defined as initial voltage when PD detector is able to recognize stable PD current pulses. During PDIV measurement it is necessary continuously increasing test voltage with the constant speed up to the initiation of PD activity. In practise there is a defined background noise level - threshold (depends on the test environment, e.g. in test labs ideally around 1 pC). After that the test voltage linearly increases and at the moment when first stable PD pulses occur, or exceed a given threshold, PDIV is recorded.
PDEV means Partial Discharge Extinction Voltage. It can be also marked as U_e (kV). PDEV is the voltage when no PD current pulses can be recorded. It is also necessary to continuously decrease the test voltage in this case. In practise the test procedure is as follows. When PDIV is reached, test voltage is slightly increased (around 20 % of PDIV) and after that test voltage is linearly decreased until no PD current pulses can be recorded - this voltage level is PDEV. After that it is necessary to decrease applied test voltage (around 20 % of PDEV) and then increase test voltage to reach PDIV again. Based on the field experience this test procedure should be repeated at least five times, to obtain statistically plausible value of PDIV and PDEV.

[2] Discharge current is one of the very important parameters as was shown in chapter 5. It gives global overview about PD activity. Opposite to the apparent charge, discharge current value cannot be compared between various PD detectors, as was explained in 2.3.1 and chapter 2.4. But it can provide valuable information about PD activity behaviour and possible changes. It should have a function as a complementary guarding parameter, which should remain the same if no changes are expected.

[3] PRPD pattern is one of the key elements for PD-AC evaluation. It can help to distinguish between various types of PD activity. For evaluation of this diagram particular experience is necessary and hence it is only an additional parameter, which is evaluated just in case of a non-standardised (problematic) behaviour. It can be recommended to record bipolar PRPD pattern, since better PD source/type can be done. Closer description can be found in chapter 0.

6 Analysis of time- and frequency- domain of partial discharge activity

This chapter shows and discusses new potential benefits and evaluation features of partial discharge behaviour in time- and frequency- domain. Thanks to the PD measurement it is possible to identify that tested device has some problems in insulation system, but in many cases to also recognise which type of failure causes PD activity or where failure is located. This chapter does not discuss the localisation of PD sources, such as reflectometry technique in case of cables [35, 36, 75-78]. Acoustic localisation [35, 79-82] (triangulation) in case of transformers, chokes etc. or particularly topical UHF measurement and localisation [86-91]. In case of rotating machines, various location techniques are used, for example inductive or capacitive sensors [33, 83-85]. This chapter deals with PD fault recognition. Currently in case of PD measurement under AC stress, PRPD pattern (fingerprint) tool is used for PD type discrimination. Thanks to the PRPD diagram/pattern, it is possible to distinguish between many types of PD sources, such as corona discharges, surface discharges, internal discharges, slot discharges or floating potential discharges. Problem arises when multiple PD sources occur. Patterns in PRPD diagram are then superimposed and it can be complicated or even impossible to distinguish between individual PD sources. In this case time- or frequency- domain based recognition can be helpful and solve this issue. This chapter also discusses the problem of measuring sensitivity of measurement. Chapter 2.2 demonstrated that a coupling capacitor C_k should be used as high as, which brings other limitations that are necessary to be taken into account.

6.1 PD pulse shape characteristic

Shape of the PD pulse is an important or even key parameter. The pulse shape determines behaviour in frequency domain. General opinion exists, saying that the frequency domain behaviour of PD pulse is mainly or exclusively given by the rise time t_r of the pulse, and that rough estimation of cut-off frequency can be done by formula $BW = 0.35 / t_r$ (BW – bandwidth, t_r – rise time) [100]. In fact, both of those assumptions are inaccurate and can lead to erroneous conclusions. Cut-off frequency (which can be defined by - 3 dB or - 6 dB signal drop; in this work is taken - 3 dB signal drop into account) is given not only by the rise time of the pulse, but also by the total pulse duration. Formula mentioned above gives the minimum bandwidth to the pulse shape (mainly rise time, which has usually shortest

time) and could be correctly recorded without any distortion or inaccuracy. It is not related to the cut-off frequency of the pulse at all. This can be clearly seen in Table 5, where pulses with various rise time t_r, fall time t_f and total pulse duration t_t are shown (Fig. 35). Calculations were done in Spice based simulation software LTSpice [93] by default FFT (discuss Fast Fourier Transform) integrated function. Topic of this work is not to discuss FFT itself or various types of possible used windows and FFT calculation. FFT it this work is used as tool only.

Table 5: PD pulse time- and frequency- characteristic

Rise Time t_r (ns)	**Fall Time t_f (ns)**	**t_{on} (ns)**	**Total Pulse Duration t_t (ns)**	**Cut-off frequency f_c (MHz)**
3	25	2	30	19.6
25	3	2	30	19.6
14	14	2	30	21.4
14	44	2	60	10.2
3	55	2	60	9.5
55	3	2	60	9.5

As can be seen in Table 5, cut-off frequency does not depend only or mainly on rise time not even on the fall time (if it is shorter), but it depends on total pulse duration. Needless to say that rise time vs. fall time relation has specific influence to pulse's cut-off frequency.

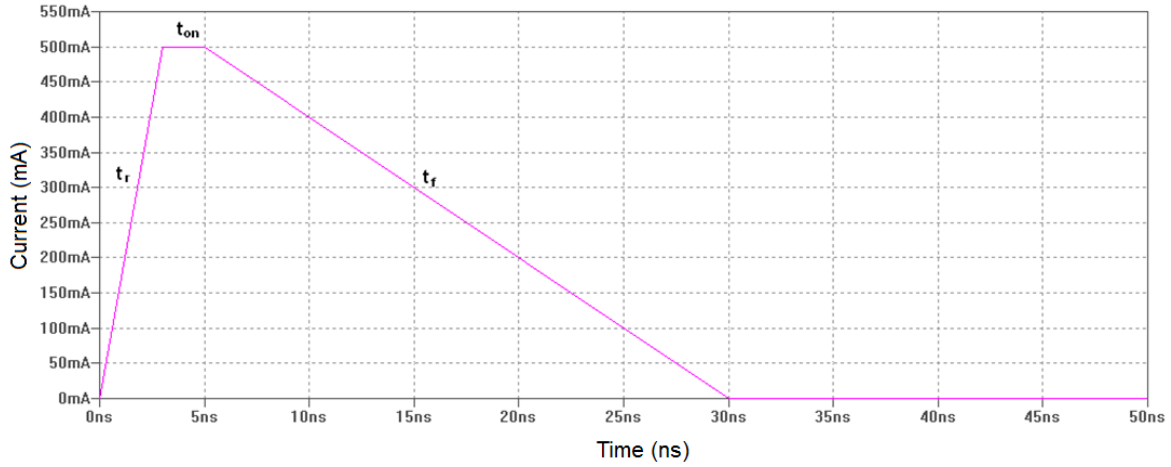

Fig. 35 PD pulse shape description

6.2 Pulse shapes of different PD phenomena

This chapter shows pulse shapes of various, most typical PD phenomena, namely corona, surface (gliding or creeping discharges) and internal discharges. Author of this work has done the measurement on basic test arrangements for above mentioned phenomena. Only a pure resistor 50 Ω in grounding area was connected in the test circuit. Signal from the resistor (measuring quadripole) was connected directly to the 50 Ω input of Agilent Infinity 2.5 GHz, 20 GSa/s oscilloscope. Hence real PD pulses could have been recorded. The goal of this test was to exclude or minimise as many causes influencing the pulse's shape as possible (see chapter 6.1). Travelling path of PD pulses was minimised to approximately 1.5 meter from the point of PD pulses origin. No High Pass filter caused by measuring impedance and coupling capacitor was realised (in fact it is not possible to exclude stray capacitance of test circuit, which can work like coupling capacitor). An ultra wide-band oscilloscope was used to record real pulse shape (not limited bandwidth like it is in case of PD detectors). Identical test arrangements to simulate corona, surface and internal discharges were used, as described in Annex 1.

6.2.1 Corona discharges

Fig. 36 shows oscilloscope screen where corona discharge pulses are recorded. A time window corresponds to one period of 50 Hz AC signal. Negative Trichel pulses in negative half sinus wave and one positive streamer in positive half sinus wave can be observed. Closer description of corona discharge behaviour is included in Annex 1.

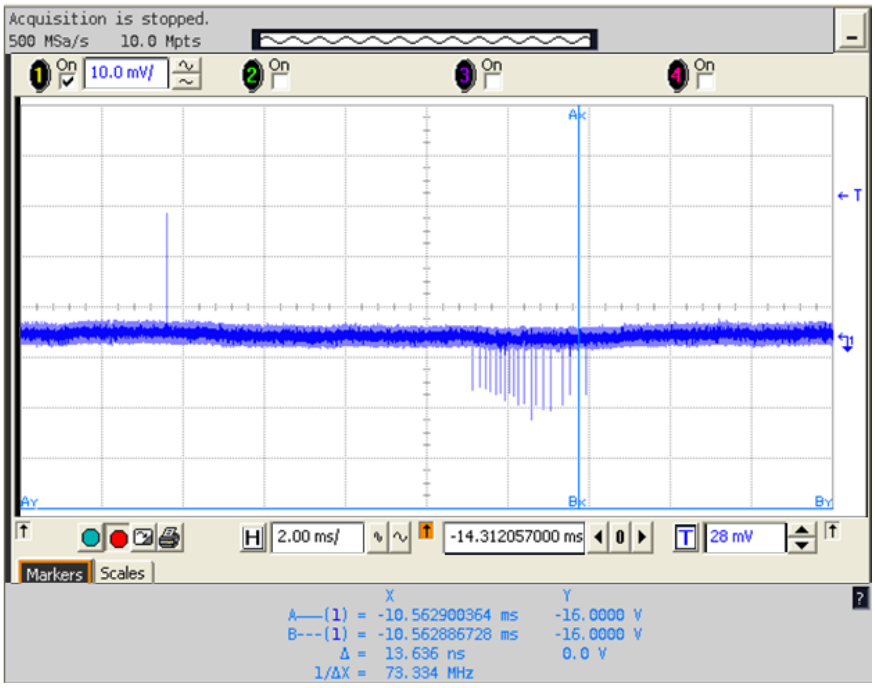

Fig. 36 Corona discharge pulses recorded with Agilent Infinity oscilloscope

Single Trichel corona pulse is displayed in Fig. 37. Typical rise time t_r of Trichel pulse is sharp, in this case $\mathbf{t_r}$ **= 2 ns**. Pulse duration $\mathbf{t_t}$ is approximately **90 ns**. In general Trichel pulses can be defined as very short pulses with very sharp rise time. Corona streamers located in positive half sinus wave have significantly longer rise time and pulse duration.

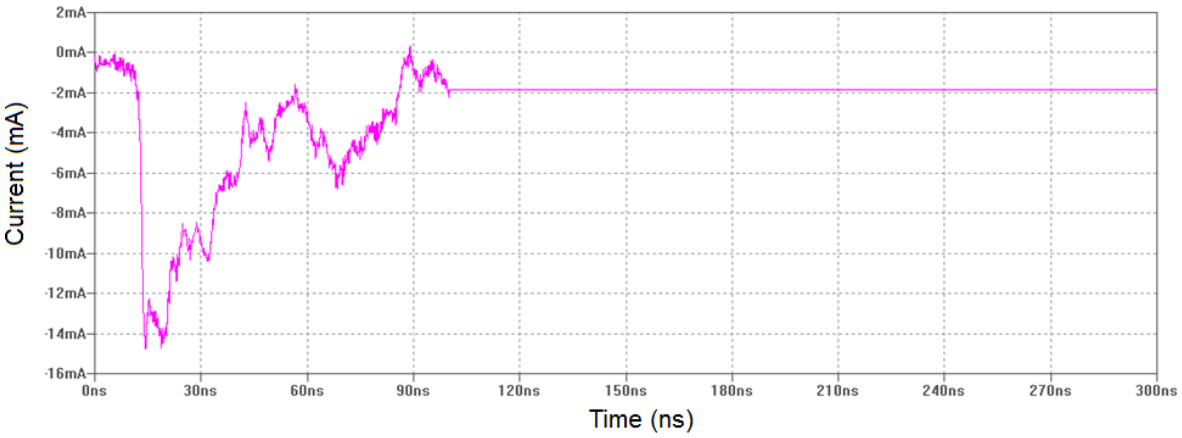

Fig. 37 Corona discharge current pulse

Frequency response (Fig. 38) can be derived based on pulse shape. Cut-off frequency (- 3 dB) in this case is **7.5 MHz**.

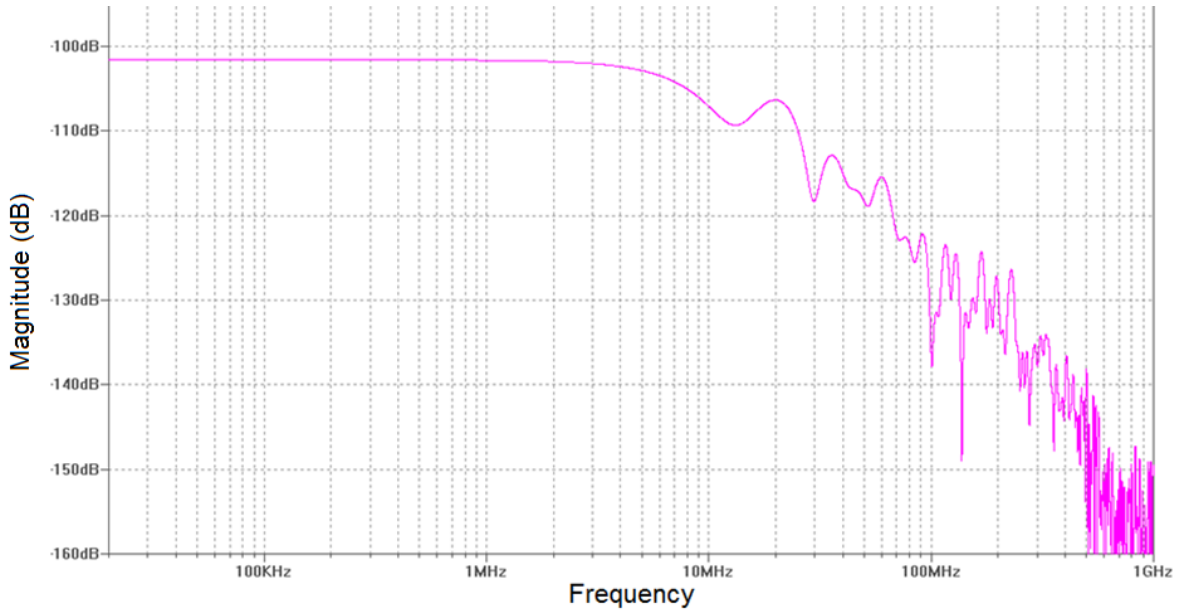

Fig. 38 Corona discharge current pulse in frequency- domain

As mentioned above, pulse shape depends on many factors. Several additional measurements were done with different needle shapes or measuring resistors. Slightly different results were obtained, but the character of the pulse shape remains. Rise time of Trichel pulses was from 2 ns up to 10 ns. Pulse duration was from 30 ns up to 100 ns. It

means that the frequency response was also changing. Maximum reached cut-off frequency was around 10 MHz.

6.2.2 Surface (gliding/creeping) discharges

Fig. 39 shows a single surface discharge pulse. The rise time $\mathbf{t_r}$ is **9 ns**. Pulse duration $\mathbf{t_t}$ is several **hundreds of nanoseconds**. Pulse duration is in this case hard to estimate precisely, since the measuring circuit caused pulse oscillations. In general, it can be assumed that surface discharges have quite fast values of rise times, but long total pulse duration. Also the amplitude of the surface pulses is significantly high. This is caused by the relatively high energy which is connected with surface discharges.

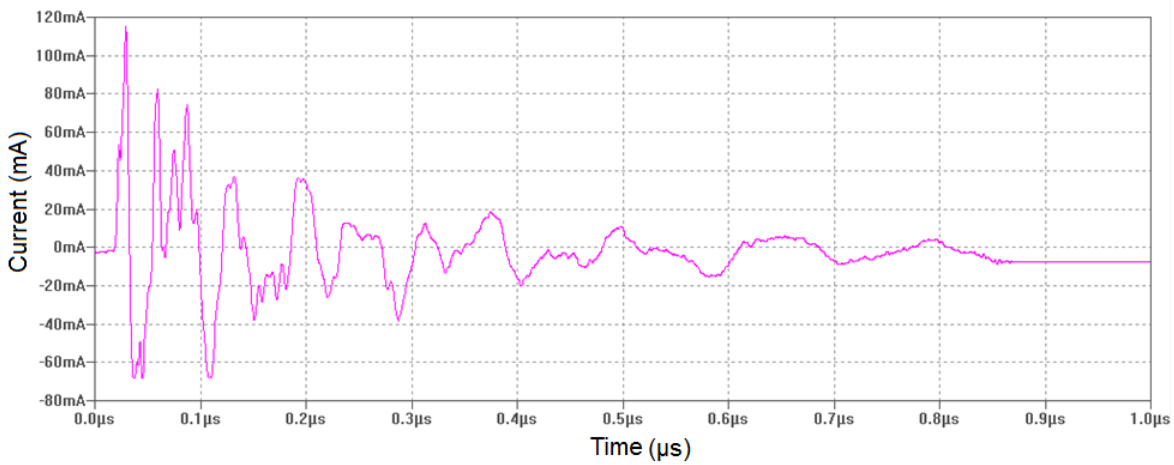

Fig. 39 Surface discharge current pulse

Frequency response (Fig. 40) can be derived based on pulse shape in Fig. 39. Cut-off frequency (- 3 dB) in this case is **450 kHz**. This is caused by the long total pulse duration which is nearly 1 µs. Several additional measurements were done with various test objects (different electrodes and insulation materials) and similar results were obtained. Rise time from 7 to 10 ns and pulse duration several hundreds of ns up to 1 µs. In case of corona Trichel pulses substantial similarity of single pulses can be observed. Opposite to that surface discharge pulses have significant dissimilarity, especially in case of the amplitude.

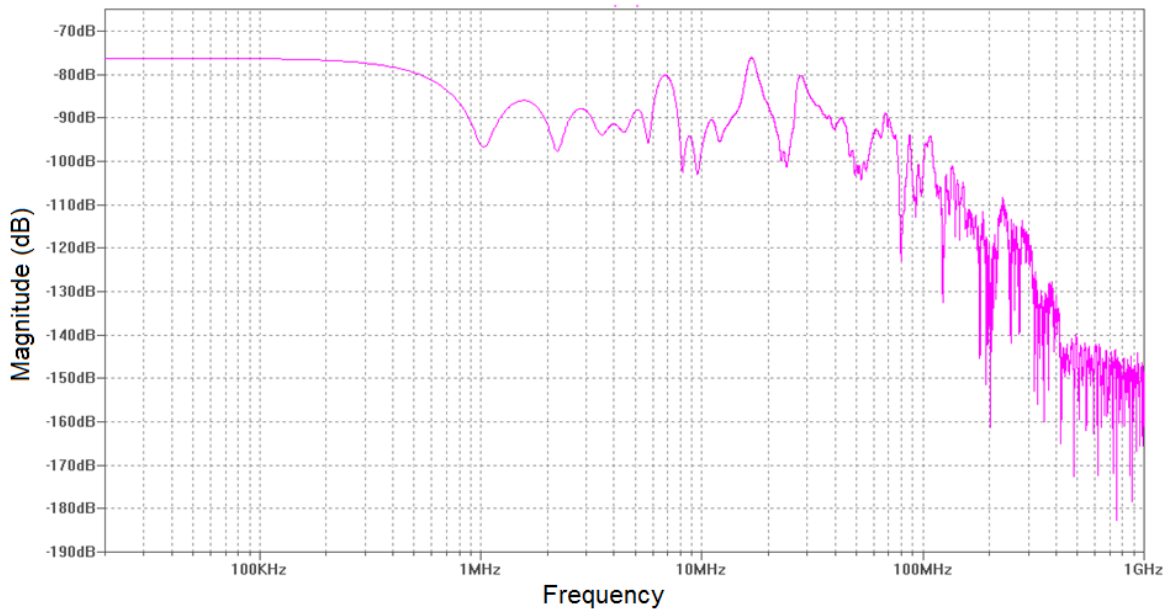

Fig. 40 Surface discharge current pulse in frequency- domain

6.2.3 Internal discharges

Fig. 41 shows a single internal partial discharge pulse. The rise time $\mathbf{t_r}$ is **26.5 ns**. Pulse duration $\mathbf{t_t}$ is estimated up to **200 ns**. The measuring circuit caused pulse oscillations. In case of internal PD, it can be assumed that it has relatively longer rise time, but rather short total pulse duration. It is important to remind that these parameters depend on many aspects, including for e.g. the material of origin.

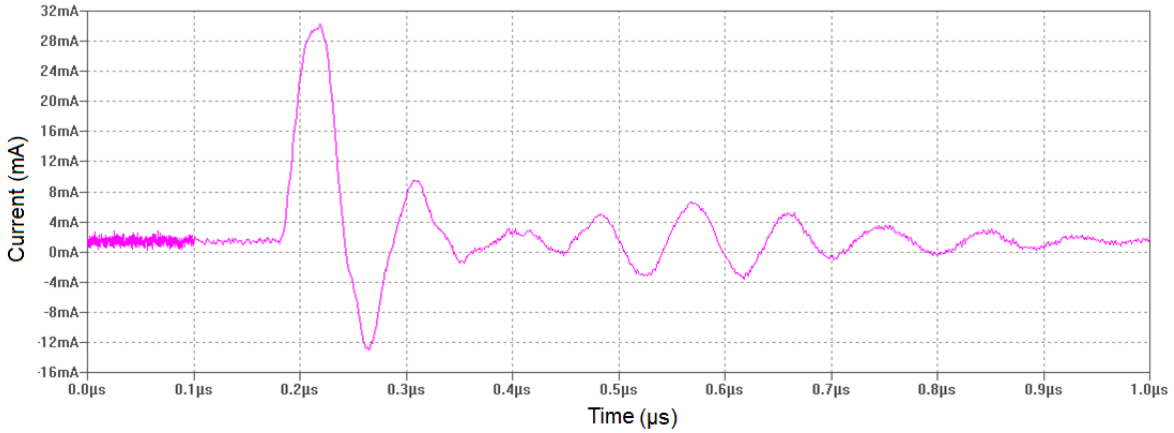

Fig. 41 Internal discharge current pulse

Frequency response (Fig. 42) shows that cut-off frequency (- 3 dB) in this case is **15 MHz**. In general, internal PD pulses have one of the highest cut-off frequencies from observed PD defects. Even shorter rise times and shorter total pulse durations were also recorded.

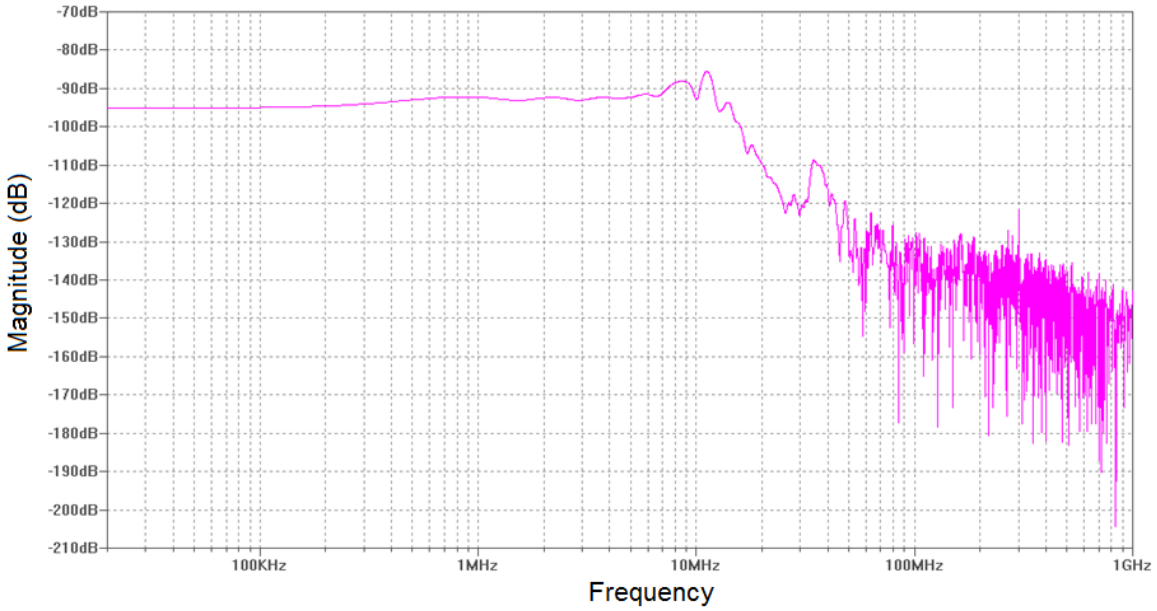

Fig. 42 Internal discharge current pulse in frequency- domain

6.2.4 Summary

As mentioned before, PD pulse shape depends on several aspects. Nevertheless it can be assumed that every single PD defect has its original pulse shape, such as rising time and pulse duration. In frequency domain, various defects can overlap themselves despite various pulse shape parameters. In other words, PD pulses can differ quite dramatically in rise time values and also in total pulse duration, but finally in frequency- domain they can have a very similar behaviour. Hence it can be strongly recommended to evaluate PD pulses in time- domain, since pulse shape is original for every single PD event.

This behaviour can be utilised for multiple PD source recognition. There are already a few techniques which operate in frequency- domain and try to distinguish between various PD pulses. However, the evaluation in time- domain seems to be much more effective and convenient. Nowadays, fast digital post-processing of large amounts of data is not a big issue. Relatively cheap and fast reading units/cards, which are able to record short pulses, also exist. Based on previous facts, it seems to be very useful to take advantage of recognition of various PD pulses based on their characteristics. PD detector can record various PD pulses and sort them to groups based on their rise time (t_r) and fall time (t_f) or total pulse duration (t_t), to name a few. And afterwards, the PRPD patterns for every single PD group can be displayed which helps to distinguish between various PD sources

occurring in the observed device. An operator can then more easily recognise the point of issue e.g. it would be possible to exclude external corona or distinguish between surface discharges and internal discharges with similar amplitude. In this case typical PRPD clusters in pattern can be overlapped and it can be difficult to discriminate all PD faults.

6.3 Example of PD recognition and differentiation in frequency- domain

Previous chapter mentions the advantages of time- and frequency- domain PD behaviour evaluation. This chapter deals with the PD measurement in different frequency range conditions, discusses adequate measuring problems and necessary test procedure which should be fulfilled in case of these unconventional measurements.

6.3.1 Experimental test procedure

The test procedure was carried out at a model of winding bars (same as described in chapter 5.2) which have a corona slot protection, an end bar corona protection. The procedure was done in two stages as described in Annex 1 in detail. In general, inception and extinction voltage was measured in the first stage. The second stage measured time-dependencies of PD values and a Q(t) behaviour. The maximum test voltage was set to 9 kV with respect to the nominal operating voltage of the model ($U_n = 15.75/\sqrt{3} \approx 9\ kV$). Waiting time to observe a so-called self- extinguish phenomenon was around 15 minutes. In case of rotating machines this waiting time is very necessary and appropriate, because of the generated space charge inside the insulation cavities during the test. Voltage down step was set to 1 kV up to extinction voltage U_e. For PD testing a standardised test circuit described in Annex 1 was used. The measuring sensitivity was less than 3 pC. The PD testing was performed using a commonly available test system, which allowed the measurement of the recommended IEC- magnitudes including the description of the PD behaviour in a well-known PRPD- pattern. The test system consists of partial discharge free oil power transformer up to 110 kV, coupling capacitor, PD detector and PC with evaluation software.

Frequency filter settings of measuring device was done according to IEC 60270 for Δf = 100 - 500 kHz and , additionally, the measurement was performed at frequency ranges (Δf) out of this IEC- range especially in different range steps - (5 - 6 MHz), (7 - 8 MHz). In all cases, the lower frequency value was the high- pass- "cut-off" frequency (f_{HP}) and the higher value was the low- pass "cut-off" frequency (f_{LP}). so- called wide band measurement

with f_{HP} - 100 kHz (acc. to IEC), but f_{LP} - 4 MHz was also performed. Note that for every frequency range a re-calibration of the measuring system was done. Frequency ranges not according to IEC were chosen based on the lowest background noise, which depends on location of measurement, current conditions etc.

6.3.2 Measurement results

In all tests PD phenomena were observed typically for rotating machines, so internal partial discharges generated in small cavities inside the mica-resin insulation, slot discharges caused by imperfect slot insulation and surface (creeping/gliding) discharges occurring in stator end-winding, because of high field gradient.

6.3.2.1 Standardized measurement (IEC- range)

In this test the following results were obtained:

Table 6: IEC- frequency range (100 kHz - 500 kHz)

U_i [kV]	4.6	N [1/s]	12000
U_e [kV]	4.1	I [µA]	8.1
Q_{iec} [nC]	4.23	P [µW]	4.12

Besides the small hysteresis expressed by the different values of U_i and U_e the typical problem of measuring Q_{iec} value can be seen in Table 6. Because of the special procedure of calculating the Q_{iec} value mentioned in IEC 60270, there is no agreement with the other measured parameters as PD current or PD power P. The Q_{iec}- time dependence curve has a local minimum and increases at lower voltage (Fig. 43).

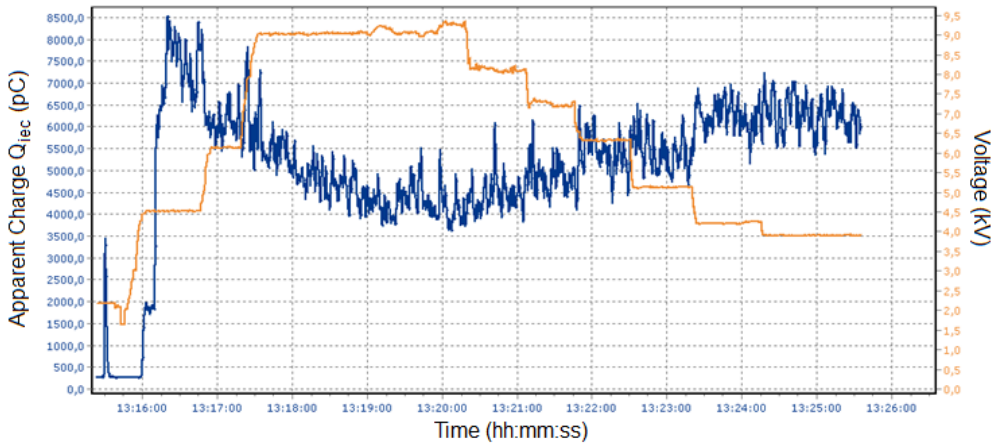

Fig. 43 Q_{iec} ,U_{test} versus time (U_{test} = [9 –> 4] kV)

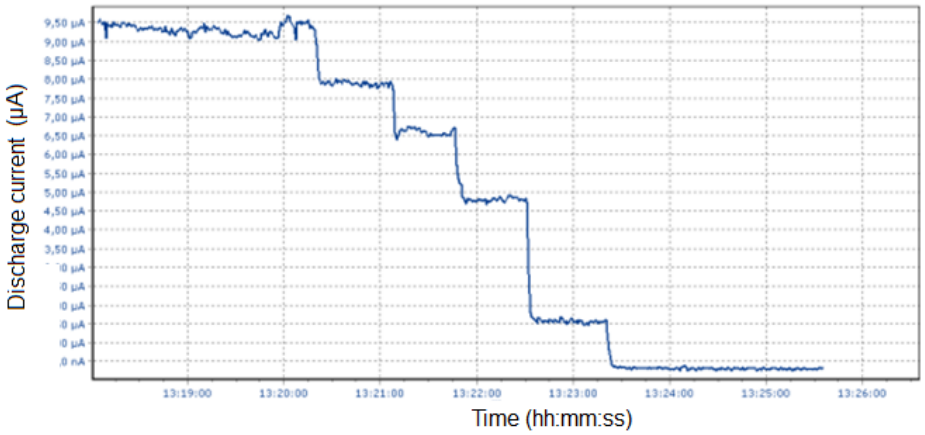

Fig. 44 Discharge current I versus time (U_{test} = [9 –> 4] kV)

This behaviour could be explained by the fact that the slot and surface (gliding) discharges has a major influence on the PD activity above all by its repetition rate at higher voltage level. This is confirmed by the PRPD- pattern, which shows some typical “clusters” caused by the different PD sources (Fig. 45, Fig. 46). Therefore, according to the IEC procedure, the Q_{iec} value is focused at/in the cluster produced by slot and surface (gliding) discharges and the other typical cluster for cavity discharges (so- called “rabbit ears") having higher amplitude of apparent charge but lower pulse repetition rate is partially ignored. This behaviour is changed by the decrease of test voltage, where slot and surface discharges also decrease its intensity, and at the same time the internal PD activity remains unchanged and the Q_{iec} value calculation also takes into account this cluster. Slot and surface discharges have typically more or less linear increasing dependence on applied test voltage, whereby internal PD has specific voltage dependence, see Annex 1. If the inception voltage of internal PD is reached and the space charge attenuation is passed, the PD activity level (Q) is more or less stable and value stays the same. It shall be noticed that the derived quantities as repetition rate N or power P follow at least the summarised PD activity (Fig. 47).

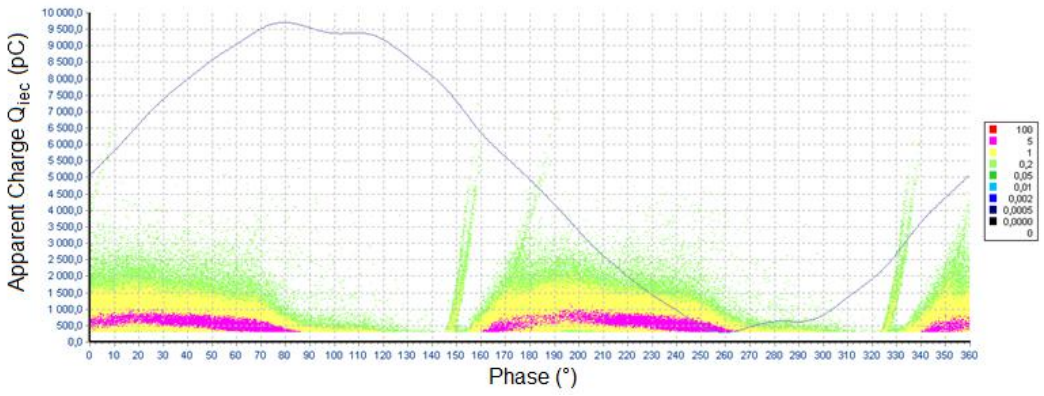

Fig. 45 PRPD pattern, U_{test} = 9 kV, Q_{iec} ~ 4.2 nC

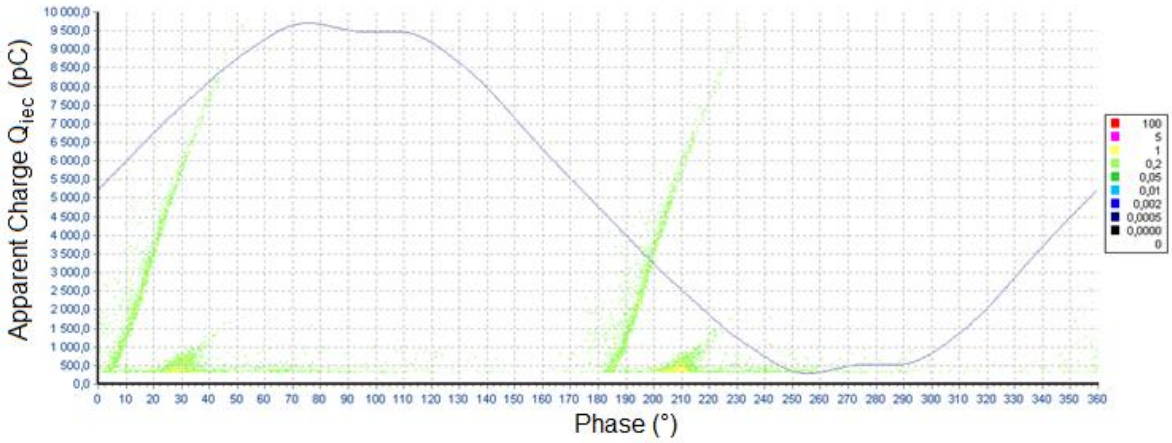

Fig. 46 PRPD pattern, U_{test} = 4 kV, Q_{iec} ~ 6.2 nC

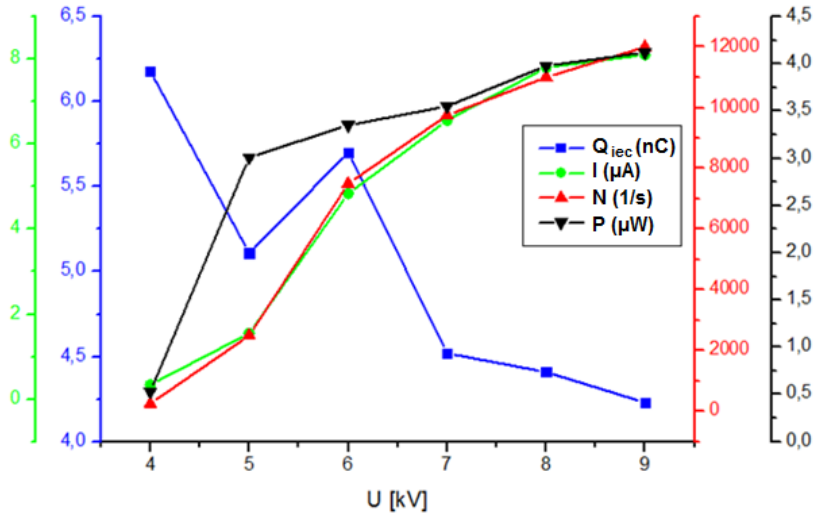

Fig. 47 Q_{iec} and derived magnitudes I, N, P dependent on test voltage

6.3.2.2 Non- standardized measurement (Δf ≠ IEC- range)

For better understanding of the measured results obtained at different frequency ranges, the frequency spectrum of two PD pulses which are similar to the investigated PD sources were analysed. The shorter PD pulse (similar to the cavity discharges) has a rise time of t_r ~ 60 ns, the longer pulse was with a rise time of t_r ~ 650 ns (similar to surface (gliding) discharges),Fig. 48, Fig. 49. As shown in chapter 6.2, the pulse shape in time- domain differs and hence does the PD pulses' behaviour in frequency- domain. In this case, the rise time and total duration is longer, since the influence of measuring circuit was taken into account. The important observation is that the pulses' characteristics remained the same.

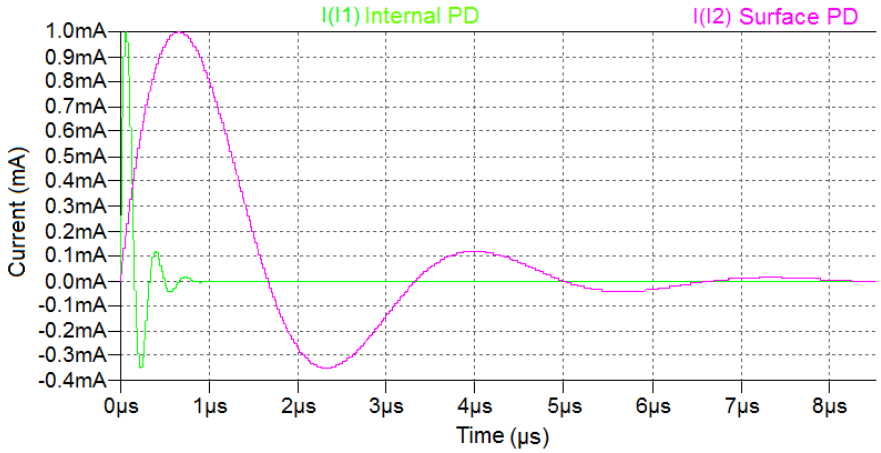

Fig. 48 Analysed PD pulses

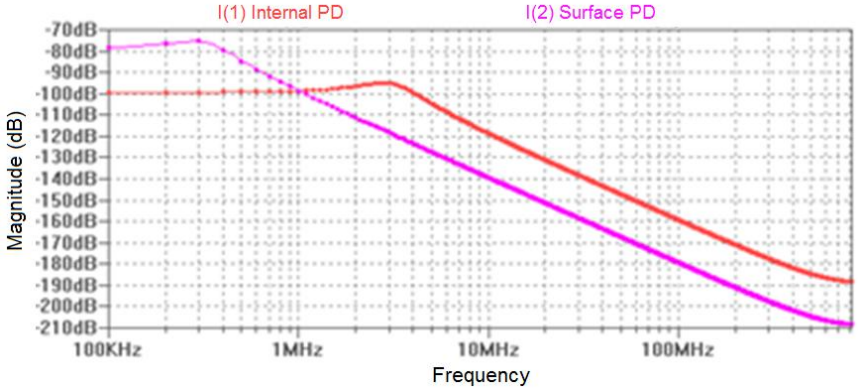

Fig. 49 FFT- spectrum of analysed PD pulses

As expected, the frequency spectrum of the shorter pulse (~ cavity discharge) reaches much higher frequency than the pulse, similar to the surface (gliding) discharge.

6.3.2.2.1 Frequency range 100 Hz – 4 MHz

In this frequency range, the measured quantities correspond with the observed PD activity (Fig. 50, Fig. 51). When comparing the measured data to IEC standard it is shown that the Q_{iec}- time dependence curve does not have a local minimum as applicable in Fig. 44. The Q_{iec}- time dependence curve follows the voltage steps and changes.

As expected from the frequency spectrum investigations in this frequency range, the components of the gliding discharges are not suppressed and, at the same time, the (higher frequency) components of the internal PD are dominant. This can be seen in the PRPD pattern (Fig. 50).

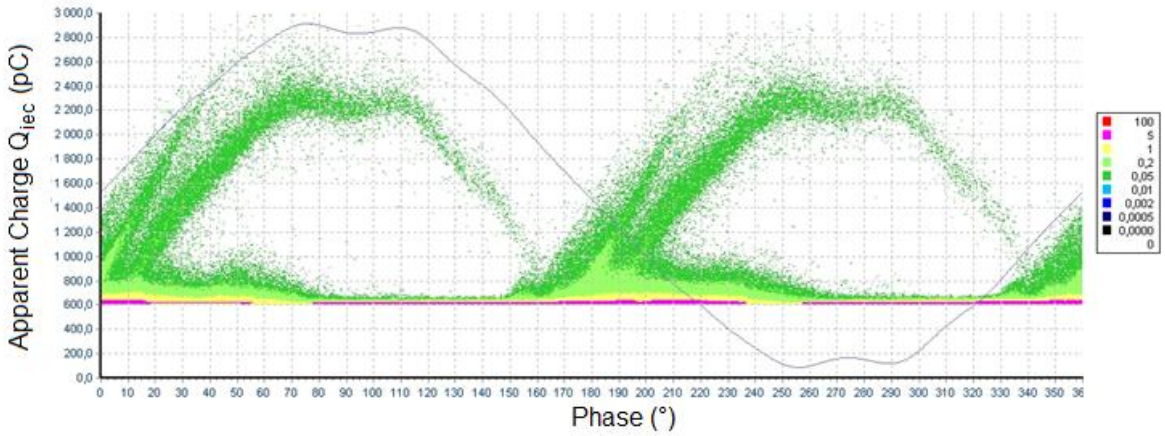

Fig. 50 PRPD pattern, U_{test} = 9 kV, Q_{iec} = 2,2 nC

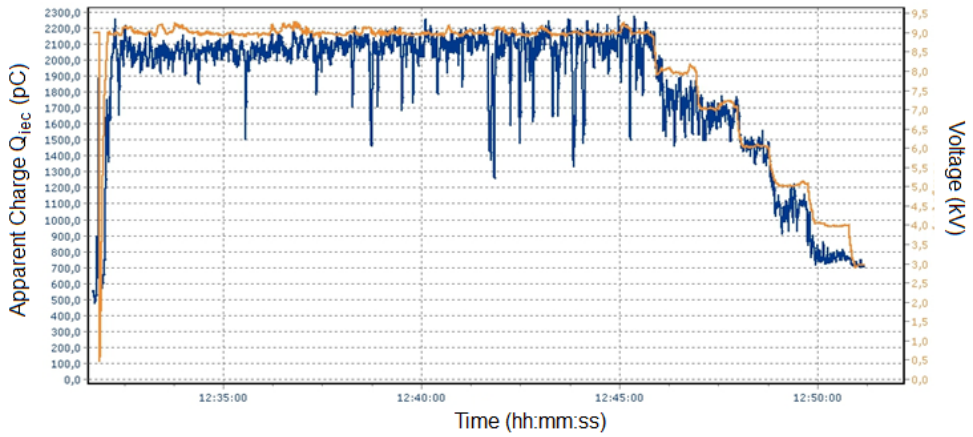

Fig. 51 Q_{iec} ,U_{test} versus time (U_{test} = [9 –> 4] kV)

6.3.2.2.2 Frequency range 5 MHz – 6 MHz

In this frequency range the measured quantities correspond with the observed PD activity are shown in Fig. 52 - Fig. 56.

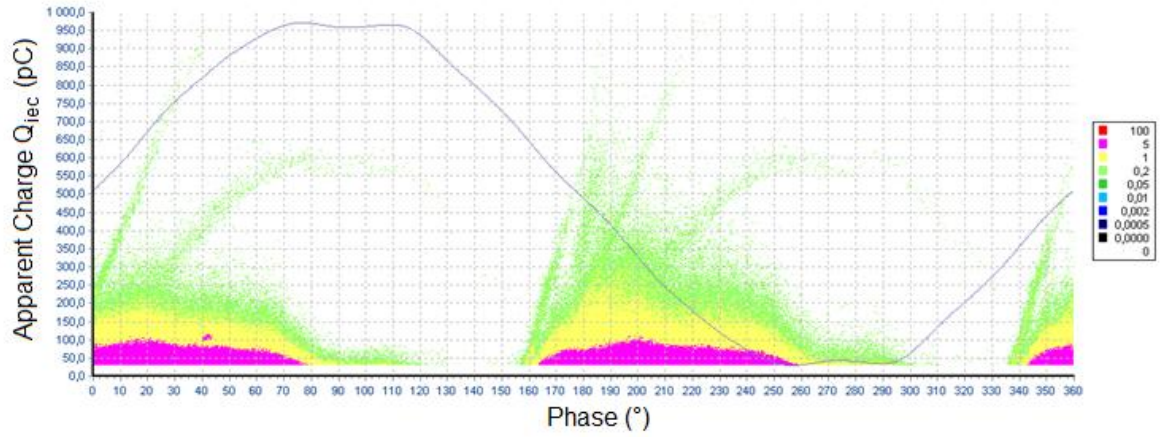

Fig. 52 PRPD pattern, U_{test} = 9 kV, Q_{iec} = 648 pC

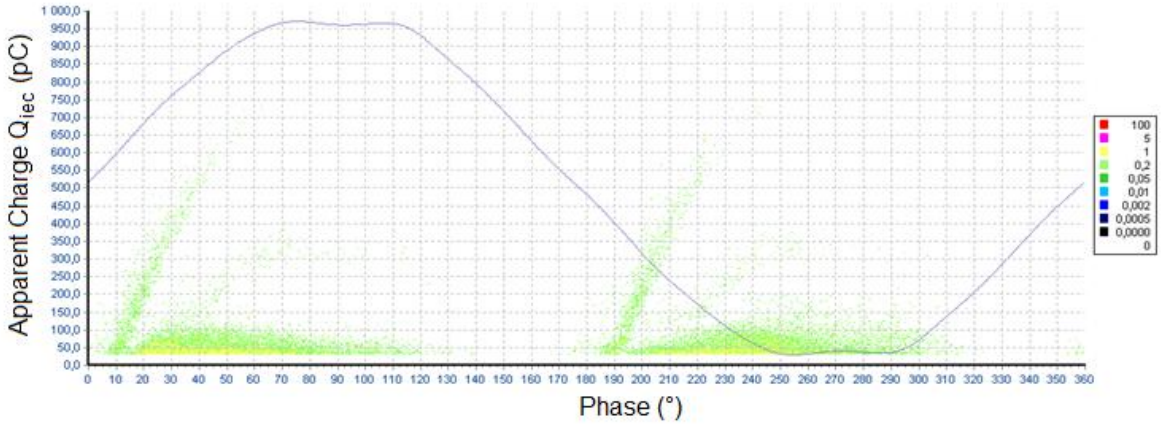

Fig. 53 PRPD pattern, U_{test} = 5 kV, Q_{iec} = 456 pC

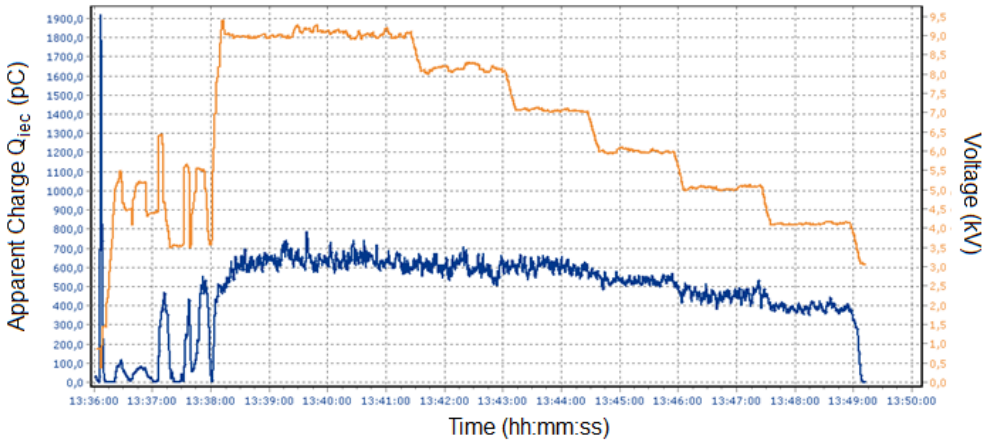

Fig. 54 Q_{iec} ,U_{test} versus time (U_{test} = [9 –> 4] kV)

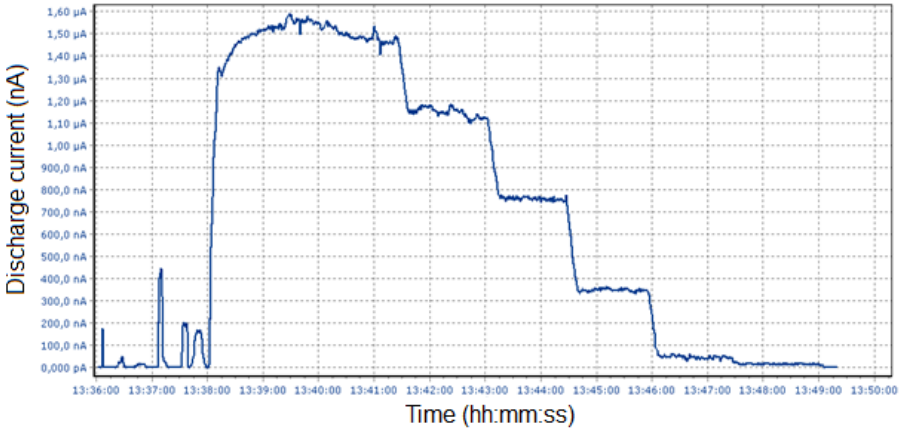

Fig. 55 Discharge current I versus time (U_{test} = [9 –> 4] kV)

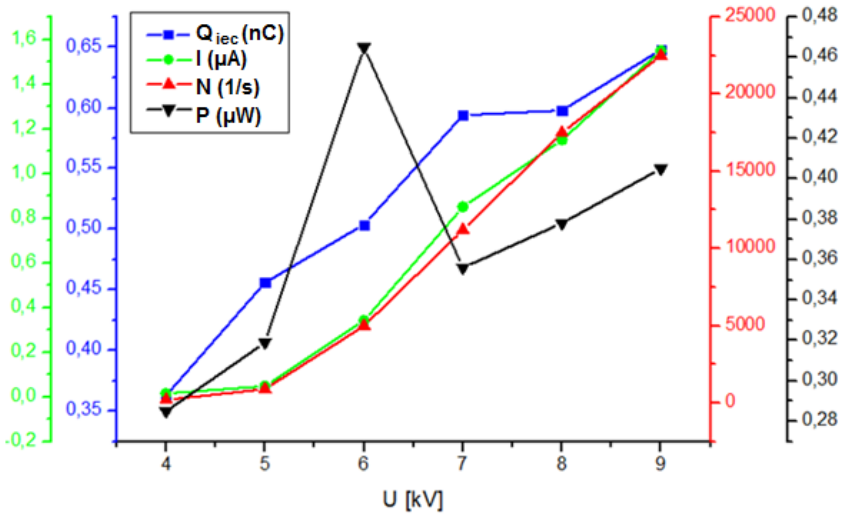

Fig. 56 Q_{iec} and derived magnitudes I, N, P dependent on test voltage

Note that at test voltage of ~ 6 kV, the power P has a local maximum, which could be explained only by a possible local degradation inside of a test object or more probably by a measurement error. Generally, the measured components of the PD activity in this frequency range (cavities and gliding/slot discharges) are quasi balanced, meaning that the summarised PD activity will be measured more and less correctly, even by the Q_{iec} value.

6.3.2.2.3 Frequency range 7 MHz – 8 MHz

As expected from the frequency spectrum investigations in this frequency range, the components of the surface (gliding) discharges will be suppressed and, at the same time, the (higher frequency) components of the internal PD are dominant. This can be seen in the PRPD pattern, where only typical cluster, so- called "rabbit ears", can be recognised (Fig. 57, Fig. 58).

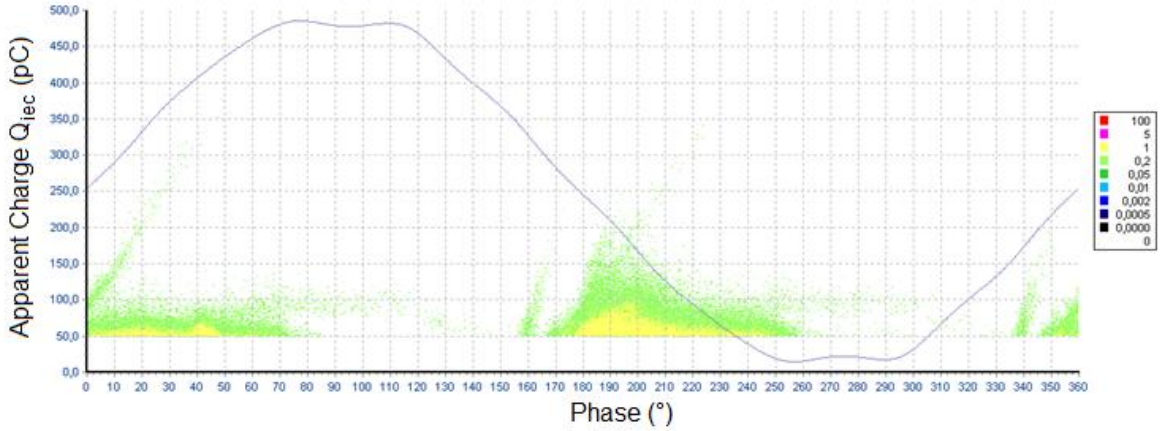

Fig. 57 PRPD pattern, U_{test} = 9 kV, Q_{iec} = 163 pC

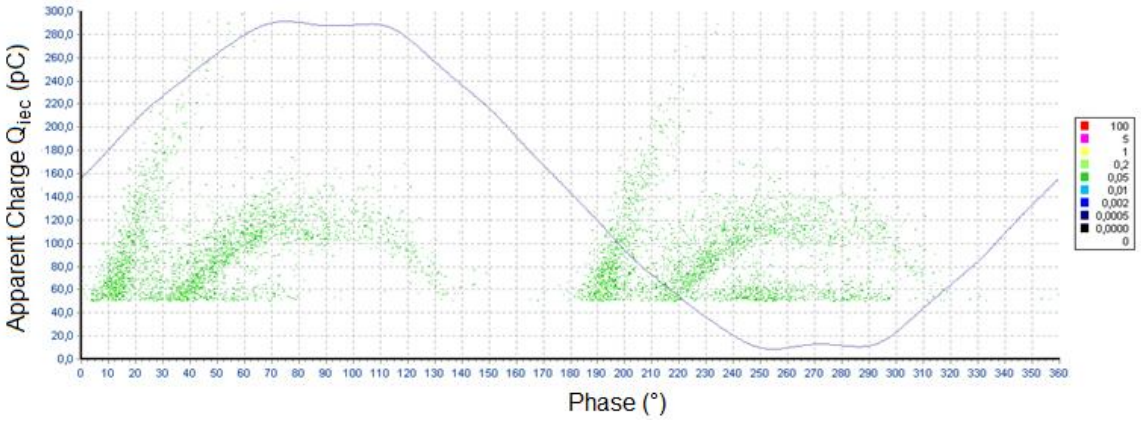

Fig. 58 PRPD pattern, U_{test} = 5 kV, Q_{iec} = 133 pC

A similar behaviour can be observed at the measured quantities (Fig. 59 - Fig. 61). The quasi constant values of Q versus testing time and, at the same manner, the increasing of the measured values up to a certain voltage (~ 6 - 7 kV) are typical for internal PD activity. If the test voltage is further increased, the quantities are decreasing, excluding the repetition rate and the PD current. This behaviour, especially in case of the power P, should be investigated more in details.

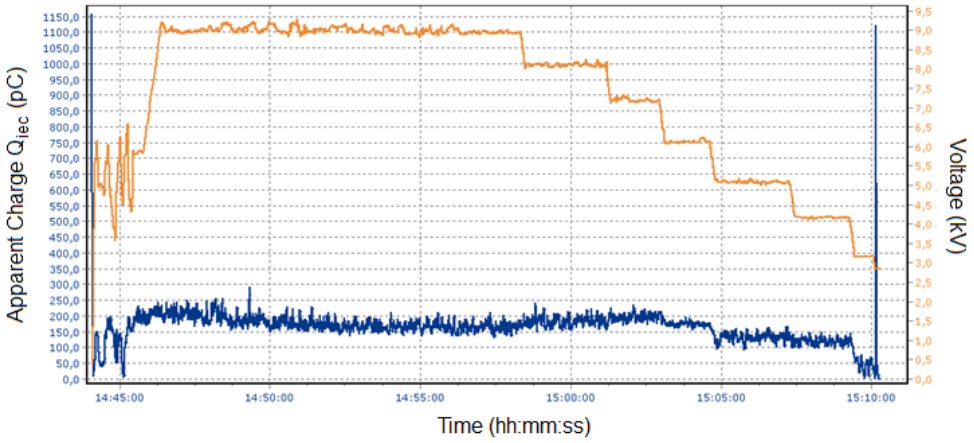

Fig. 59 Q_{iec} ,U_{test} versus time (U_{test} = [9 –> 4] kV)

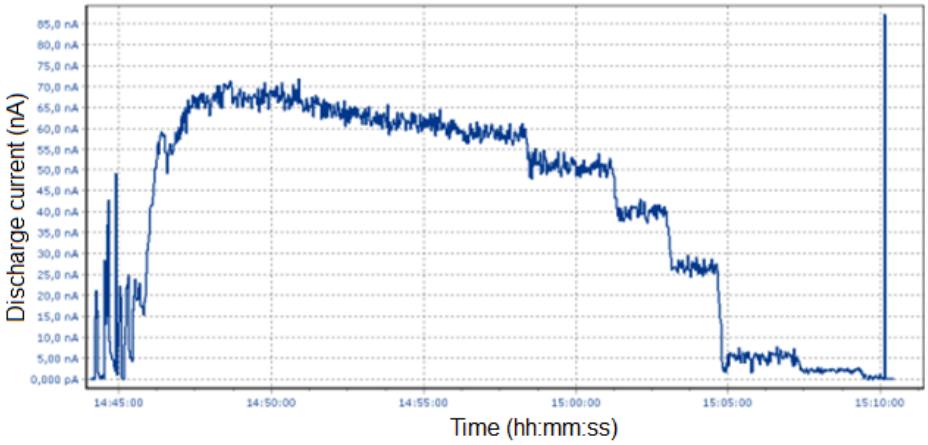

Fig. 60 Discharge current I versus time (U_{test} = [9 –> 4] kV)

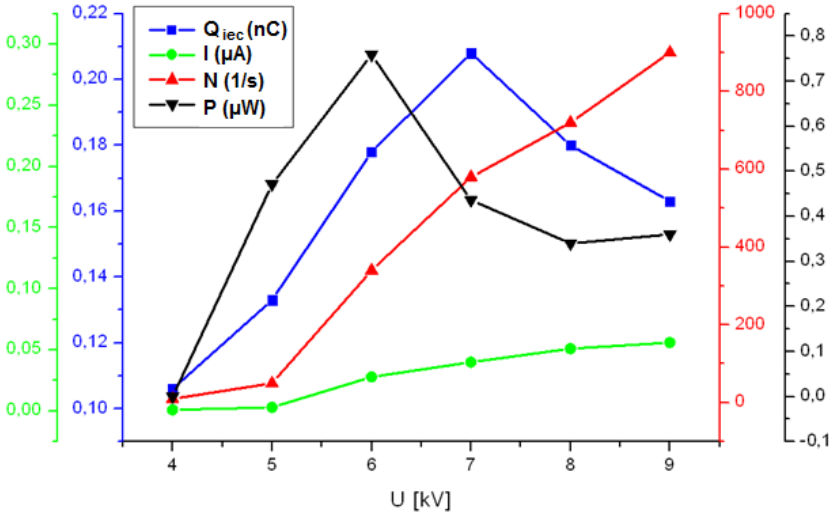

Fig. 61 Q_{iec} and derived magnitudes I, N, P dependent on test voltage

6.3.3 Discussion

Amplitudes or absolute values of all magnitudes differ in every frequency range. It is caused by different signal amplitude/attenuation over the frequency spectrum. In specific frequency ranges different PD defects have a different intensity and occurrence, which is caused by its relevant frequency spectrum signal behaviour. However, the measured PD parameters show different values at a different frequency range of the measuring system (Table 7). This fact must be considered during evaluation of PD activity for the investigated test objects. Fig. 61 shows local maximum of apparent charge Q_{iec} and power P. It is important to mention that peak values are not significant in the manner of PD measurement. The peaks could be caused by different distribution of the single PD events over the test voltage, since the discharge power P calculates with every single PD event and its

instantaneous test voltage level. PD activity in general is not absolutely stable and the reading changes over the time. It is appropriate to evaluate absolute or average values of PD magnitude. Evaluating of the trending over the time seems to be more convenient and more important for PD measurement in general.

Table 7: Overview about all PD test results for U_{test} = 9 kV

	100 - 500 kHz	**0.1 - 4 MHz**	**5 - 6 MHz**	**7 - 8 MHz**
U_i	4.6	4.3	5.2	5.7
U_e	4.1	3.9	4.6	4.9
Q_{iec} (nC)	4.23	2.1	0.648	0.163
N (1/s)	12000	9000	1200	900
I (µA)	8.1	1.1	1.55	0.056
P (µW)	4.12	0.73	0.405	0.36

6.3.4 Summary

The PD measurement of a test object with multiple PD sources shows problems in the evaluation of PD activity based on the measured parameters. Especially the parameter Q_{iec} recommended by the IEC standard does not fully and unambiguously describe the existing PD phenomena in a correct way. One possibility to avoid that is to measure it in different frequency windows, which can help to further specify and distinguish the existing PD activity. Admittedly, special calibration must be done in every frequency range to measure real values. Measured magnitudes cannot be compared between each other in case of a different spectrum, but the main character and core of PD behaviour remain and can be supplemented. The main and prime application and advantage of using various frequency ranges is to suppress the external background noise and to better distinguish and separate the PD sources and behaviour. Measurement in different frequency ranges make sense regarding points mentioned above and, finally, may give a contribution to a better evaluation and understanding of PD activity in real equipment.

6.4 Influence of measuring circuit

A basic partial discharge circuit (Fig. 62) was used for simulation of different PD events. Current source I represents PD current pulse occurring in defect of insulation. C_t represents

a capacity of test object (DUT), C_k represents a coupling capacitor and Z represents ideal measuring impedance.

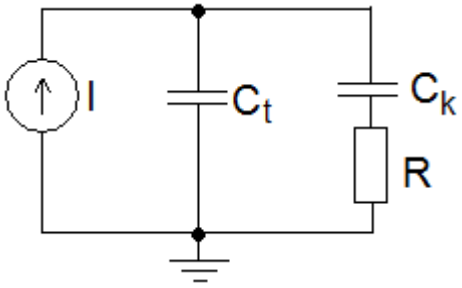

Fig. 62 Basic PD measuring circuit

Shape of the pulses was changed by the influence of test circuit. Hence the frequency response was changed as well. Several typical coupling capacitors' values were tested. Namely C_k = 80 pF / 1 nF / 5 nF / 10 nF. And two different loads were tested C_t = 1 nF and 1 µF. Measuring sensitivity in the meaning of maximum amplitude of the pulse was observed and the frequency response of de-coupled pulses was evaluated.

Following figures are for the pulse shape with Rise Time (t_r) = 3 ns and Fall Time (t_f) = 10 ns, total pulse duration (t_t) = 15 ns with C_t = 1nF and various C_k values. The differences of the amplitude of decoupled pulses, and differences in total pulse duration and hence various frequency responses can be seen.

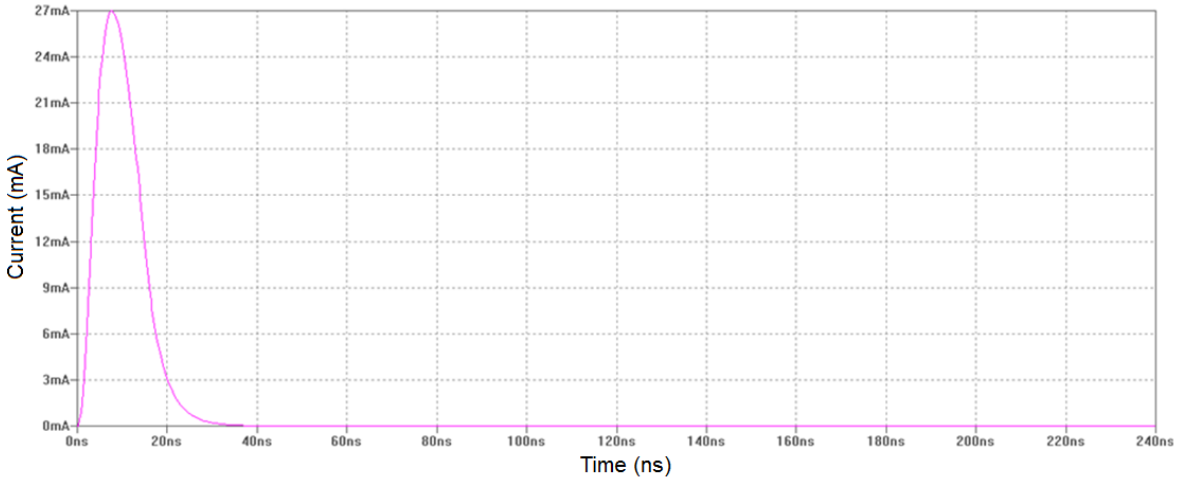

Fig. 63 PD pulse shape for C_k = 80 pF

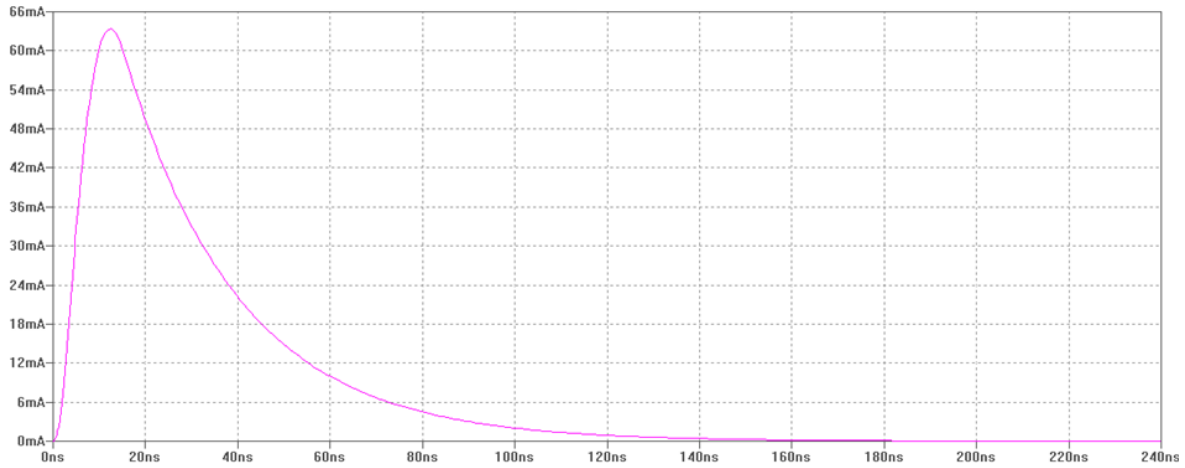

Fig. 64 PD pulse shape for C_k = 1 nF

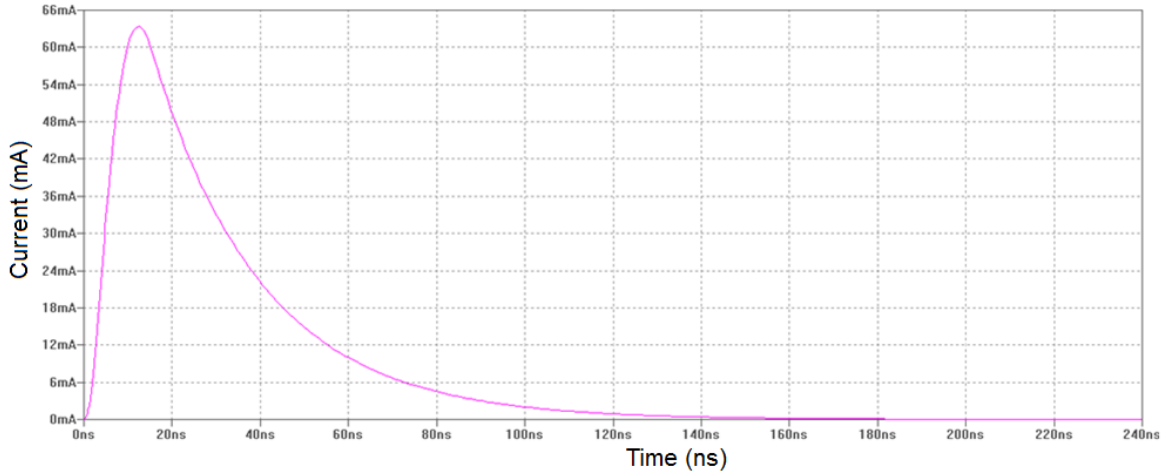

Fig. 65 PD pulse shape for C_k = 5 nF

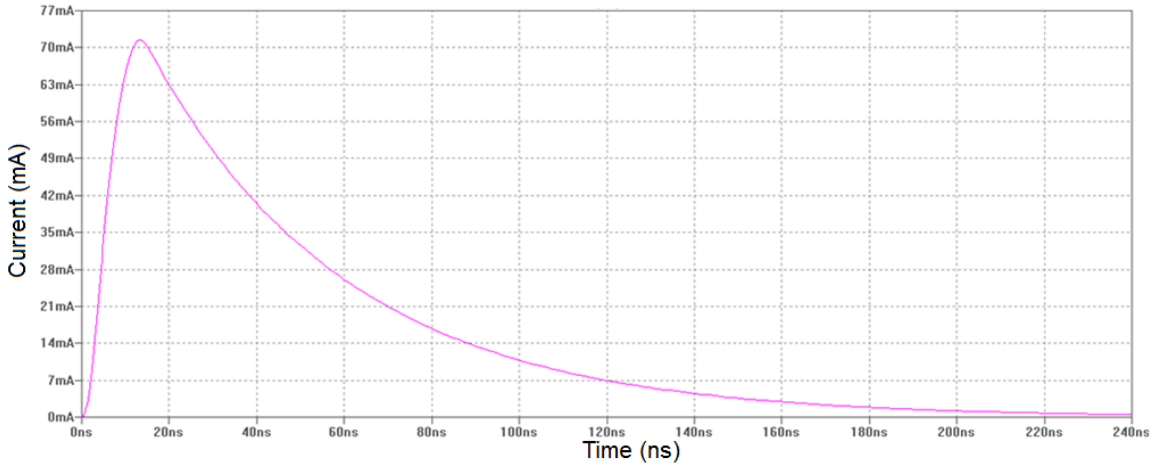

Fig. 66 PD pulse shape for C_k = 10 nF

1. Capacitance of test object C_t = 1 nF

Table 8: C_t = 1 nF; t_r = 3 ns, t_f = 10 ns

C_k (nF)	Amplitude (mA)	Cut-off frequency f_c (MHz)
0.08	27	28
1	64	6
2	67	5
5	70	4
10	71	3.2

For short pulses and relatively low load, it can be assumed that coupling capacitor C_k = 80 pF has significantly lower measuring sensitivity, but the frequency response goes to higher frequencies.

Table 9: C_t = 1 nF; t_r = 200 ns, t_f = 300 ns

C_k (nF)	Amplitude (mA)	Cut-off frequency f_c (MHz)
0.08	37	1.3
1	240	1.3
2	305	1.1
5	370	1.1
10	400	1.1

For longer pulses and relatively low load, it can be assumed that coupling capacitor C_k = 80 pF has even lower measuring sensitivity and the frequency response remains approx. the same for all coupling capacitors.

2. Capacitance of test object C_t = 1 µF

Table 10: C_t = 1 µF; t_r = 3 ns, t_f = 10 ns

C_k (nF)	Amplitude (uA)	Cut-off frequency f_c (MHz)
0.08	28	28
1	72	3
2	79	1.8
5	82	0.65
10	83	0.32

For short pulses and extremely high load, it can be assumed that coupling capacitor C_k = 80 pF has low measuring sensitivity and the frequency response goes to higher frequencies.

Measuring sensitivity does not change dramatically for coupling capacitors with higher capacity, from 1 nF to 10 nF.

Table 11: C_t = 1 μF; t_r = 200 ns, t_f = 300 ns

C_k (nF)	Amplitude (uA)	Cut-off frequency f_c (MHz)
0.08	40	1.3
1	440	1.2
2	750	1
5	1300	0.6
10	1750	0.4

For long pulses and extremely high load, it can be assumed that coupling capacitor C_k = 80 pF has low measuring sensitivity and the frequency response remains more or less same. In comparison with previous case increasing of capacity of coupling capacitors has extreme influence to the measuring sensitivity.

For long pulses and large load, it can be assumed that coupling capacitor C_k = 80 pF has significantly lower measuring sensitivity and the frequency response remains more or less same. The frequency response limitations of coupling capacitors with higher capacity are given by limitations of C_k and R which is in fact high pass filter. For example the theoretical bandwidth of C_k = 80 pF is 39 MHz and theoretical bandwidth of C_k = 2 nF is 1 MHz. So in general, it can be assumed that C_k = 80 pF has low measuring sensitivity of decoupled PD signal. As the best solution seems to be usage of C_k = 1 nF or 2 nF. With higher capacitances significantly higher measuring sensitivity is not gained in certain cases. It is also necessary to take into account that it is not possible to increase value of coupling capacitor C_k up to excessively high values, because a time constant $\tau = R \times C_k$ increases. This causes longer pulse duration and hence shorter cut-off frequency in frequency-domain. See Fig. 63 - Fig. 66 and Table 8 - Table 11. In certain cases, when the value of C_k is high enough, the cut-off frequency in frequency- domain can be under the IEC 60270 frequency range (100 - 500 kHz).

6.5 Influence of filter settings to the PD pulse shape and recognition

This chapter deals with the influence of filter (High Pass and Low Pass) settings and its influence to PD recognition technique and pulse shape. Corona discharge behaviour was used as representative sample. Special focus was applied to the phenomenon of "pulses less area". It is located in the middle of Trichel pulses cluster. In general, the following

statement is accepted. no PD pulses can be observed in this area with common partial discharge detectors. In fact, the repetition rate of pulses in this area is so high, that common PD analysers are unable to recognise them. For closer description of corona behaviour see Annex 1.

In the experiment an oscilloscope LeCroy was used to record raw data of corona behaviour. A standard basic test arrangement was used (needle-plane, 10 mm air gap), which is also described in Annex 1. Oscilloscope provides an ultra-wide bandwidth 500 MHz. Afterwards, a Butterworth filter (4th order) with various Low-Pass cut-off frequencies was applied on the raw data.

6.5.1 Case one - Low-Pass filter 2MHz

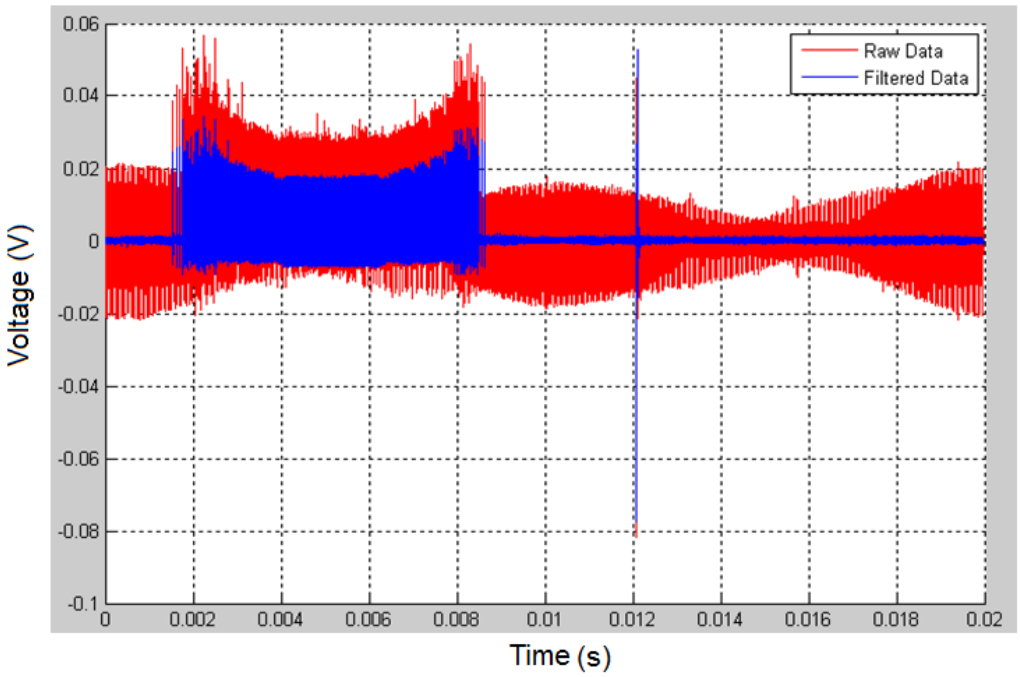

Fig. 67 Recorded PD corona signal by LeCroy Oscilloscope, LP filter 2 MHz

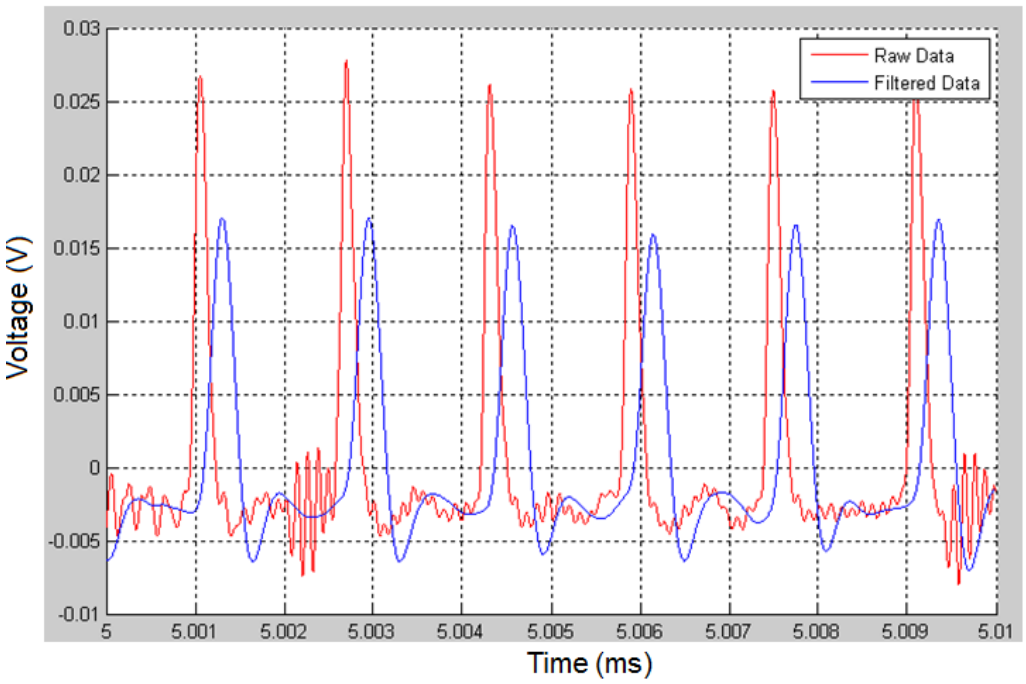

Fig. 68 Zoom to the middle of Trichel pulses cluster, LP filter 2 MHz

6.5.2 Case two – Low-Pass filter 500 kHz

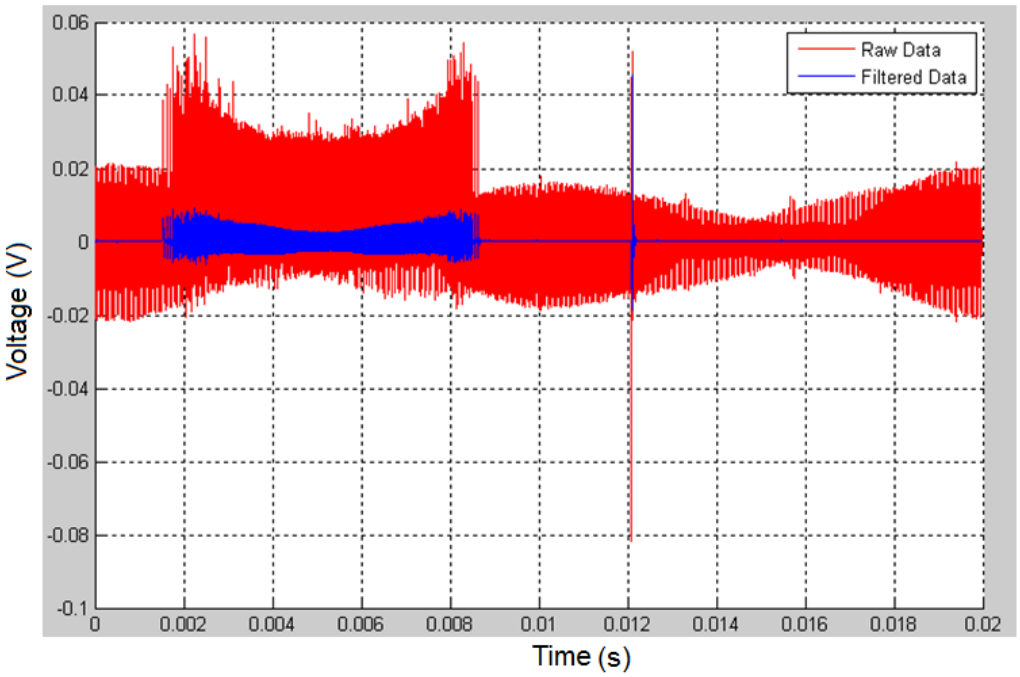

Fig. 69 Recorded PD corona signal by LeCroy Oscilloscope, LP filter 500 kHz

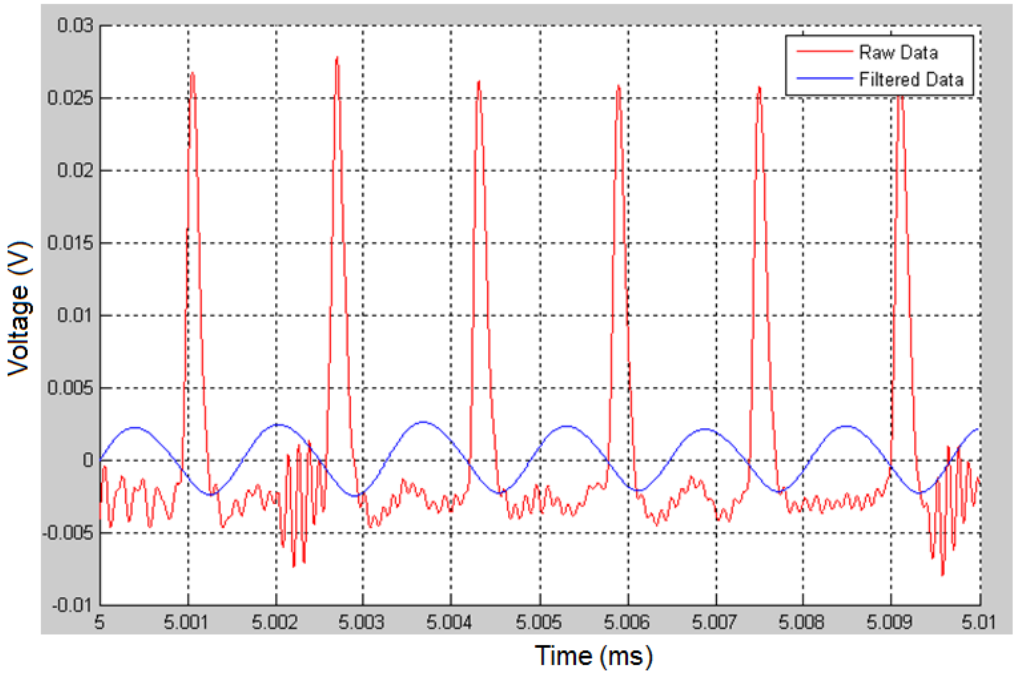

Fig. 70 Zoom to the middle of Trichel pulses cluster (recorded time is 10 µs, number of possible recorded pulses is 6), LP filter 500 kHz

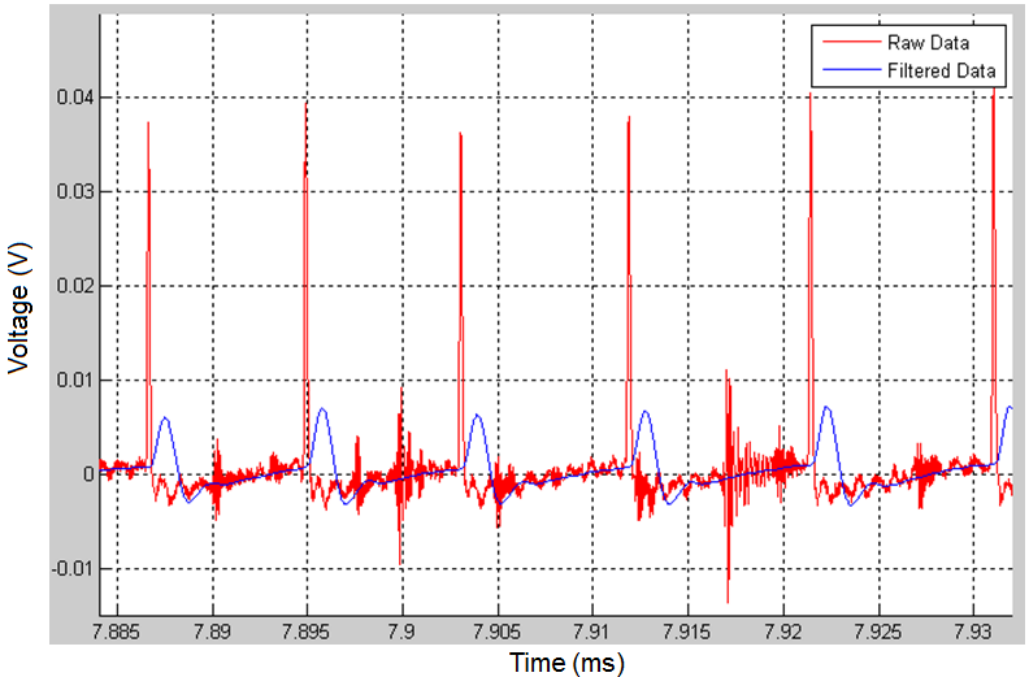

Fig. 71 Zoom to the right side of Trichel pulses cluster (recorded time is 100 µs, number of possible recorded pulses is 6).

Clear difference can be seen between the repetition rate in the middle and on sides of Trichel pulses cluster (see Fig. 70 and Fig. 71). The repetition rate In the middle of Trichel

pulses cluster (Fig. 70) is 10 times higher than on the side of Trichel pulses cluster (Fig. 71). Hence on the sides of Trichel pulses cluster pulses are not so close to each other and the filter does not have such a large oscillation (Fig. 71) at the output as in case of a high repetition rate in the middle of the Trichel pulses cluster (Fig. 70). If the repetition rate is too high (the distance between the single pulses is too small), the filter has more or less the sine oscillation at its output. This effect causes that no PD pulses are recognised.

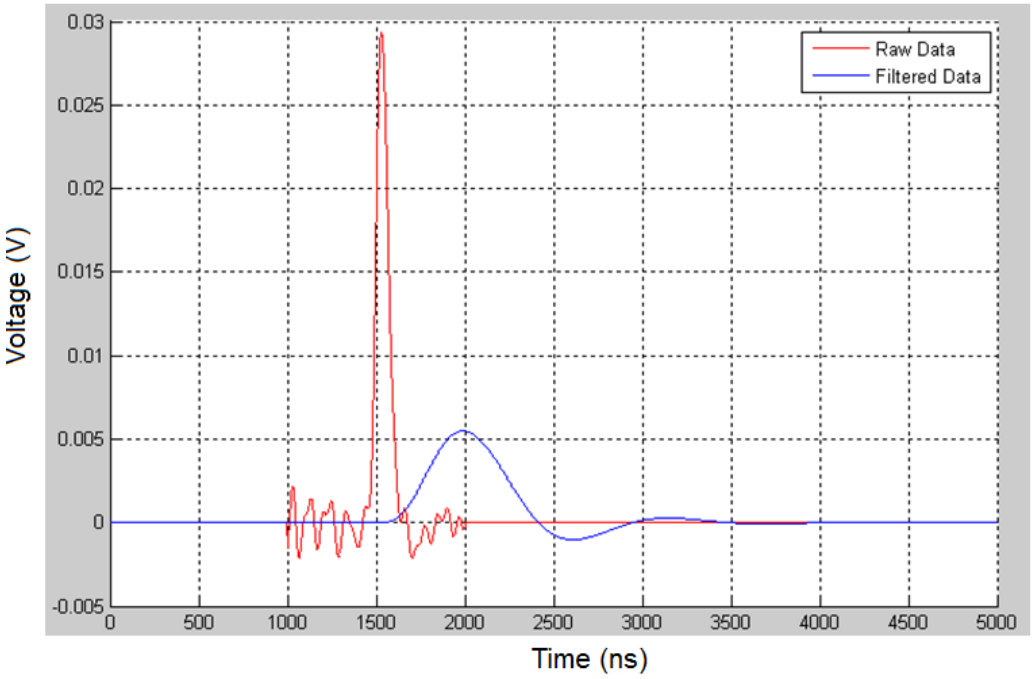

Fig. 72 Single pulse from 5.000 ms to 5.002 ms from Fig. 70

A pulse in Fig. 72 is processed by filter as a single pulse. In Fig. 70, the filter signal is more or less sine wave with frequency 1 MHz. On the other hand, if only s single pulse is processed by the filter, the output of still looks like a PD pulse and not like a sine wave, and a PD pulse recognition can be done by the PD detector. It can be concluded that the statement at the beginning of this chapter is therefore inaccurate. The pulse-less area is caused by the filter settings required by the IEC 60270, which requires a maximum LP value 500 kHz. If the LP = 2 MHz is used, clear PD pulses recognition can be done, as shown in Fig. 68.

7 Evaluation of measurement issues of test objects with winding

Chapter 2.2 introduced the relation between C_k:C_t and the consequent Q_m/Q behaviour. It was shown that the ratio 100:1 (C_k:C_t) is required to reach a 100 % Q_m/Q ratio. Ratio 10:1 gives 90 % Q_m/Q sensitivity. As measurement limit can be defined ratio 1:1 when the Q_m/Q ratio drops to 50 %. In case of PD measurement on bushings or small or middle size (e.g. distribution) transformers, it is not a problem to fulfil the recommended ratio between coupling capacitor and test object capacity. Problems can arise in case of large power transformers and rotating machines, where the capacitances are relatively high. Rotating machine capacities are in range from 100 nF up to 1 μF and more in case of large hydro generators. A brief overview of electrical device capacitances can be found in Annex 2. In these cases, it is simply impossible to fulfil recommended values of the coupling capacitor. First of all the size and price of the coupling capacitor would be too high and second of all the power source to energise the entire system would be too large and expensive. In practise, coupling capacitors with maximum size 10 nF – 40 nF are used.

Transformers and rotating machines are complex RLC networks with specific resonances. Measurement of machine's capacity is normally done together with dissipation factor measurement at 50 Hz. However the capacitance changes over the frequency due to the resonances caused by RLC character of the device. Hence it is not appropriate to derive the size of coupling capacitors based on the standard capacitance measurement.

7.1 Theoretical background

For standard measurement of transfer frequency characteristics, Spectrum Analysers or Network Analyser is usually used. However these devices are optimised for 50 Ω loads, but electrical devices, such as rotating machines or transformers have various impedance outputs caused by specific RLC elements arrangement. So an application of these measuring devices seems to be too complicated or even impossible. Next disadvantage of such measuring devices is their fragility. Their main purpose is therefore lab use.

Due to the limitations mentioned above, a new measuring technique was developed, taking the advantage of Frequency Response Analysis (FRA) device into account. FRA is a

method to measure the frequency response of passive elements (RLC) of electrical devices. Originally, it was developed to detect mechanical damages in the transformers. [96] FRA measuring device consists of Source probe and Receiver probe. A source probe transmits AC voltage signal (12 V or 24 V, with variable frequencies from 10 Hz to 10 MHz). A receiver receives the voltage signal and then the transfer frequency characteristic $A = 20 \log \frac{U_2}{U_1} (dB)$ can be calculated. The FRA is standartly used for measurement between transformer's phases. However the PD measurement is done in configuration phase - ground. Hence modified FRA measurement must be performed.

Fig. 73 Modified FRA measurement test set-up presents a modified FRA measurement test set-up. The measuring resistor R_M is connected to generator in series. The Device Under Test (DUT) is then connected in parallel. The receiver is also connected in parallel to the DUT. In fact, voltage divider is created. The measuring resistor R_M is variable and adapts to the impedance of the DUT. In fact it ensures a good measuring sensitivity, as shown in the following text.

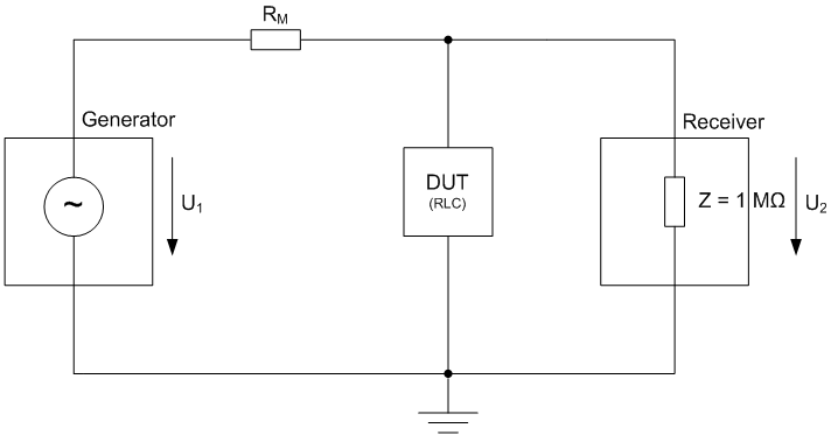

Fig. 73 Modified FRA measurement test set-up

7.2 Simulations of test method

For simulation and verification of theoretical assumptions the Spice-Based Analogue Simulation Program from Texas Instruments – Tina-Ti was used [97]. Fig. 74 shows a RLC circuit with three arms to demonstrate influences of the measuring resistor R_M.

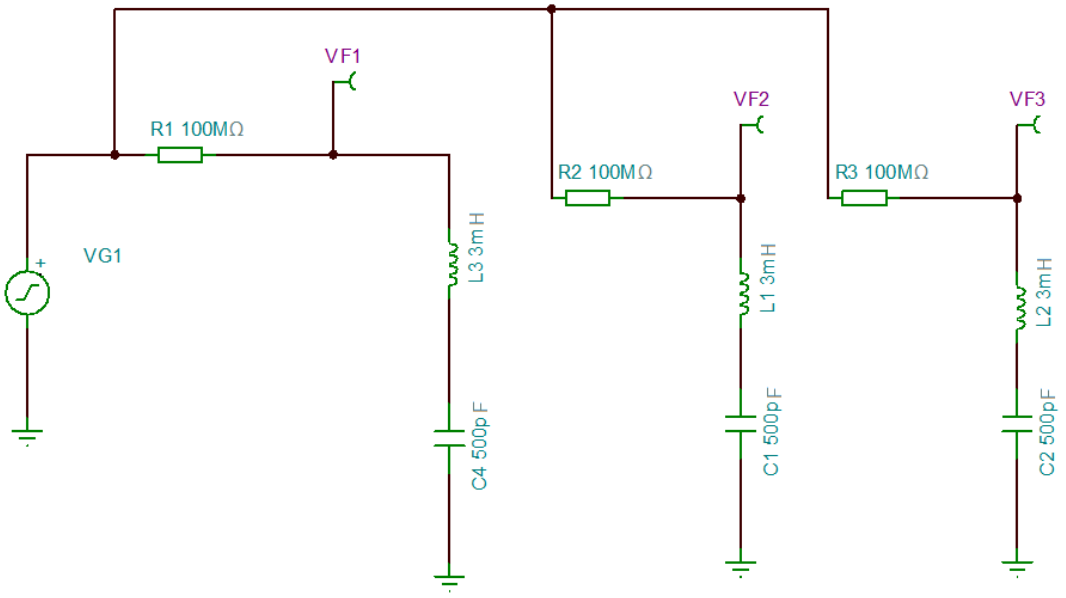

Fig. 74 RLC circuit – sensitivity check

When measuring resistor R_M (represented by resistors R_1, R_2, R_3 in circuit in Fig. 74) has the same value in all three aims of the test circuit, it generates the same frequency response.

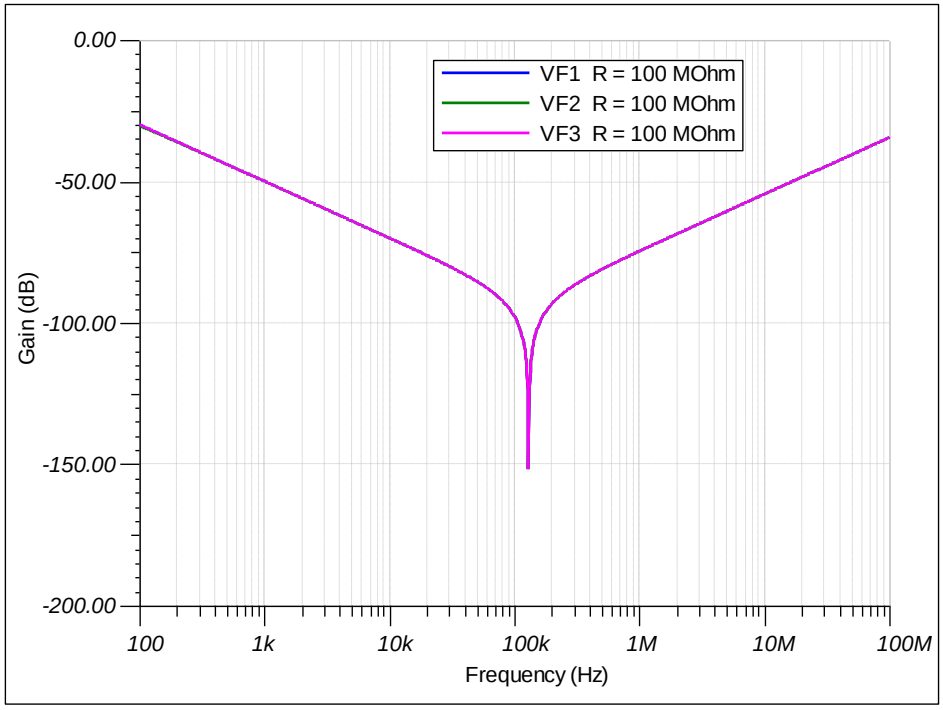

Fig. 75 Frequency response of circuit with same R_M

However when the measuring resistor decreases its value, the frequency response curve moves up in the meaning of sensitivity.

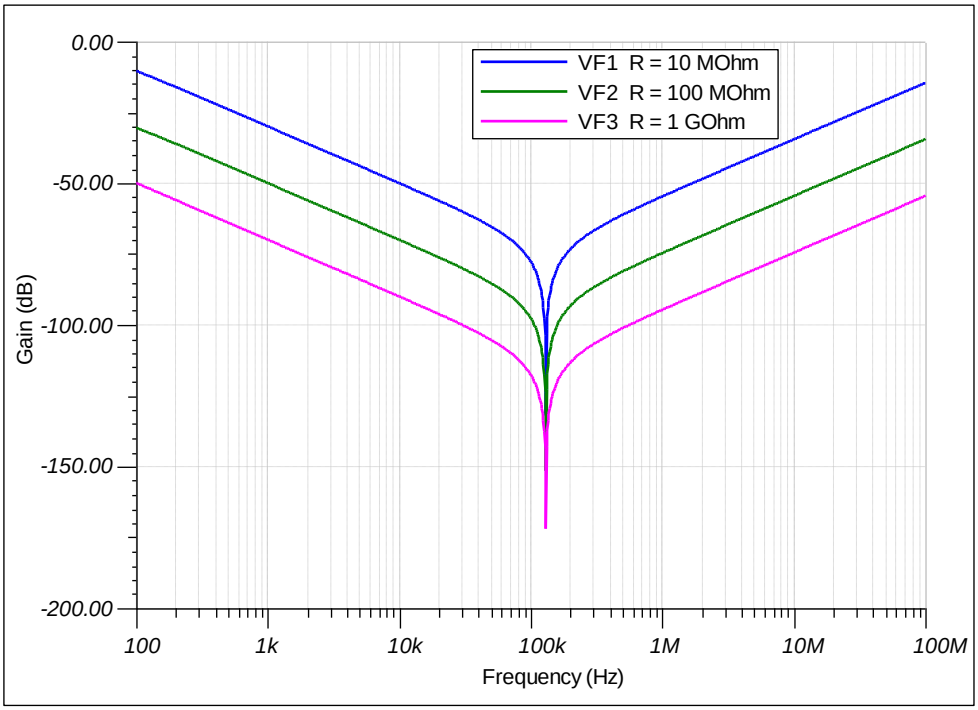

Fig. 76 Frequency response of circuit with various R_M

The RLC circuit with three various arms to show the measuring circuit behaviour is displayed in Fig. 77. Arm 1 (output VF1) represents a single RLC network with two resonances. Arm 2 represents a pure capacitor character C = 50 pF. Finally, arm 3 is the RLC network with one resonance.

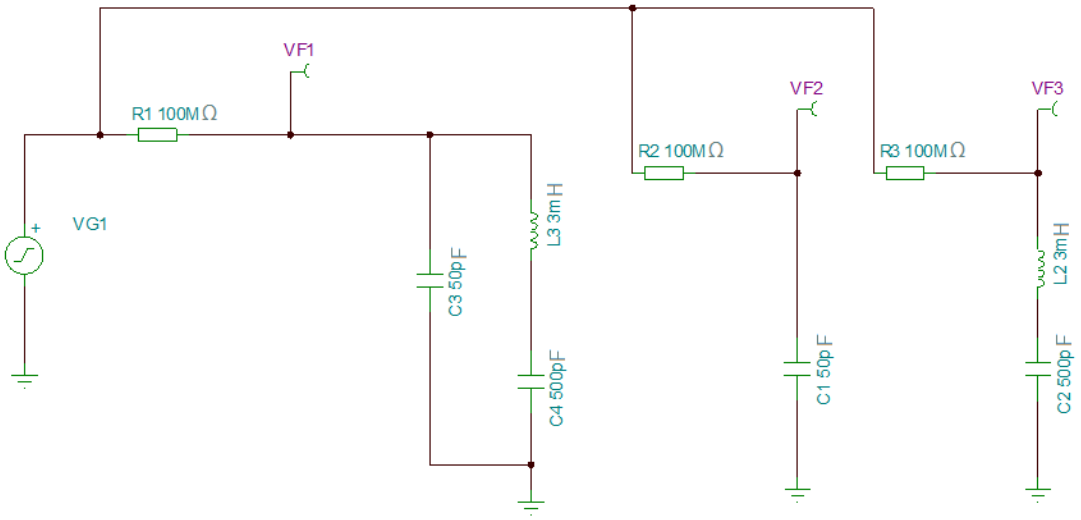

Fig. 77 RLC circuit – various arm connections

As can be seen in Fig. 78, arm 1 and 3 have the same behaviour in frequency response until the first resonance of arm 1. Afterwards arm 1 shows the second resonance. Arm 2 represented by pure capacitor shows capacitive character (since it is an ideal capacitor it

does not show its resonance frequency). It can be seen that after the resonance of arm 3, the capacitive character is changed to the inductive character. In case of arm 1 the LC sub-arm (represented by L_3 and C_4) is excluded after its resonances and only capacitor C_3 remains. This can be clearly seen from frequency 1 MHz, when the VF1 and VF2 lines overlap each other.

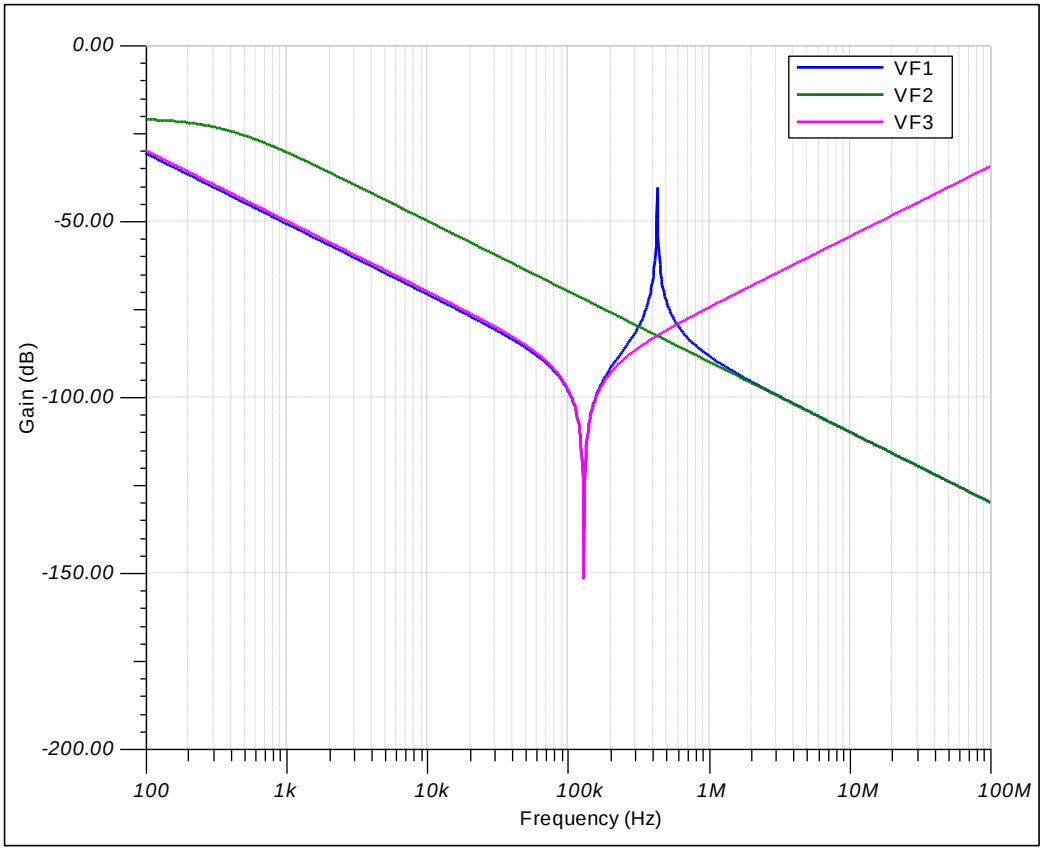

Fig. 78 Frequency response of circuit with various arms' connections

Fig. 79 introduces how determination of capacitance at given frequency ranges works. Arm 1 represents LC network (for example very simplified representation of transformer). There are three capacitors in parallel, each with capacitance 500 pF. Arm 2 represents pure capacitor with capacity 500 pF. Arm 3 represents pure capacitor with capacity 1000 pF. Arm 4 represents pure capacitor with capacity 1500 pF. In Fig. 80 can be seen the frequency response of given test circuit. As expected character of tested LC network is capacitive. Capacitance at lower frequencies (50 Hz) is 1500 pF – curves VF1 and VF4 overlapped each other. Nevertheless approximately at 500 Hz and 4 kHz two resonances occur and limit the capacitance of the test object at higher frequencies. It means that in case of PD measurement performed in frequency range 100 kHz - 500 kHz the capacitance of test circuit is not 1500 pF, but only 500 pF.

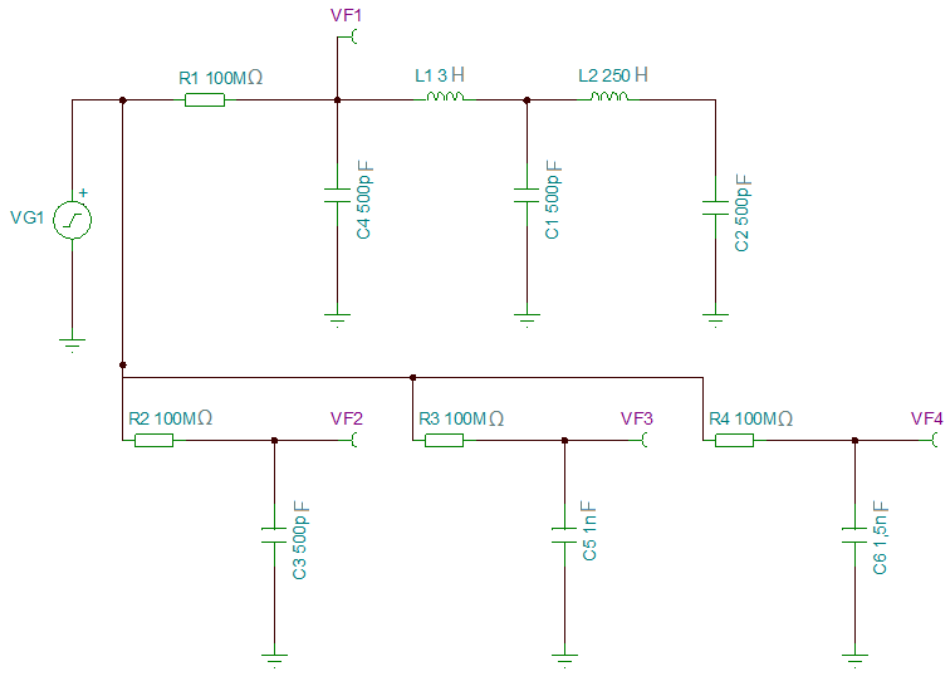

Fig. 79 LC network – determination of capacitance

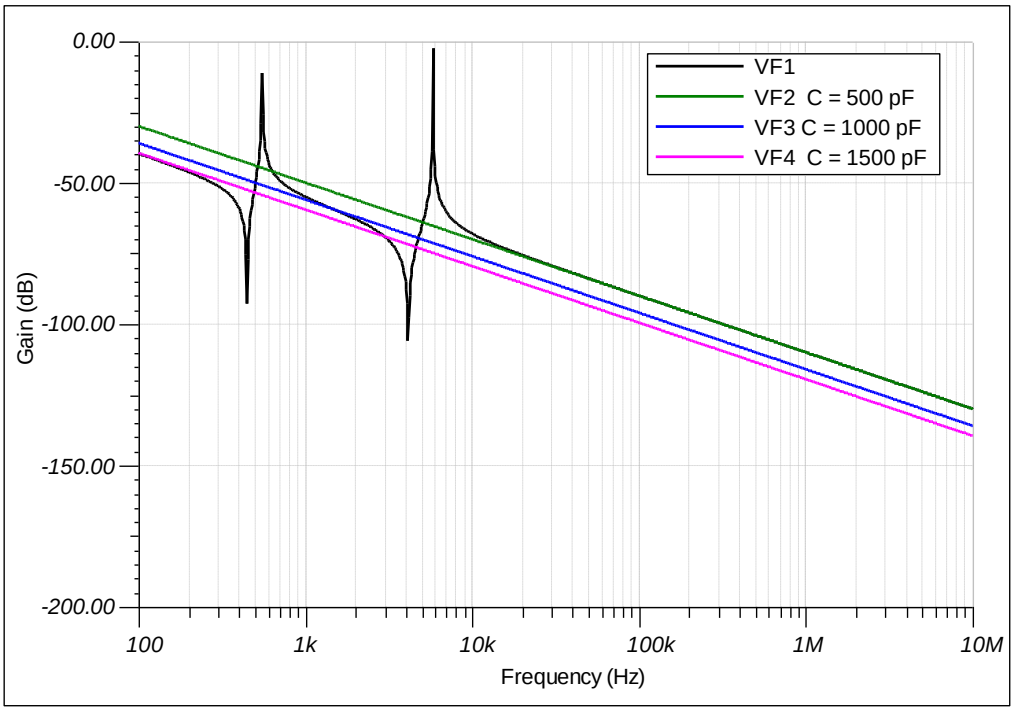

Fig. 80 Frequency domain of LC network – determination of capacitance

7.3 Practical on-side measurement examples

To verify and show the advantages of this method, several measurements on real transformers and rotating machines were done.

Following test procedure was designed:

1. Make connections according to the Fig. 73
2. Use various measuring resistor R_M to estimate proper sensitivity [1]
3. Choose the best measuring resistor concerning the best sensitivity
4. Record the impedance frequency characteristic
5. Use a database to compare measured curve with curves of pure capacitors [2]

[1] Influence of the size of measuring resistor R_M was explained in chapter 7.2, Fig. 76. It has proven as sufficient to use the following measuring resistors to cover most of the test objects' impedances R = 1 kΩ, 10 kΩ, 100 kΩ, 1 MΩ in common practise.

[2] It is recommended to create a measuring database of pure capacitors' impedance frequency characteristics. It is important to compare impedance frequency characteristics of pure capacitors and test object with the usage of the same value of measuring resistor R_M!

Magnitude of impedance function in Fig. 82 - Fig. 88 is calculated according to formula:

$$A = 20 \log \frac{U_2}{I_1} (dB) \quad (7)$$

7.3.1 Distribution transformers

First test object was the distribution transformer HV side 10.5 kV, LV voltage side 400 V (Fig. 81). Frequency response of HV phase U to ground with usage of various measuring resistors R_M was measured. As can be seen in Fig. 82, the measuring resistor R_M influences the measuring sensitivity. It fully correlates with simulation shown in Fig. 76.

Fig. 81 Distribution transformer HV side 10.5kV, LV voltage side 400 V

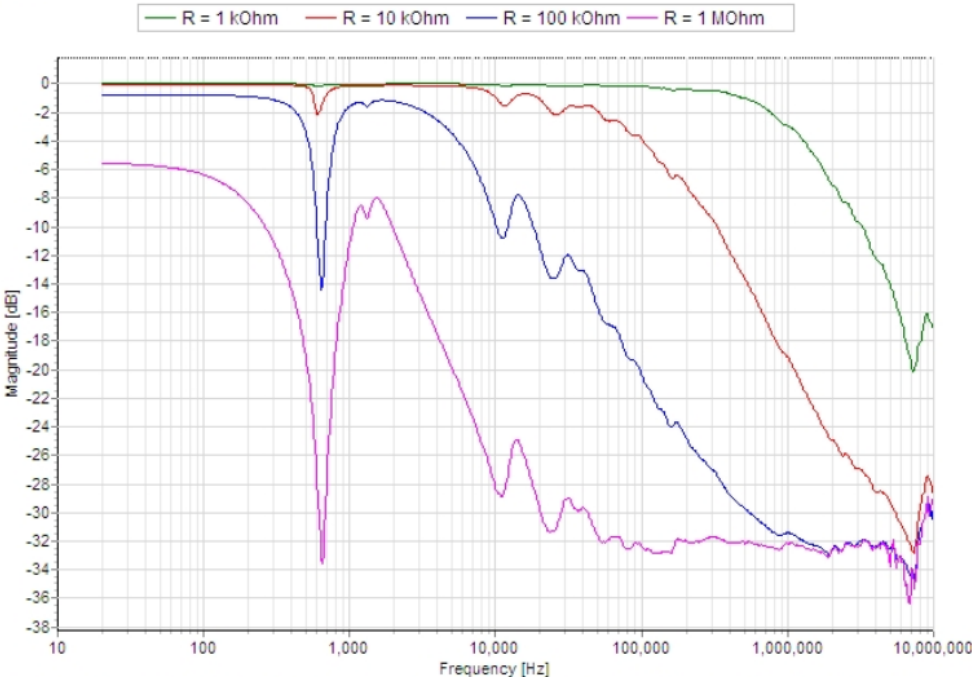

Fig. 82 Impedance frequency characteristic of distribution transformer 10.5/0.4 kV – various measuring resistors R_M

Fig. 83 shows impedance frequency characteristic of observed distribution transformer Machinenfabrik Oerlikon, Zürich (HV side 15.5 – 16.5 kV, LV 400 V, S = 75 kVA). The capacitance of single phase U by the Tettex MIDAS 288x (Mobile Insulation Diagnosis & Analyzing System) was measured [98]. MIDAS includes a capacitance and tan δ

(dissipation factor) measuring bridge. Measured capacitance was 1.3 nF. It can be noticed that the first resonances occurs at approx. 650 Hz. For comparison, several pure capacitors were measured by the same test procedure. In frequency range specified for PD measurement (100 kHz – 500 kHz) is the capacitance between the range 100 – 150 pF. It means 10 times lower value then at 50 Hz.

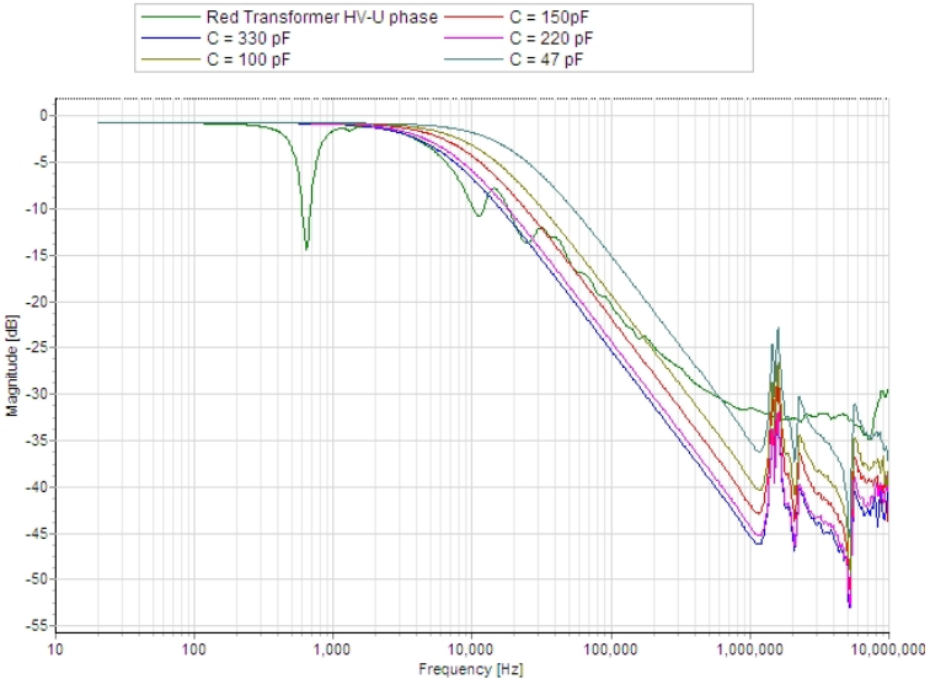

Fig. 83 Impedance frequency characteristic of distribution transformer 10.5/0.4 kV

Next two distribution transformers were measured. To gain reference capacitance at 50 Hz MIDAS system was used. First transformer was Brown Boveri (HV side 10 – 10.6 kV, LV 400 V, S = 400 kVA) - on the left hand side at Fig. 84 - $C_{HVwinding}$ = 2 nF. Second transformer Breda (HV side 19 – 21 kV, LV 400 V, S = 630 kVA) - on the right hand side at Fig. 84 - $C_{HVwinding}$ = 3.7 nF.

Fig. 84 Distribution transformers Brown Boveri and Breda

Fig. 85 shows a impedance frequency characteristic of distribution transformer Brown Boveri. Capacitance of High Voltage winding measured by MIDAS system was C = 2 nF. Capacitance derived from impedance frequency characteristic is near 2.2 nF. It proves a good correlation of both measuring techniques. At 50 kHz first resonance occurs. After that, one by one resonance occurs. Since resonances occur in continuity with each other, it is complicated to estimate the capacitance. Capacitance can be determined in a steady-state after the resonance, not during the resonance, as shown in Fig. 78. Anyway, by a rough estimation, the capacitance decreased significantly.

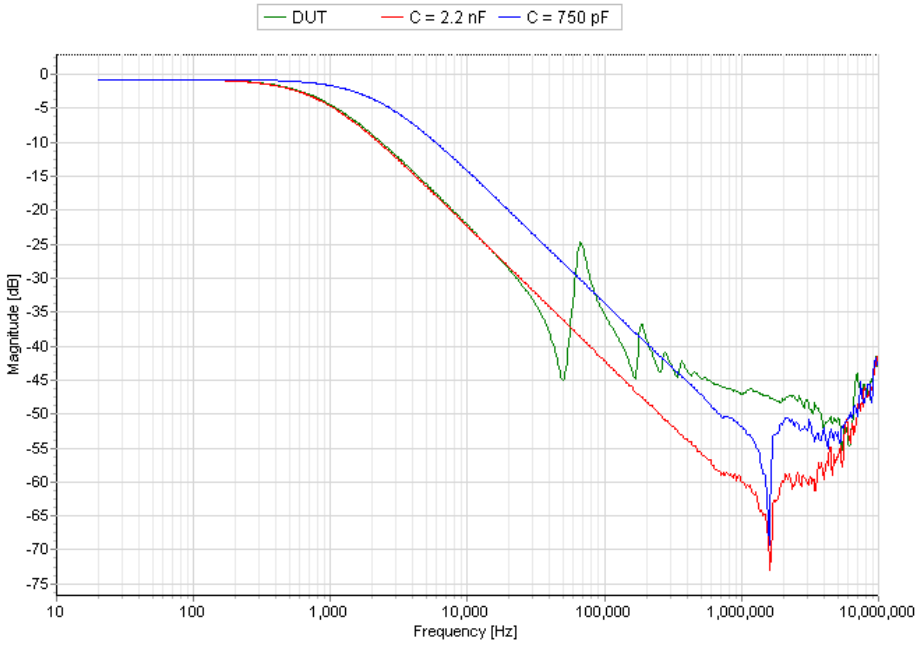

Fig. 85 Impedance frequency characteristic of distribution transformer Brown Boveri

Impedance frequency characteristic of distribution transformer Breda is shown in Fig. 86. Capacitance of High Voltage winding measured by MIDAS system was C = 3.7 nF. First resonance occurs at 300 kHz and as can be estimated from impedance frequency characteristic, capacitance decreased to 1.5 nF. At 600 kHz next resonance occurs and the capacitance drops to 750 pF. At approximately 1 MHz is the capacitance only 200 pF. This conclusion is based on the graphical agreement of given curve lines. This approach is applied in general as the core of this technique.

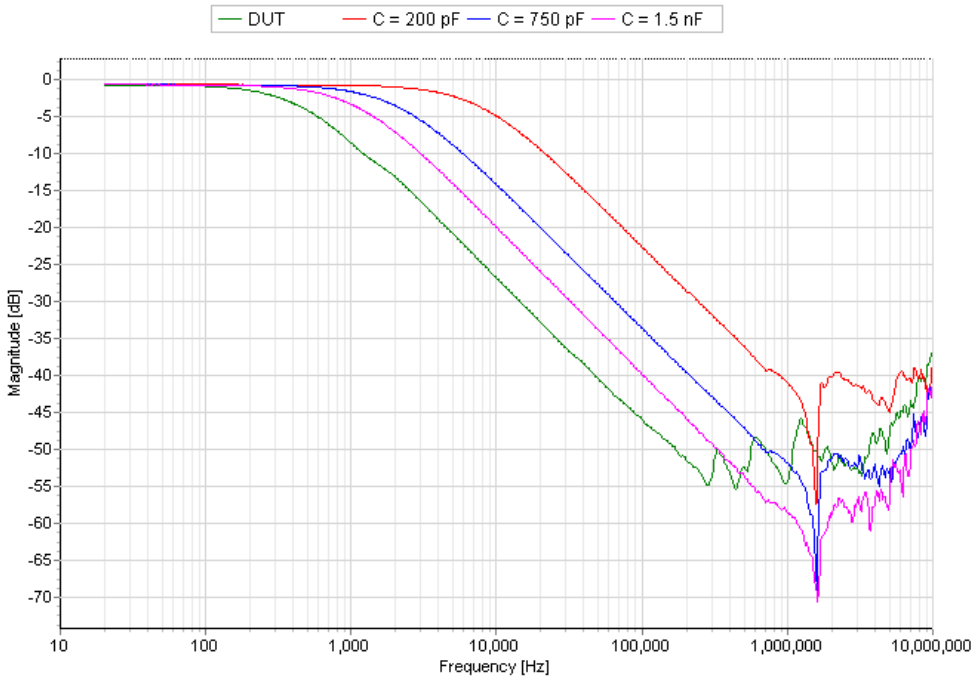

Fig. 86 Impedance frequency characteristic of distribution transformer Breda

7.3.2 Rotating machines

A stator winding of motor with nominal voltage U_n = 5.5 kV (according to the name plate of the stator) was tested. Stator winding is a very complex electrical system. Within the slot part stator winding has a transmission line character. A theoretical assumption for a large rotating machine follows. Let's assume that the stator bar has a length 5 m. From that a capacitance 5 nF can be derived (1nF per 1 m). There exist also design rule that every centimetre of leads has inductance 1 nH [100], it means 5 m lead has 5 μH inductance. From that characteristic/surge impedance can be calculated as $Z_0 = \sqrt{\frac{L}{C}} = \sqrt{\frac{5\times10^{-6}}{5\times10^{-9}}} \cong 30\ \Omega$. Outside of the slot - the end winding part - the characteristic/surge impedance is not well defined and coil end winding seems to behave as inductance, with significant mutual capacitance to other coils. [99]

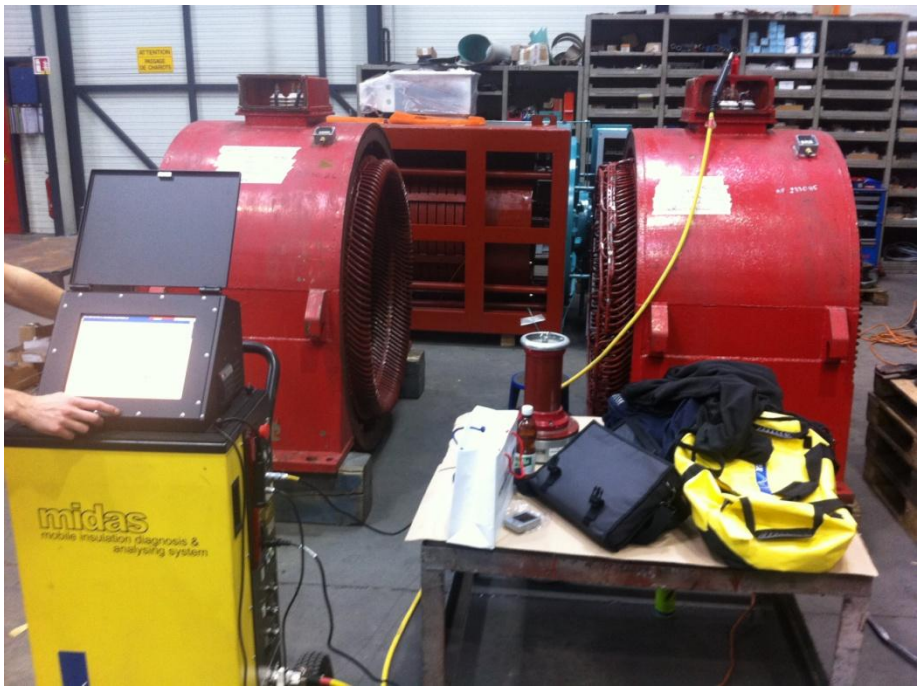

Fig. 87 Stator winding U_n = 5.5 kV.

A capacitance of the stator winding (all phases together to ground) measured by MIDAS system was C = 220 nF. That perfectly correlates with capacitances estimated from the impedance frequency characteristic show in Fig. 88. After several resonances, the capacitance in frequency range 400 kHz - 1 MHz decreased to only 2.2 nF. It means one hundred times lower value than at 50 Hz.

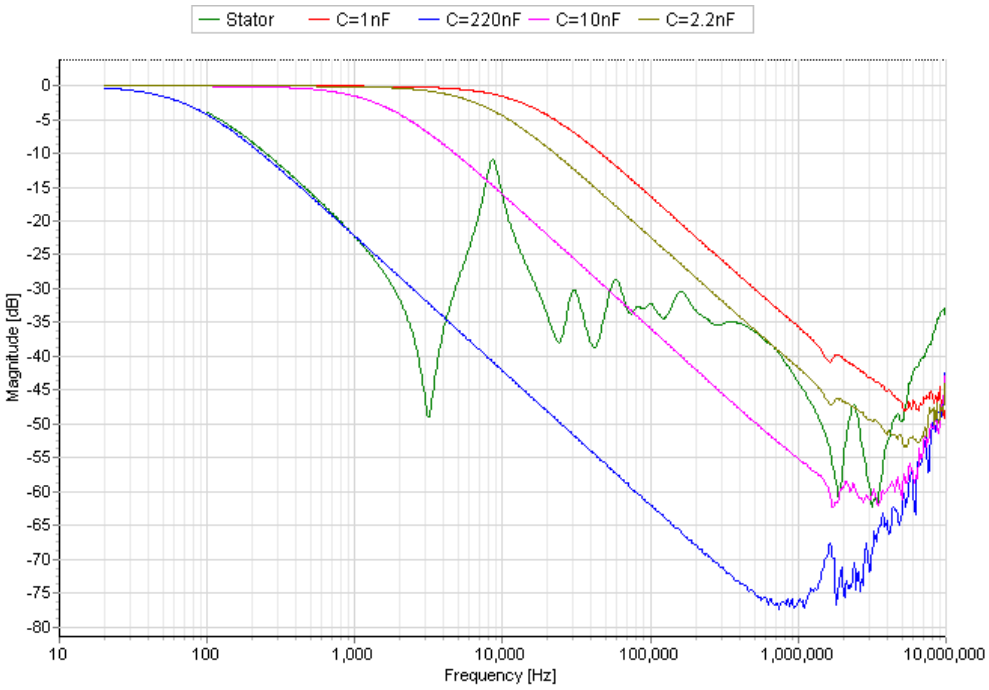

Fig. 88 Impedance frequency characteristic of stator of rotating machine

7.4 Summary

By using special new developed measuring technique it was proved that the capacitance of electrical devices with winding decreases over the frequencies. This is caused by local resonances caused by complexity of design and RLC character of these devices. By modified FRA measuring test technique, it is possible to find resonance frequencies and estimate the approximate capacitance at a specific frequency range and derive the proper coupling capacitor for PD measurement. The main advantage of this measuring technique is its simplicity of performance. Measurement can be easily done on-site, since FRA disposes with big, easy to handle connection clamps, and measurement is done under the safe conditions for both the test equipment and the operator. It is important to point out that the conclusion of this method cannot be that only a part of the machines is measured in higher frequencies, e.g. only the closest 2 stator bars to the testing point. It is clear that by resonances, the single arms of machine's equivalent circuit are excluded. Anyway, the propagation of the PD current pulse through the complex RLC network is not easy to define, since even to estimate the exact equivalent circuit of the device is not possible. Thanks to the mutual capacitance coupling, the PD pulse can cross-couple through the system – e.g. between single stator bars at end-winding part and hence even pulses originate deep inside the winding can be measured and recorded.

8 Thesis contributions

In chapter 5 the apparent charge Q_{iec} was discussed as the only evaluation PD parameter, as it is recommended in majority of international standards dealing with PD measurement on electrical devices. It was clearly shown that in certain cases the apparent charge Q_{iec} can lead to incorrect conclusions concerning PD activity. It was proven that measuring other complementary parameters such as discharge current I can be strongly recommended. New methodology of partial discharge recording and analysis was established. Following this test procedure should provide plausibility and full understanding of PD behaviour at given devices.

PRPD (Phase Resolved Partial Discharge) pattern was discussed in case of various PD sources being recognised, which showed its limitations in case of multiple PD sources. Chapter 6 presents and verifies the discrimination of PD sources in frequency- domain. Particular limitations of this technique were also introduced along with new evaluation approach for PD phenomena differentiation in time- domain. Unlimited growth of the capacity of coupling capacitor was also proven inappropriate, since duration of de-coupled PD pulses increases and subsequently causes the frequency- response to be no longer obligated to comply with IEC standard recommendations. Particular limits of IEC 60270 standard frequency range and bandwidth were shown and so called “pulse less area” phenomenon in case of corona discharges was explained. Nevertheless this particular restriction concerning limited possibility of repetition rate recording can be also noticed in other cases of PD measurement and is therefore necessary to be taken into account.

Last contribution of this work is explanation of PD measurement on high capacity electrical devices including windings. The relation between the sizes of coupling capacitor and capacity of a test object was explained as well. Capacity of the test object is much higher than in case of PD measuring frequencies if performed at the frequency of 50 Hz, at which capacitance measurement is usually done. New measurement technique of how to recognise and evaluate this behaviour was also introduced.

The following findings can be considered as original contributions of this thesis:

- Establishment of the new methodology of partial discharge recording and analysis. Specific limitation of current evaluation techniques were pointed out and appropriate new methodology was designed and verified.
- Design and verification of frequency- and time- domain multiple PD sources recognition. A problematic of multiple PD sources was discussed and limitations of current evaluation tools were described and consequently possible solution for recognition of multiple PD sources in frequency- domain was introduced and verified. A new PD source recognition technique in time- domain was shown.
- Explanation of the PD measurement on high capacity electrical devices including windings, and definition of the new unpublished measurement technique of how to recognise and evaluate the behaviour of these devices.

9 Conclusion

The thesis has shown and proved practical importance of partial discharge measurement and evaluation. Outcomes of the thesis have a significant contribution in practice. As every diagnostic method, even PD measurement technique has its particular limitations, which were introduced in this work. Currently, the apparent charge Q_{iec} is used as a major or single evaluation parameter. This work discussed limitations of this attitude and offered appropriate solution. Based upon the previously mentioned findings a new methodology of partial discharge measurement and analysis was introduced.

During the PD measurement it is necessary to take into account fundamental standard IEC 60270 along with its consequent limitations. One of the key elements of PD measurement is measuring sensitivity. Given recommendations of C_k:C_t ratio should be followed. However, it is not possible to increase the size of coupling capacitor C_k without any significant limitations while remaining in compliance to IEC standard. In case of electrical devices including winding, such as transformers or rotating machines, measuring sensitivity and C_k:C_t ratio have specific character and behaviour. Character of the test object and certain resonance behaviour must be taken into account in these particular cases. Following the special measuring technique introduced in this work allows the proper size of coupling capacitor to be derived.

Evaluation procedure follows after the measurement process. Time trends or characteristic absolute values of apparent charge and discharge current are evaluated. This helps in case of condition tests evaluation. However standard PD measuring technique is even able to define which type of PD defect causes PD activity, which helps during the troubleshooting. One of the tools to perform this process is PRPD pattern. Particular limitations can arise in case of multiple PD sources. It is then necessary to follow special PD discrimination techniques in time- or frequency- domain. These particular issues need to be examined in more detail and require further research as well as practical verification.

Concerning the new evaluation magnitudes such as discharge current I, it can be recommended to follow a trending of this value. Absolute value cannot be taken into account since every company producing PD detectors uses different pulse recognition technique, which is know-how of the company. Hence the repetition rate N, which is used

for discharge current I calculation, differs depending on the used PD instrument. Nevertheless, this thesis has shown that discharge current I is a very useful complementary parameter and together with apparent charge Q_{iec} helps to comprehensively describe the condition of observed electrical devices. Based on long-term experience, an apparent charge Q_{iec} limits were established and defined in specific standards. New PD measuring procedure was designed in Chapter 5.4. The limits for apparent charge Q_{iec} are given by international standards. In case of new complementary parameters, such as discharge current, it is recommended to compare the values of sister units and then follow the trending. In case of significant increase (which can differ depending on the parameters of the device that is being tested) of particular value further analysis, such as PRPD pattern recognition, should be performed.

Even though PD diagnostic technique is very powerful tool, it is generally not possible to evaluate the device condition solely by using one diagnostic parameter. PD measurement should be hence taken into account as one of the diagnostic tools from the wide range of complex diagnostic systems that should be designed for every tested component. PD evaluation technique depends as well as every other diagnostic tool, on the type, size, and application of the tested object. Specific limits then need to be adapted on cables (where the insulation system is very sensitive to PD activity). Different limits are set for rotating machines, where the mica material, which resists PD activity quite well, is used in the insulation system. It can be concluded that a diagnostic system with particular limits should be specifically designed for each application and each type of an electrical device.

Literature

[1] Cigre Brochure WG A1.10: Survey of Hydrogenerator Failures, 2009, p. 22

[2] Cigre Electra JWG 33/23.12: Insulation co-ordination of GIS: return of experience on site tests and diagnostic techniques, 1998, p. 32

[3] Cigre session, SC 15, Partial discharges tests on GIS installation in Malaysia. Techniques and experiences, 2000, p. 10

[4] Cigre session, SC D1, Experience of the on-line intelligent partial discharge monitoring (IPDM) system for GIS using UHF method, 2006, p. 8

[5] Cigre Electra WG A2.37: Transformer Reliability Survey: Interim Report. 2012, p. 4

[6] Cigre session, SC 15, Partial discharges in transformer insulation, 2000, p. 12

[7] Cigre session, SC D1, Partial discharge and dissolved gas analysis of common fault types in bio-degradable oil transformers, 2010, p. 10

[8] Cigre Session, SC A1: Experience with continuous monitoring partial discharge testing in a predictive maintenance application of three similar hydro machines, 2010, p. 11

[9] IEC 60270:2000 High-voltage test techniques - Partial discharge measurements

[10] IEC 60076-3:2000, Power transformers – Part 3: Insulation levels, dielectric tests and external clearances in air, second edition

[11] IEC 60044-1:2003, Instrument transformers – Part 1: Current transformers

[12] Brutsch, Rudolf, et al. Insulation failure mechanisms of power generators [feature article]. Electrical Insulation Magazine, IEEE, 2008, 24.4: 17-25.

[13] IEC 62271-203:2011 - High-voltage switchgear and controlgear – Part 203: Gas-insulated metal-enclosed switchgear for rated voltages above 52 kV

[14] Doble Lemke GmbH, internal company documents, 2012

[15] IEEE Trial-Use Guide to the Measurement of Partial Discharges in Rotating Machinery," IEEE Std 1434-2000 , vol., no., pp.i,, 2000

[16] IEC 60034-27:2006, Rotating electrical machines – Part 27: Off-line partial discharge measurements on the stator winding insulation of rotating electrical machines, first edition

[17] IEC 60885-2:1987, Electrical test methods for electric cables – Part 2: Partial discharge tests

[18] IEC 60885-3:1988, Electrical test methods for electric cables – Part 3: Test methods for partial discharge measurements on lengths of extruded power cables.

[19] IEC 60502-2:1998, Power cables with extruded insulation and their accessories for rated voltages from 1 kV (Um = 1,2 kV) up to 30 kV (Um = 36 kV) – Part 2: Cables for rated voltages from 6 kV (Um = 7,2 kV) up to 30 kV (Um = 36 kV)

[20] IEC 60840:1999, Power cables with extruded insulation and their accessories for rated voltages above 30 kV (Um = 36 kV) up to 150 kV (Um = 170 kV) – Test methods and requirements

[21] IEC 62067:2001, Power cables with extruded insulation and their accessories for rated voltages above 150 kV (Um = 170 kV) up to 500 kV (Um = 550 kV) – Test methods and requirements

[22] Cigre Session, SC A1: Experience with partial discharge (PD) monitoring system for hydro generators, 2010, p.19

[23] Cigre Brochure WG A1.01.06: Application of On-Line Partial Discharge Tests to Rotating Machines, 2004, p.12

[24] Cigre Session, SC A1: Field experience in monitoring partial discharges in rotating machines, 2010, p.8

[25] Tozzi, M.; Salsi, A.; Busi, M.; Montanari, G.C.; Cavallini, A.; Hart, P.M., "Permanent PD monitoring for generators: Smart alarm management," Innovative Smart Grid Technologies Asia (ISGT), 2011 IEEE PES , vol., no., pp.1,6, 13-16 Nov. 2011

[26] Fornasari, L.; Montanari, G.C.; Cavallini, A., "Alarm management in permanent PD monitoring for generators," Electrical Insulation (ISEI), Conference Record of the 2012 IEEE International Symposium on , vol., no., pp.571,575, 10-13 June 2012

[27] Renforth, L.; Goodfellow, S.; Foxall, M.; Clark, D.; Shuttleworth, R., "On-line partial discharge testing of in-service rotating machines in ex hazardous environments by employment of central monitoring solutions," Electrical Insulation (ISEI), Conference Record of the 2012 IEEE International Symposium on , vol., no., pp.565,570, 10-13 June 2012

[28] Kheirmand, A.; Leijon, M.; Gubanski, S.M., "Advances in online monitoring and localization of partial discharges in large rotating machines," Energy Conversion, IEEE Transactions on , vol.19, no.1, pp.53,59, March 2004

[29] Stone, G.C., "A perspective on online partial discharge monitoring for assessment of the condition of rotating machine stator winding insulation," Electrical Insulation Magazine, IEEE , vol.28, no.5, pp.8,13, September-October 2012

[30] Gross, D.W., "Partial discharge measurement and monitoring on rotating machines," *Electrical Insulation, 2002. Conference Record of the 2002 IEEE International Symposium on* , vol., no., pp.570,574, 7-10 Apr 2002

[31] Bethge, A.; Lo, P.K.-W.; Phillipson, J.T.; Weidner, J.R., "On-line monitoring of partial discharges on stator windings of large rotating machines in the petrochemical environment," *Industry Applications, IEEE Transactions on* , vol.34, no.6, pp.1359,1365, Nov/Dec 1998

[32] Mentlík, Václav. Dielektrické prvky a systémy. 1. vyd. Praha: BEN - technická literatura, 2006, 235 s. ISBN 80-730-0189-6.

[33] Mentlík, V., Pihera, J., Polanský R., Prosr P., Trnka, P. Diagnostika elektrických zařízení. 1. vyd. Praha: BEN - technická literatura, 2008, 439 s. ISBN 978-80-7300-232-9.

[34] Kučerová, Eva. Elektrotechnické materiály. 1. vyd. V Plzni: Západočeská univerzita, 2002, 174 s. ISBN 80-708-2940-0.

[35] König, Dieter and Y. Narayana Rao. Partial discharges in electrical power apparatus. Berlin [u.a.], 1993. ISBN 38-007-1760-3.

[36] Kreuger, F.H. Partial discharge detection in high-voltage equipment. London: Butterworths. ISBN 0408020636.

[37] Weber, H. J. Partial Discharge Measuring Techniques. Tettex-Information 21, 1984

[38] Osvath, P.; Zaengl, W.; Weber, H. J. Measurement of Partial Discharge – Problems and how they can be solved with a flexible measuring system. Tettex-Information 23, 1985

[39] Mráz, P. Problematika částečných výbojů v elektrických zařízeních. Work for State doctoral exam. WBU in Pilsen. 2011.

[40] Lemke, E., "A critical review of partial-discharge models," Electrical Insulation Magazine, IEEE , vol.28, no.6, pp.11,16, Nov.-Dec. 2012

[41] Lemke, E., "Analysis of the partial discharge charge transfer in extruded power cables," Electrical Insulation Magazine, IEEE , vol.29, no.1, pp.24,28, January-February 2013

[42] Záliš, Karel. Částečné výboje v izolačních systémech elektrických strojů. Vyd. 1. Praha : Academia, 2005. 140 s. ISBN 80-200-1358-X.

[43] Mráz, P., Mentlík, V., Pihera, J. Aspekty měření a vyhodnocování částečných výbojů. In Proceedings of the 13th International Scientific Conference Electric Power Engineering 2012. Brno: Brno University of Technology, 2012. s. 791-796. ISBN: 978-80-214-4514-7

[44] Umemura, T.; Nakamura, S.; Hikita, M.; Maeda, T.; Higashiyama, M., "Partial discharges of small-air-gap in cast-resin insulation system," Dielectrics and Electrical Insulation, IEEE Transactions on , vol.20, no.1, pp.255,261, February 2013

[45] Tanaka, T.; , "PD pulse distribution pattern analysis," Properties and Applications of Dielectric Materials, 1994., Proceedings of the 4th International Conference on , vol.2, no., pp.662-665 vol.2, 3-8 Jul 1994

[46] Welsch, A.; Haller, R. Partial Discharge Diagnostics for Localisation of Defect Parts in Gas Insulated Medium Voltage Swithgear. XV International Symposium on High Voltage Engineering. 2007, Ljubljana, Slovenia

[47] Kornhuber, Stefan; Boltze, Matthias; Haller, Rainer; Mraz, Petr; Pihera, Josef; , "PD behaviour of basic test arrangements under different measurement conditions," Condition Monitoring and Diagnosis (CMD), 2012 International Conference on , vol., no., pp.557-560, 23-27 Sept. 2012

[48] Gross, D., W. „Locating partial discharge using acoustic sensors", HighVolt Kolloquium '11, May 19-20, 2011, Dresden, Germany, pp. 99-106

[49] Bodega, R.; Morshuis, P.H.F.; Lazzaroni, M.; Wester, F.J.; , "PD recurrence in cavities at different energizing methods," Instrumentation and Measurement, IEEE Transactions on , vol.53, no.2, pp. 251- 258, April 2004

[50] Gross, D.W.; Fruth, B.A.; , "Characteristics of phase resolved partial discharge pattern in spherical voids," Electrical Insulation and Dielectric Phenomena, 1998. Annual Report. Conference on , vol., no., pp.412-415, vol. 2, 25-28 Oct 1998

[51] Das, S.; Purkait, P.; , "ϕ-q-n pattern analysis for understanding partial discharge phenomena in narrow voids," Power and Energy Society General Meeting - Conversion and Delivery of Electrical Energy in the 21st Century, 2008 IEEE , vol., no., pp.1-7, 20-24 July 2008

[52] Nakao, K.; Suzuoki, Y.; Mizutani, T.; , "PD patterns and PD current shapes of LDPE specimen with a void," Conduction and Breakdown in Solid Dielectrics, 1998. ICSD '98. Proceedings of the 1998 IEEE 6th International Conference on , vol., no., pp.157-160, 22-25 Jun 1998

[53] Mizutani, T.; Kondo, T.; , "PD patterns and PD current shapes of a void in LDPE," Properties and Applications of Dielectric Materials, 2000. Proceedings of the 6th International Conference on , vol.1, no., pp.276-279 vol.1, 2000

[54] Wu, K.; Okamoto, T.; Suzuoki, Y.; , "A simulation model for PD patterns in voids with consideratio of PD discharge areas," Electrical Insulation and Dielectric Phenomena, 2000 Annual Report Conference on , vol.2, no., pp.649-652 vol.2, 2000

[55] Ijichi, K.W.T.; Kojima, A.; Komori, F.; Suzuoki, Y.; , "Influence of PD rest time on φ-q-n patterns from voids," Solid Dielectrics, 2001. ICSD '01. Proceedings of the 2001 IEEE 7th International Conference on , vol., no., pp.93-96, 2001

[56] Wu, K.; Komori, F.; Suzuoki, Y.; , "Effects of oxygen on the formation of rabbit-like PD pattern in a void between metal surfaces," Electrical Insulating Materials, 2001. (ISEIM 2001). Proceedings of 2001 International Symposium on , vol., no., pp.37-40, 2001

[57] Kim, C.-S.; Kondo, T.; Mizutani, T.; , "Change in PD pattern with aging," Dielectrics and Electrical Insulation, IEEE Transactions on , vol.11, no.1, pp. 13- 18, Feb. 2004

[58] Junhao Li; Wenrong Si; Xiu Yao; Yanming Li; , "Partial discharge characteristics over differently aged oil/pressboard interfaces," Dielectrics and Electrical Insulation, IEEE Transactions on , vol.16, no.6, pp.1640-1647, December 2009

[59] Berg, G.; Lundgaard, L.E.; , "Discharges in combined transformer oil/paper insulation," Dielectric Liquids, 1999. (ICDL '99) Proceedings of the 1999 IEEE 13th International Conference on , vol., no., pp.144-147, 1999

[60] Yang Jia-xiang; Chi Xiao-Chun; Ding Li-Jian; Liu ji; , "Creeping discharge performance of oil-paper insulation with streaming electrification," Dielectrics and Electrical Insulation, IEEE Transactions on , vol.4, no.6, pp.780-784, Dec 1997

[61] Beroual, A.; Kebbabi, L.; , "Analysis of cumulative number and polarity of creeping discharges initiated at solid/liquid interfaces subjected to AC voltage," Electrical Insulation and Dielectric Phenomena, 2009. CEIDP '09. IEEE Conference on , vol., no., pp.380-383, 18-21 Oct. 2009

[62] Kiiza, R.C.; Niasar, M.G.; Nikjoo, R.; Wang, X.; Edin, H.; Ahmed, Z.; , "Comparison of phase resolved partial discharge patterns in small test samples, bushing specimen and aged transformer bushing," Electrical Insulation and Dielectric Phenomena (CEIDP), 2012 Annual Report Conference on , vol., no., pp.88-91, 14-17 Oct. 2012

[63] Hudon, C.; Belec, M.; , "Partial discharge signal interpretation for generator diagnostics," Dielectrics and Electrical Insulation, IEEE Transactions on , vol.12, no.2, pp. 297- 319, April 2005

[64] Mráz, P., Mentlík, V., Pihera, J. Partial Discharge Apparent Charge Measurement. In Elektroenergetika 2013 : proceedings of the 7th International Scientific Symposium on Electrical Power Engineering. Košice: Technical University, 2013. p. 409-412. ISBN: 978-80-553-1441-9

[65] Šašek, L., Alexa, L.: O příčinách vzniku a formě projevu povrchových výbojů v drážkách elektrických točivých strojů, EO n.3/1981, p. 139-147

[66] Šašek, L.: Aktuální problémy údržby statorových vn vinutí elektrických točivých strojů, EO n.7/1984, p.359-362

[67] J. S. Johnson and M. Warren, "Detection of slot discharges in high-voltage stator windings during operatio," Trans. Am. Inst. Electr. Eng., vol. 70, no. 2, pp. 1998–2000, 1951.

[68] G. C. Stone, E. A. Boulter, I. Culbert, H. Dhirani, "Electrical Insulation for Rotating Machines: Design, Evaluation, Aging, Testing, and Repair," Wiley-IEEE Press, December 2003

[69] Niu, H.Q.; Cavallini, A.; Montanari, G.C., "Identification of Partial Discharge Phenomena in HVDC Apparatus," Electrical Insulation, 2008. ISEI 2008. Conference Record of the 2008 IEEE International Symposium on , vol., no., pp.373,376, 9-12 June 2008

[70] Cavallini, A.; Montanari, G.C.; Tozzi, M.; Chen, Xiaolin, "Diagnostic of HVDC systems using partial discharges," Dielectrics and Electrical Insulation, IEEE Transactions on , vol.18, no.1, pp.275,284, February 2011

[71] Jiang, T., Grzybowski, S., He, Z., Liao, R., "Statistical Features Used for Recognition of Partial Discharge under AC-DC Combined Voltages," In 17th International Symposium on High Voltage Engineering. Berlin: VDE Verlag Gmbh, 2011. ISBN: 978-3-8007-3364-4

[72] Liu, Y., Du, B. X., "Acoustic Characteristics of Surface Discharge for Hydrophobicity Evaluation of HVDC Insulator," In ISH 2013 : proceedings : 18th International Symposium on High Voltage Engineering. Seoul: Hanyang University, 2013. p. 1529-1534. ISBN: 978-89-86510-18-8

[73] Swanson, A., Grant, M. D., Jandrell, I. R., Hofsajer, I., "HVDC Corona - Experimental Setup and Measurements," In ISH 2013 : proceedings : 18th International Symposium on High Voltage Engineering. Seoul: Hanyang University, 2013. s. 2328-2333. ISBN: 978-89-86510-18-8

[74] Fabian, J.; Muhr, M.; Jaufer, S.; Exner, W., "Partial discharge behavior of mineral oil and oil-board insulation systems at HVDC," Condition Monitoring and Diagnosis (CMD), 2012 International Conference on , vol., no., pp.285,288, 23-27 Sept. 2012

[75] Xinyan Wu; Hengkun Xie; Zongren Peng; Qingping Pang, "Partial discharge detection and location in cable joint," Electrical Insulating Materials, 1998. Proceedings of 1998 International Symposium on , vol., no., pp.721,723, 27-30 Sep 1998

[76] Gross, D.W.; Herbig, J.G., "Partial discharge fault location and diagnosis on HV power cables," Electrical Insulation and Dielectric Phenomena, 2000 Annual Report Conference on , vol.2, no., pp.630,633 vol.2, 2000

[77] Miri, S. M.; Privette, A., "A survey of incipient fault detection and location techniques for extruded shielded power cables," System Theory, 1994., Proceedings of the 26th Southeastern Symposium on , vol., no., pp.402,405, 20-22 Mar 1994

[78] Mashikian, M.S.; Bansal, Rajeev; Northrop, R.B., "Location and characterization of partial discharge sites in shielded power cables," Power Delivery, IEEE Transactions on , vol.5, no.2, pp.833,839, Apr 1990

[79] R. Bartnikas, “Partial discharges. Their mechanism, detection and measurement”, IEEE Trans. Dielectr. Electr. Insul., Vol. 9, pp. 763-808, 2002.

[80] Sikorski, W.; Siodla, K.; Moranda, H.; Ziomek, W., "Location of partial discharge sources in power transformers based on advanced auscultatory technique," Dielectrics and Electrical Insulation, IEEE Transactions on , vol.19, no.6, pp.1948,1956, December 2012

[81] Cole, P. T., "Location of partial discharges and diagnostics of power transformers using acoustic methods," Condition Monitoring of Large Machines and Power Transformers (Digest No: 1997/086), IEE Colloquium on , vol., no., pp.8/1,8/3, 19 Jun 1997

[82] Jones, S.L., "The detection of partial discharges in power transformers using computer aided acoustic emission techniques," Electrical Insulation, 1990., Conference Record of the 1990 IEEE International Symposium on , vol., no., pp.106,110, 3-6 Jun 1990

[83] Sedding, H.G.; Stone, G.C., "A discharge locating probe for rotating machines," Electrical Insulation Magazine, IEEE , vol.5, no.5, pp.14,17, Sept.-Oct. 1989

[84] Candela, R.; Contin, A., "A portable instrument for the location and identification of defects generating PD," Electrical Insulation Conference (EIC), 2011 , vol., no., pp.469,473, 5-8 June 2011

[85] Kheirmand, A.; Leijon, M.; Gubanski, S.M., "New practices for partial discharge detection and localization in large rotating machines," Dielectrics and Electrical Insulation, IEEE Transactions on , vol.10, no.6, pp.1042,1052, Dec. 2003

[86] Hoek, S.M.; Kraetge, A.; Kessler, O.; Broniecki, U., "Time-based partial discharge localization in power transformers by combining acoustic and different electrical methods," Condition Monitoring and Diagnosis (CMD), 2012 International Conference on , vol., no., pp.289,292, 23-27 Sept. 2012

[87] Sinaga, H.H.; Phung, B.T.; Blackburn, T.R., "UHF sensor array for partial discharge location in transformers," Condition Monitoring and Diagnosis (CMD), 2012 International Conference on , vol., no., pp.979,982, 23-27 Sept. 2012

[88] Mirzaei, H.R.; Akbari, A.; Zanjani, M.; Gockenbach, E.; Borsi, H., "Investigating the partial discharge electromagnetic wave propagation in power transformers considering active part characteristics," Condition Monitoring and Diagnosis (CMD), 2012 International Conference on , vol., no., pp.442,445, 23-27 Sept. 2012

[89] Tenbohlen, S.; Denissov, D.; Hoek, S.M.; Markalous, S.M., "Partial discharge measurement in the ultra high frequency (UHF) range," Dielectrics and Electrical Insulation, IEEE Transactions on , vol.15, no.6, pp.1544,1552, December 2008

[90] Coenen, S.; Tenbohlen, S.; Markalous, S.M.; Strehl, T., "Sensitivity of UHF PD measurements in power transformers," Dielectrics and Electrical Insulation, IEEE Transactions on , vol.15, no.6, pp.1553,1558, December 2008

[91] Tenbohlen, S.; Pfeffer, A.; Coenen, S., "On-site experiences with multi-terminal IEC PD measurements, UHF PD measurements and acoustic PD localisation," Electrical Insulation (ISEI), Conference Record of the 2010 IEEE International Symposium on , vol., no., pp.1,5, 6-9 June 2010

[92] Linear Technology - Design Simulation and Device model. [online]. 2014 [cit. 2014-06-06]. Accessible from: http://www.linear.com/designtools/software/

[93] Haller, R., “Partial Discharge Measurement – an essential tool for diagnosis of electrical equipments”, Electrical Power & Environmental Engineering, University of West Bohemia Pilsen, Czech Republic

[94] Omicron Electronics GmbH. [online]. 2014 [cit. 2014-29-06]. Accessible from: https://www.omicron.at/fileadmin/user_upload/pdf/literature/MPD-600-Brochure-ENU.pdf

[95] Power Diagnostix Systems. [online]. 2014 [cit. 2014-29-06]. Accessible from: http://www.pdix.com/products/pd-measurement-devices/icmsystem.html

[96] Haefely Test AG, "FRA 5310 - Sweep Frequency Response Analyser for Power Transformer Diagnosis ", Product brochure, Switzerland, p. 3, 2014

[97] Texas Instruments - Tina, Spice-Based Analog Simulation Program. [online]. 2014 [cit. 2014-03-07]. Accessible from: http://www.ti.com/tool/tina-ti

[98] Haefely Test AG, "MIDAS 288x Mobile Insulation Diagnosis & Analyzing System", Operating Instructions, Version 1.9, Switzerland, p. 168, 2012

[99] Stone, G., "Importance of bandwidth in PD measurement in operating motors and generators," Dielectrics and Electrical Insulation, IEEE Transactions on , vol.7, no.1, pp.6,11, Feb 2000

[100] Tektronix, Inc. [online]. 2014 [cit. 2014-09-06]. Accessible from: http://www2.electron.frba.utn.edu.ar/~jcecconi/Bibliografia/06%20-%20Osciloscopios%20de%20Almacenamiento%20Digital/Understanding_Oscilloscope_BW_RiseT_And_Signal_Fidelity.pdf

List of author's publications

[1] PIHERA, J., MRÁZ, P., HALLER, R., MENTLÍK, V. Partial discharges and breakdown voltage diagnostics during thermal aging of insulating materials. In Diagnostika '11. Pilsen: University of West Bohemia, 2011. s. 130-136. ISBN: 978-80-261-0020-1

[2] PIHERA, J., TRNKA, P., MENTLÍK, V., ŠIRŮČEK, M., MRÁZ, P. Corona Discharge within Organic Oil Insulations. In 2011 IEEE International Conference on Dielectric Liquids. Trondheim: SINTEF Energi AS, 2011. s. 1-4. ISBN: 978-1-4244-7355-7

[3] MRÁZ, P., MENTLÍK, V., PIHERA, J., HALLER, R. Aspects of partial discharge behaviour - voltage dependence. In Diagnostika '13. Pilsen: Universtiy of West Bohemia, 2013. s. 202-206. ISBN: 978-80-261-0210-6

[4] MRÁZ, P. Možnosti odstranění rušení při měření částečných výbojů. In Elektrotechnika a informatika 2013. Část 1., Elektrotechnika. Plzeň: Západočeská univerzita v Plzni, 2013. s. 87-90. ISBN: 978-80-261-0233-5

[5] MRÁZ, P., MENTLÍK, V., PIHERA, J. Partial discharge activity of thermally aged stator winding bars. In Annals of DAAAM for 2011 & Proceedings. Vienna: DAAAM International Vienna, 2011. s. 957-958. ISBN: 978-3-901509-83-4 , ISSN: 1726-9679

[6] DONČUK, J., MRÁZ, P. Možnosti stanovení vlhkosti v pevné izolaci transformátoru. Electroscope, 2012, roč. 2012, č. 2, s. 1-5. ISSN: 1802-4564

[7] MRÁZ, P. Posouzení stárnutí izolačních systémů sledováním výbojové činnosti. Plzeň, 2010., ISBN: 978-80-7043-913-5,

[8] MRÁZ, P. Posouzení stárnutí izolačních systémů sledováním výbojové činnosti. Plzeň, 2010., ISBN: 978-80-7043-913-5,

[9] MRÁZ, P., KINDL, V., HRUŠKA, K. INFLUENCE OF LOW–CONDUCTIVE COATING ON INSULATION SYSTEM OF ROTARY ELECTRIC MACHINE. Journal of ELECTRICAL ENGINEERING, 2012, roč. 63, č. 3, s. 180-185. ISSN: 1335-3632

[10] MRÁZ, P., PIHERA, J., MENTLÍK, V. Partial discharge measurement - state of the art. In ELEN 2012. Praha: České vysoké učení technické, 2012. s. 1-6. ISBN: 978-80-01-05096-5

[11] MRÁZ, P., MENTLÍK, V., PIHERA, J. A new approach in partial discharge activity: Observing of the consecutive pulses. In Diagnostika '11. Plzeň: University of West Bohemia, 2011. s. 24-28. ISBN: 978-80-261-0020-1

[12] KUPKA, L., PIHERA, J., MRÁZ, P., ŠIRŮČEK, M. Weibull statistic in material diagnostics. In Sborník z konference Diagnostika 11. Plzeň: Západočeská univerzita v Plzni, 2011. s. 28-31. ISBN: 978-80-261-0020-1

[13] MRÁZ, P. Problematika částečných výbojů v elektrických zařízeních. FEL, ZČU v Plzni : ZČU, 2011, 77 s. ISBN: neuvedeno

[14] HALLER, R., PIHERA, J., MRÁZ, P., KORNHUBER, S., BOLTZE, M. PD Behaviour Of Basic Test Arrangements Under Different Measurement And Evaluation Conditions. In 2011 Annual Report Conference on Electrical Insulation

and Dielectric Phenomena. Piscataway, NJ 0885 -1331.: Institute of Electrical and Electronics Engineers, 2011. s. 275-279. ISBN: 978-1-4577-0986-9 , ISSN: 0084-9162

[15] PIHERA, J., HALLER, R., MRÁZ, P. Evaluation Conditions for PD Measurement on Basic Test Ar-rangements. In Proceedings of the 13th International Scientific Conference Electric Power Engineering 2012. Brno: Brno University of Technology, 2012. s. 827-832. ISBN: 978-80-214-4514-7

[16] KORNHUBER, S., BOLTZE, M., HALLER, R., MRÁZ, P., PIHERA, J. PD Behaviour of Basic Test Arrangements under Different Measurement Conditions. In Proceedings of 2012 IEEE International Conference on Condition Monitoring and Diagnosis. Red Hook: IEEE, 2012. s. 557-560. ISBN: 978-1-4673-1020-8

[17] MRÁZ, P., MENTLÍK, V., PIHERA, J. Aspekty měření a vyhodnocování částečných výbojů. In Proceedings of the 13th International Scientific Conference Electric Power Engineering 2012. Brno: Brno University of Technology, 2012. s. 791-796. ISBN: 978-80-214-4514-7

[18] MRÁZ, P. Problémy měření částečných výbojů v elektrických zařízeních a jejich řešení. In Elektrotechnika a informatika 2012, část první Elektrotechnika. Plzeň: Západočeská univerzita v Plzni, 2012. s. 79-80. ISBN: 978-80-261-0120-8

[19] MRÁZ, P., MENTLÍK, V., PIHERA, J. Partial Discharge Apparent Charge Measurement. In Elektroenergetika 2013 : proceedings of the 7th International Scientific Symposium on Electrical Power Engineering. Košice: Technical University, 2013. s. 409-412. ISBN: 978-80-553-1441-9

[20] PIHERA, J., HALLER, R., MENTLÍK, V., MRÁZ, P. PARTIAL DISCHARGES OF THERMALLY AGED INSULATION. In 17th International Symposium on High Voltage Engineering. Berlin: VDE Verlag Gmbh, 2011. s. 212-213. ISBN: 978-3-8007-3364-4

[21] MRÁZ, P. Nové možnosti měření a vyhodnocování výbojové činnosti. In Elektrotechnika a informatika 2011 část první Elektrotechnika. Plzeň: Západočeská univerzita v Plzni, 2011. s. 83-86. ISBN: 978-80-261-0016-4

[22] ŠIRŮČEK, M., MENTLÍK, V., TRNKA, P., PIHERA, J., BOČEK, J., MRÁZ, P. Cole-Cole diagram as Diagnostic Tool for Dielectric Liquids. In 2011 IEEE International Conference on Dielectric Liquids. Trondheim: SINTEF Energi AS, 2011. s. 120-124. ISBN: 978-1-4244-7355-7 , ISSN: 2153-3725

[23] PIHERA, J., MRÁZ, P., HALLER, R., MENTLÍK, V. Partial Discharges and Breakdown Voltage Diagnostics during Thermal Aging of Insulating Materials. ElectroScope, 2011, roč. 2011, č. 5, s. 1-5. ISSN: 1802-4564

[24] KRPAL, O., MRÁZ, P., ŠIRŮČEK, M. Influence of Renewable Energy on Power Transformer Insulating System. In Annals of DAAAM for 2012 & Proceedings of the 23rd International DAAAM Symposium. Vídeň: DAAAM International, 2012. s. 569-574. ISBN: 978-3-901509-91-9 , ISSN: 1726-9679

[25] MRÁZ, P., MENTLÍK, V., ROK, M. Evaluation of a stator end winding bracing system to be used in large rotating machines. In 2013 IEEE International Conference on Solid Dielectrics. S.l.: IEEE, 2013. s. 517-520. ISBN: 978-1-4673-4459-3

[26] HALLER, R., MRÁZ, P., PIHERA, J. Partial Discharge Measurement on Stator Bar Insulation. In ISH 2013 : proceedings : 18th International Symposium on High

Voltage Engineering. Seoul: Hanyang University, 2013. s. 1929-1934. ISBN: 978-89-86510-18-8

[27] PIHERA, J., MRÁZ, P., HALLER, R. PARTIAL DISCHARGES UNDER AC AND DC TEST CONDITIONS. In Proceedings of the 14th international scientific conference Electric power and engineering 2013. Ostrava: VSB - Technical University, 2013. s. 1-6. ISBN: 978-80-248-2988-3

10 Annex 1

For interpretation of PD activity evaluated by the measured PD parameters very often the dependency on the applied test voltage is used. The common existing evaluation for this kind of measurement is that with increasing test voltage the PD parameters are increased too and the measured values are more or less linear dependent on the applied test voltage. In this chapter is shown that the PD parameter depending on the applied test voltage could have a different behaviour caused by different PD sources. The described investigations were made with some well-known basic (artificial) PD sources, which are typical for relevant defects in electrical apparatus, such as transformers, rotating machines, switchgears/ GIS or cables. The PD activity was evaluated by the PD parameter Q_{iec} (apparent charge) as well as PRPD patterns according to the recommendations mentioned above. The obtained results should give a contribution to a better interpretation of measured PD activity under real test conditions and give overview about basic PD phenomenon.

10.1 Test and measurement conditions

10.1.1 Test objects description

For the measurement three basic test arrangements were chosen simulating typical corona -, gliding – and internal discharges (Table I). First one was needle-plane arrangement (Table I.-A) to simulate corona discharge. Brass needle tip shape was 24 μm before the test voltage was applied (electrical stress) and lower brass circular electrode has diameter 75 mm, gap distance was 10 mm.

Gliding discharge phenomenon was measured according to the arrangement which is shown in Table I.-B. Top electrode had circular shape and its diameter was 50 mm. Lower electrode had circular shape as well and its diameter was 75 mm. Insulating material was represented by block made of Poly(methyl methacrylate) (PMMA). Dimensions of this insulating material were 140x140 mm, thickness 10 mm. Top electrode was pressed to the insulating material by constant and defined pressure, which was ensured by spring located in a holder system of the top electrode.

Internal partial discharges were measured according to arrangement shown in Table I.-C. The top (high voltage)-electrode had a circular shape with a diameter of 50mm. The ground-electrode was circular shaped too (diameter 75mm). The top-electrode was pressed to the

dielectric material by a constant and defined pressure, which was given by a spring located in a holder system of the top electrode. The whole test setup was completely immersed into transformer oil to suppress the gliding discharge on surface of specimen.

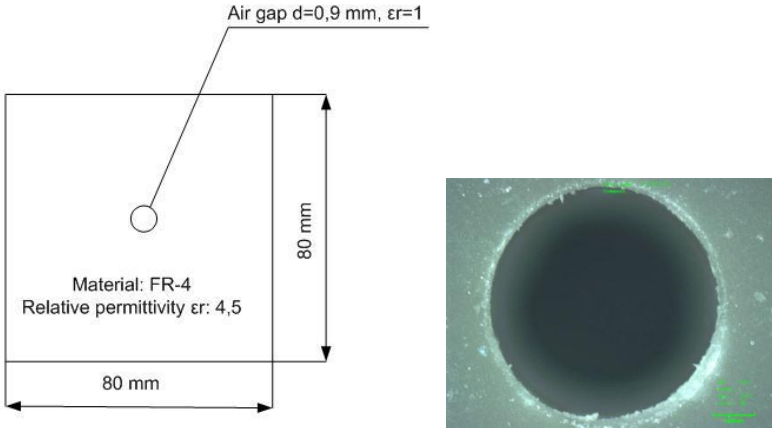

Fig. 89 Diameters of internal PD sample and microscopic view

The dielectric material was realized by sheets of FR4 (FR4 is a composite material composed of woven fibreglass cloth with an epoxy resin binder that is flame resistant) with dimensions of 80 x 80 mm and thickness of 3 x 0.6mm. The diameter of cavity was 0.9 mm round shape and was measured microscopically by Stereomicroscope Olympus SZX10, see Fig. 89.

Table I. Test arrangements overview

A	**Corona** Needle-plane	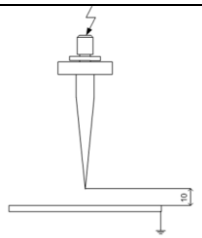
B	**Gliding discharge**	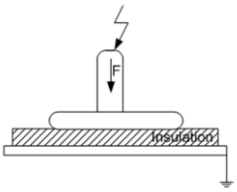
C	**Internal discharge**	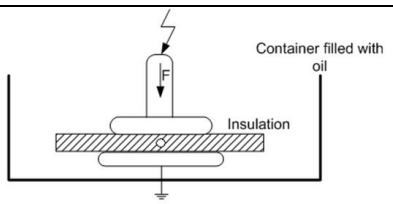

10.1.2 Test circuit

Measurement was performed using a test circuit according to IEC 60270 (Fig. 90), [9]. It consists of a 50 Hz- power transformer (0-50 kV), coupling capacitor (C = 1000pF), measuring impedance (Z = 50 Ω) and partial discharge analyser PD SMART (LDIC PD fully digital measuring system (Doble Lemke). The whole test circuit was located into a shielded test room, where a PD sensitivity of less than 1 pC was reached at a test voltage value up to 30 kV.

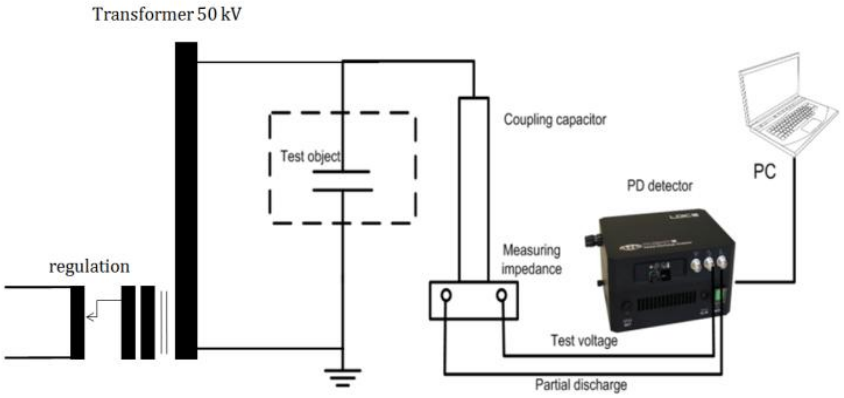

Fig. 90 Test circuit

10.1.3 Test procedure

The test procedure was carried out in two stages (Fig. 91 and Fig. 92).

FIRST STAGE

Increasing the test voltage up to U_i (inception voltage), measuring the Q_{iec}-value, increasing the test voltage up to 1.2 U_i, decreasing the test voltage to 0.8 U_e (extinction voltage) and repeating the procedure 5 times. For evaluation an averaging of the measured values was made.

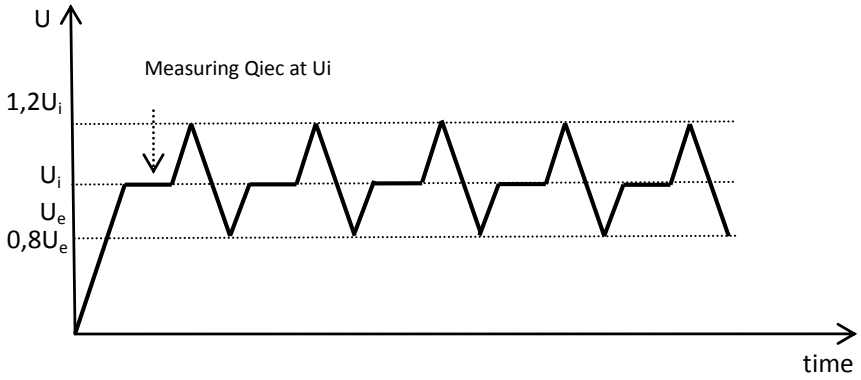

Fig. 91 First stage measurement (principle)

SECOND STAGE

For measuring of any time-dependencies of PD- values the Q(t)- behaviour was measured in the second stage procedure according to Fig. 92. Time dependence of corona discharge was set to 15 minutes at 350 % U_i (self-extinction phenomenon). Decreasing test voltage from 350% U_i to U_e with 35 % U_i steps – measuring Q_{iec} and PRPD (Phase resolved PD characteristics or Φ-q-n) and Φ-q diagrams for each voltage step. Time dependence of gliding discharge was 5 minutes at 135 % U_i. Decreasing test voltage from 135 % U_i to U_e with 0.5 kV voltage- steps and time dependence of internal partial discharge was 10 minutes at 120 % U_i. Decreasing test voltage from 120 % U_i to U_e with the same (0.5 kV) steps.

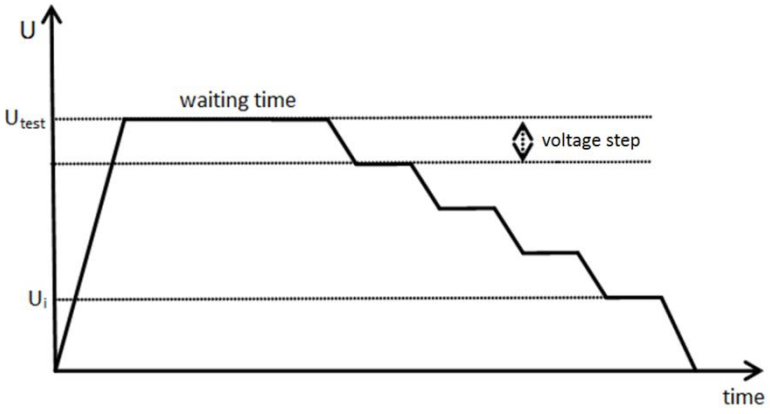

Fig. 92 Second stage measurement (principle)

10.2 Experiment results

10.2.1 Corona discharges

Table II. Measured values for corona discharges

Average Inception voltage U_i	1.56 kV
Average Apparent Charge at inception voltage Q_{iec}	37.8 pC
Average extinction voltage U_e	1.43 kV

There are four phases of corona to breakdown development

- First phase ($U_{test} = U_i \sim 1.6$ kV)

If AC voltage is applied to the needle, pulses can be observed in negative half sinus wave. These pulses have relatively small amplitude (depending on the tip shape), high repetition rate and they are time- stable. This phenomenon is called Trichel pulses. They are caused by fast transfer of electrons from voltage electrode (needle) to ground electrode (plane). Electrons leave behind themselves slow positive ions, which create space charge around the tip and suppress the electron´s movement for a certain time. If the ions are moved away, the next pulse is possible (Fig. 93).

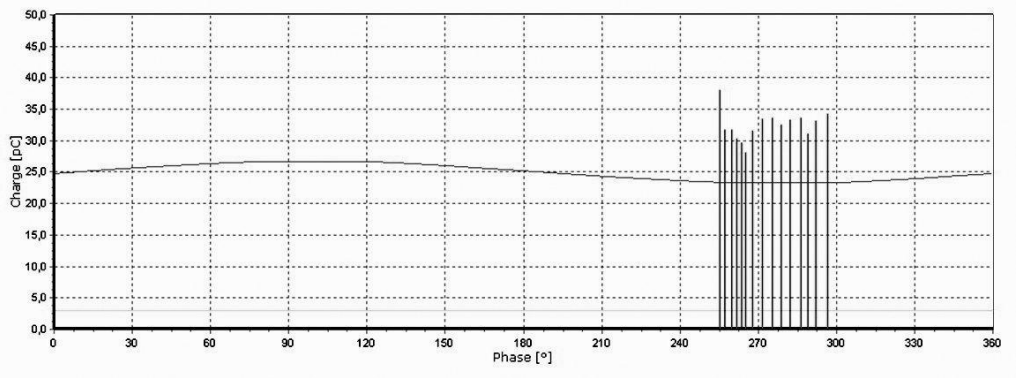

Fig. 93 Φ-q diagram - first phase of corona

- Second phase ($U_{test} = 200$ % $U_i \sim 3.1$ kV)

Increasing of test voltage causes that the range of the Trichel pulses over the voltage (or the area of phase angle) gradually spreading - between the electrodes flow more and more electrons- avalanches, a higher PD repetition rate could be measured too (Fig. 94).

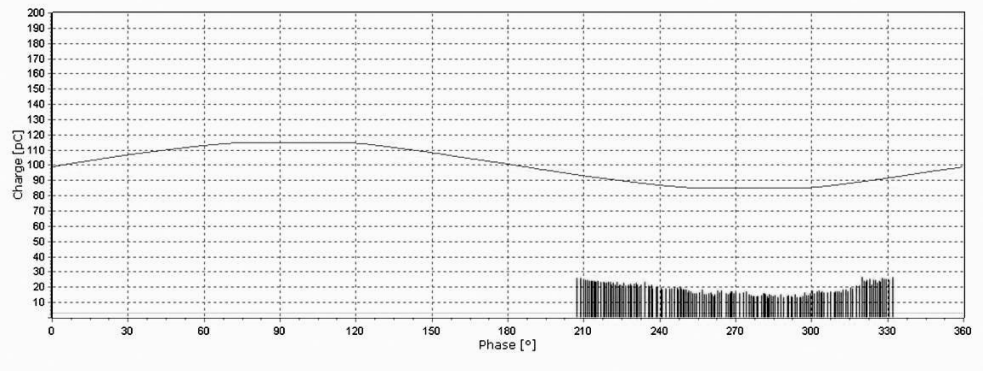

Fig. 94 Φ-q diagram - second phase of corona

- Third phase (U_{test} = 263 % U_i ~ 4.1 kV)

With higher value of test voltage a special PD behaviour can be observed, so called "pulses less area". It is located in the middle of Trichel pulses cluster (Fig. 95). With common partial discharge detectors, which operates according to IEC 60270 no PD pulses can be observed in this area. In fact the repetition rate of pulses in this area is so high, that common PD analysers are not able to recognize them, due to the filter settings according to the IEC 60270, as explained in chapter 6.5.

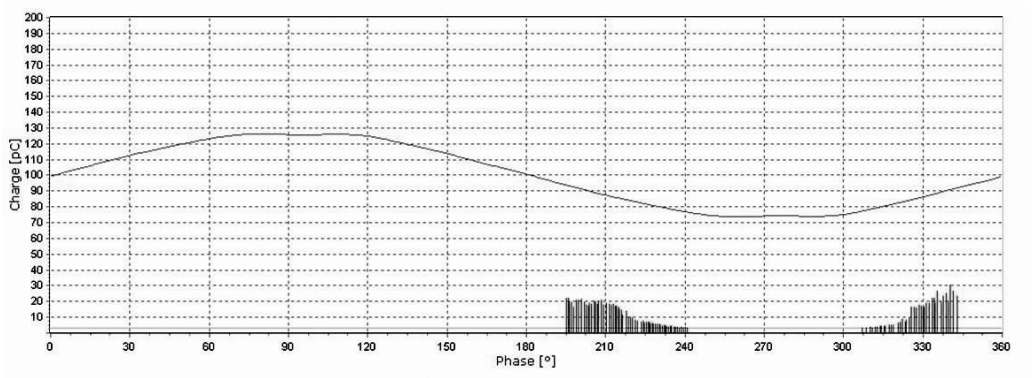

Fig. 95 Φ-q diagram - third phase of corona

- Fourth phase (U_{test} = 350 % U_i ~ 6 kV)

If the test voltage is increased even more - close to breakdown voltage - high energy pulses occur in positive half sinus wave of test voltage. These pre-breakdown or onset streamers are typical with their high charge resp. energy levels (significantly several times higher than Trichel pulses) and with their instability - this is a phase very close to breakdown. These pulses are located in positive half sinus wave of test voltage (needle) because this arising instable conduct channel consists of positive streamers. This fourth phase can be very easily turned to the breakdown thanks to their instability. In that case onset streamers can be observed in both polarities of test voltage. Fourth phase is characterized by an audible (acoustic) effect (Fig. 96, Fig. 97).

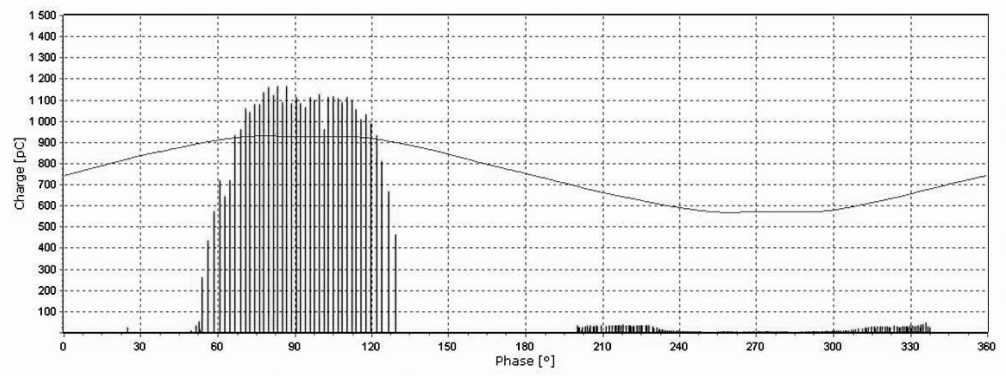

Fig. 96 Φ-q diagram - fourth phase of corona

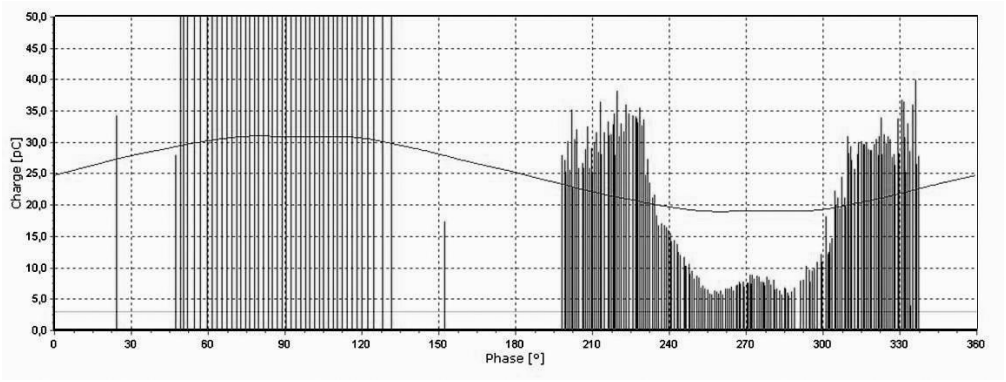

Fig. 97 Φ-q diagram - fourth stage of corona - zoom to negative half sinus wave

The charge- voltage dependency shows the typical characteristics of this PD behaviour (Fig. 98). In the first phase a quasi-constant charge level over the voltage will be obtained. Therefore, this behaviour was in the past particular used like a high- voltage- calibrator [36]. It should be noticed, that the level of measured charge is dependent on the tip- radius. The described phenomenon is valid only in a certain range of test voltage. If the voltage is increased, the stability of the charge value is lost (see Fig. 98 - higher dispersion).

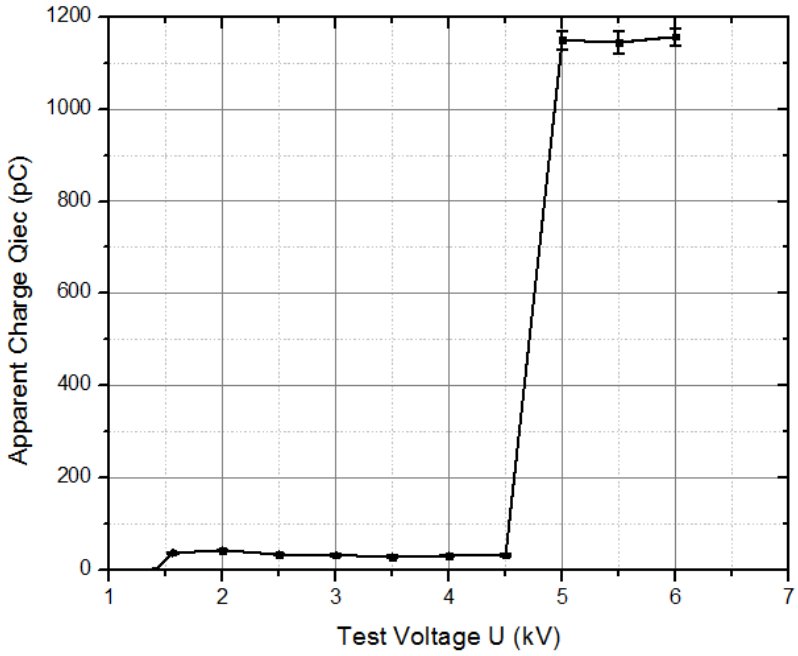

Fig. 98 Charge- voltage dependence of corona

Fig. 99 on the left side shows the shape of the needle before and after the electrical stress. The initial thickness of the tip was 20 µm. Fig. 99 on the right side shows the shape of the needle after the electrical stress - 15 minutes under 6 kV. The thickness of the point was 55 µm. The shape changes depend on material of the needle, on initial thickness, on the level of voltage and finally on operation time. This effect clearly demonstrates degradative impacts of partial discharge activity.

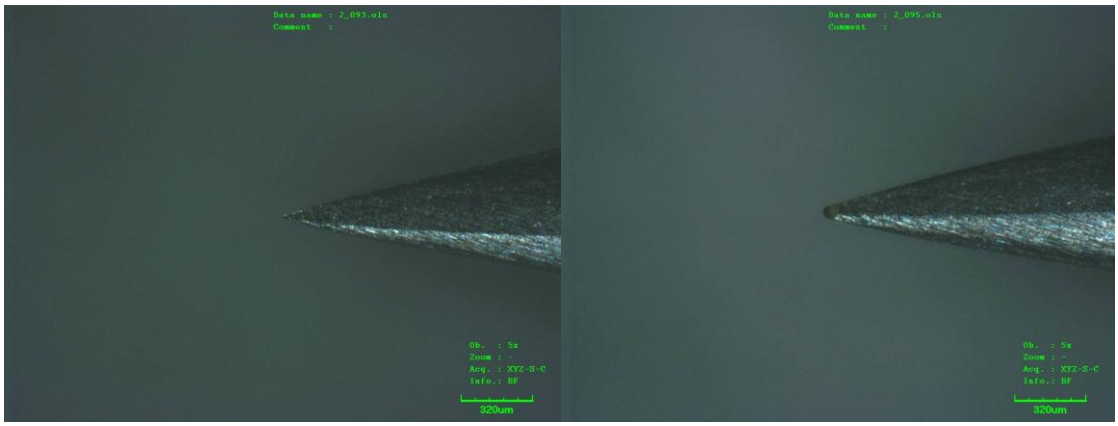

Fig. 99 Needle tip before (left side) and after (right side) electrical stress

10.2.2 Surface (gliding/creeping) discharges

Table III. Measured values for corona discharges

Average Inception voltage U_i	7.1 kV
Average Apparent Charge at inception voltage Q_{iec}	1310 pC
Average extinction voltage U_e	6.8 kV

Fig. 100 shows the typical PD behaviour of gliding discharge at ϕ-q-n diagram. There is no phase shift during test voltage increasing. Gliding discharge activity is characteristic by two symmetric triangle diagrams, one is in positive half sinus wave and the second is on the negative half sinus wave of test voltage. The peaks are at 60° of phase in positive half sinus wave, respectively in 240° of phase in negative half sinus wave. When the arrangement has different layout (different size of electrodes etc.) the cluster in negative half sinus wave of test voltage can have smaller amplitude of charge. Only the size (the level of apparent charge) of diagram is changing with voltage increasing, clusters' shape remain the same.

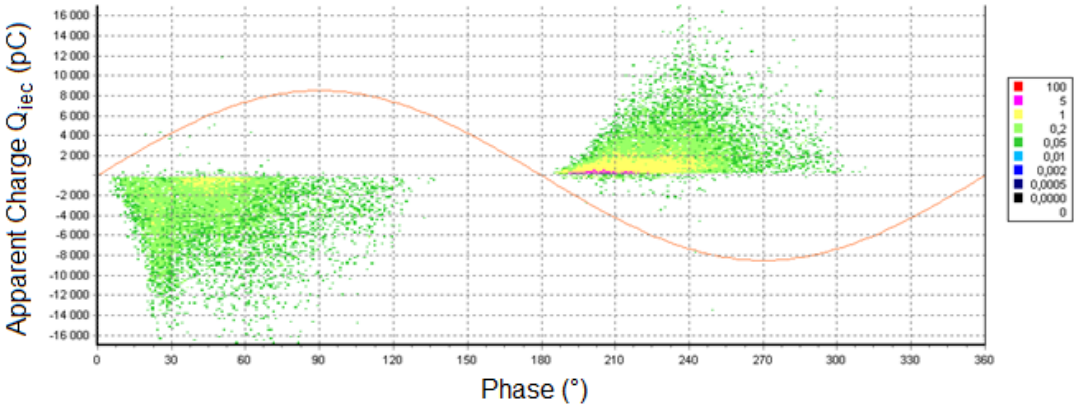

Fig. 100 Φ-q-n / PRPD pattern for gliding discharge

At the same time the charge- voltage dependency is typically for gliding discharges (Fig. 101), [60-63]. All values are in the nC range, with relative high dispersion behaviour, the PD activity is monotonously increased at higher test voltage.

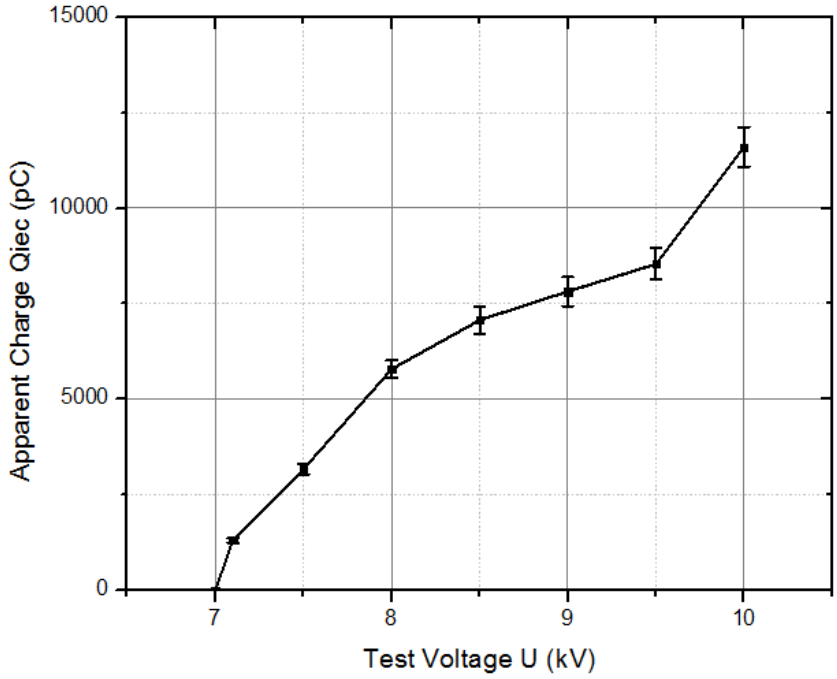

Fig. 101 Charge- voltage dependency of gliding discharge

10.2.3 Internal discharges

Table IV. Measured values for internal discharges

Average Inception voltage U_i	3.65 kV
Average Apparent Charge at inception voltage Q_{iec}	240 pC
Average Extinction voltage U_e	3.1 kV

The typical PD behaviour of an internal cavity is characterized by a hysteresis at test voltage up and down (Fig. 102). It is supposed, that the avalanche of fast electrons in the cavity let the slow ions behind itself. The ions then create space charge and it receives on the inner surface of the cavity. It causes deformation of the original electrical field.

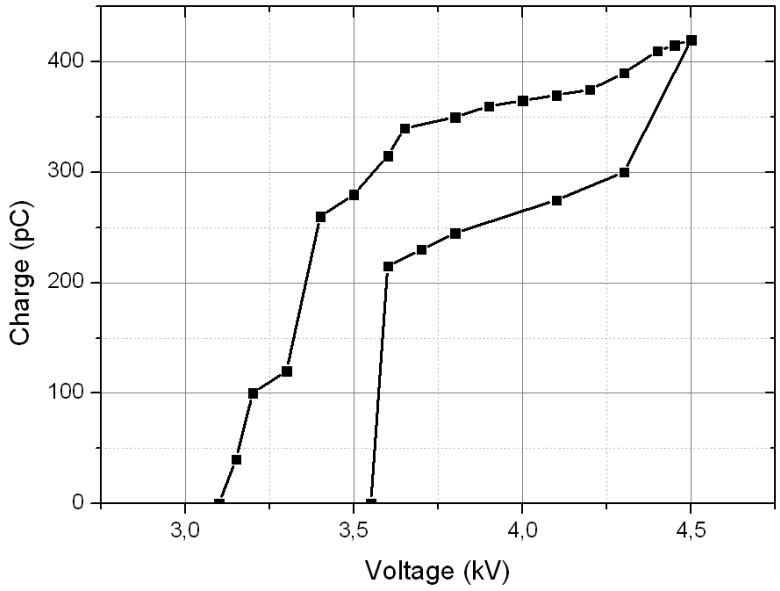

Fig. 102 Charge- voltage dependency of internal discharge (inception and extinction voltage area)

Space charge has an opposite field influence in comparison with the external field, the resulting field within the cavity is weaker. Therefore in comparison with the inception voltage the extinction voltage is lower caused by the space charge inside the internal defect. In some cases this behaviour can be used for identification of the existing PD sources.

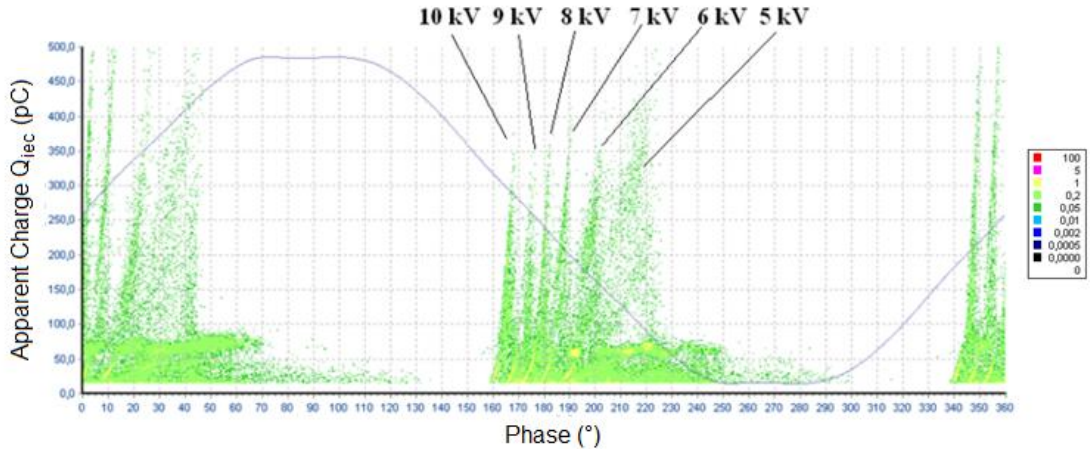

Fig. 103 Φ-q-n / PRPD pattern for internal discharges at different test voltages

A typical PD behaviour can be obtained by measuring the PRPD- pattern (Fig. 103), [47-50]. There are two symmetrical clusters in both half sinus waves and with higher test voltage the PD activity "cluster" (so-called rabbit ears) is shifted to a lower phase angle and at the same time the PD activity is limited to a smaller "phase- area".

In Fig. 104 PRPD pattern construction principle for internal PD activity is shown. In case of internal discharges is created cluster which follows sinus shape of applied voltage. With increasing test voltage, sinus shape gets sharper and also internal PD cluster increase its angel of occurrence as can be seen in Fig. 103. This behaviour is symmetrical in both half sinus waves. Fig. 103 shows unipolar PRPD pattern. In case of bipolar PRPD pattern so called "rabbit ears" cluster would be displayed in negative axial orientation since half sinus wave has negative character which is followed by the internal PD activity.

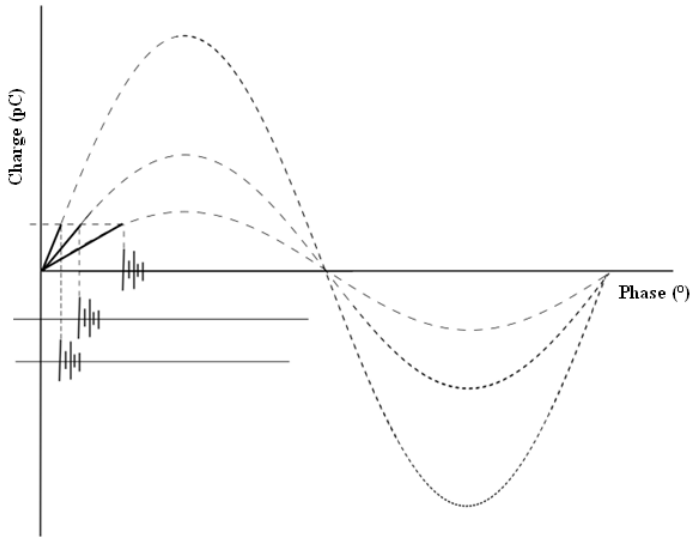

Fig. 104 Internal PD activity PRPD pattern construction principle

Even the charge- voltage dependency shows a characteristic behaviour (Fig. 105). After the PD inception and small increasing of the test voltage the PD activity expressed by the measured charge is even quasi unchanged at higher test voltages. It should be noticed, that the dispersion of the charge values is much higher than at corona- PD´s, the value of the charge is determined by the size of the cavity. In case of several cavities with different size also levels of inception voltages can be changed. Also this typical behaviour could be used in some cases for a better identifying of the existing PD sources.

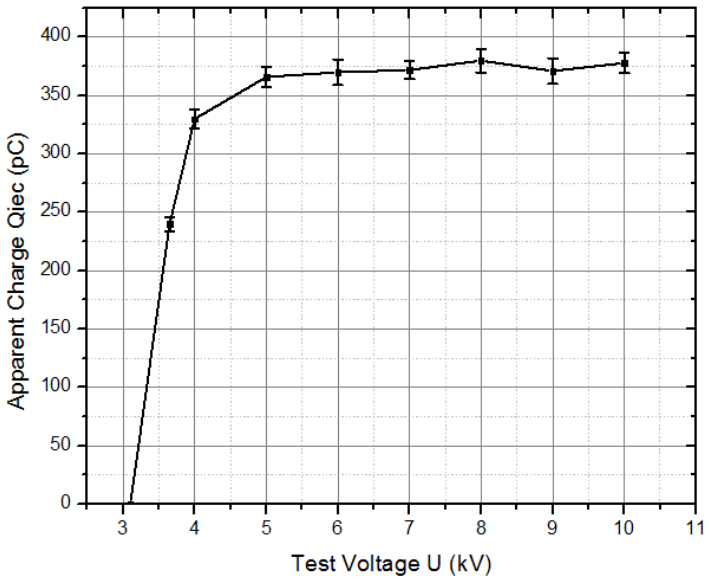

Fig. 105 Charge- voltage dependency of internal discharge

10.3 Conclusion

In this chapter some aspects of PD evaluation are discussed – in detail the charge- voltage behaviour and accompanied PD parameters- of basic PD arrangements typical for real existing PD defects. The obtained results confirm that each type of PD defect has its specific PD behaviour and especially its charge- voltage dependency. Not all of them have a monotonously increasing PD activity at higher applied test voltage. As example the corona PD activity has a special charge- voltage characteristic, which is characterized by Trichel pulses up to final pre-breakdown onset streamers. Surface (gliding/creeping) discharges in general have more or less linear increasing character of PD activity with rising test voltage, caused by linear increase of electrical field inhomogeneity. Internal discharges have first part of charge- voltage characteristics similar to the corona, but higher dispersion of measured values but then it differs. Despite of another physical background of PD activity of internal defects is strongly dependent on size and filling material of cavity. Therefore, it is not convenient to evaluate the PD activity only by an absolute value of apparent charge or by generalized charge- voltage behaviour.

11 Annex 2

In following tables a brief overview of electrical devices' capacitances can be found.

11.1 Rotating machines

Turbo – generators / motors

U_n (kV)	P (MW)	C (nF)	Core length (mm)	Frequency (Hz)	Note
11.5	50	220	2900	50	-
13.8	38	110	1700	60	-
13.8	13	470	5200	60	-
13.8	125	440	3300	60	-
13.8	116	290	4000	60	-
15	135	490	4550	50	-
15.75	190	570	5000	60	-
15.75	150	610	4550	50	-
19	240	850	5700	60	Theoretical calculation
15.75	270	480 - 510	4100	50	$H_2O + H_2$ cooling, JE Mochovce
24	1000	ca. 1000	7500	50	$H_2O + H_2$ cooling, JE Temelín
11	78	340	ca. 3000	50	Škoda, model 2004
11	-	210	-	50	Siemens unit
11.5	-	330	-	50	ABB unit

Hydro- generators are mostly over 1000 nF, usually 1200 - 1300 nF.

11.2 Instrument transformers

Type	U_n (kV)	C (pF)
VT	245	470
VT	420	185
CT	420	850
CT	245	600

VT … Voltage Transformer

CT … Current Transformer

11.3 Bushings

U_n (kV)	C (pF)
420	500
245	550
123	300
52	250

11.4 Power transformers

Unit S = 350 MVA, U = 400/110 kV

Winding	C (nF)
HV + LV	22
TV (tertiary)	40